Published for SISSA by Springer

Received: December 5, 2019
Revised: May 17, 2020
Accepted: June 30, 2020
Published: July 22, 2020

Dark fermions and spontaneous CP violation in SU(2)-axion inflation

Azadeh Maleknejad

Max-Planck-Institute for Astrophysics,
Karl-Schwarzschild-Str. 1, 85741 Garching, Germany

E-mail: amalek@mpa-garching.mpg.de

Abstract: Remarkably, if CP was spontaneously broken in the physics of inflation, fermions would notice and remember it. Based on that, we present a new (non-thermal) mechanism for generating self-interacting dark Dirac fermions prior to the Hot Big Bang. The non-Abelian gauge fields and axions are well-motivated matter contents for the particle physics of inflation. In this background, we analytical study Dirac fermion doublets charged under the SU(2) gauge field and use point-splitting technique to regularize the currents. We show that the non-trivial CP-violating vacuum structure of SU(2)-axion models naturally leads to an efficient mechanism for generating massive fermions during inflation. The size of the fermionic backreaction and the density fraction of dark fermions put upper bounds on the fermion's mass. For a GUT scale inflation, the generated dark fermions, only gravitationally coupled to the visible sector, can be as heavy as $m \lesssim 10\,\mathrm{TeV}$.

Keywords: Discrete Symmetries, Effective Field Theories, Spontaneous Symmetry Breaking

ArXiv ePrint: 1909.11545

https://doi.org/10.1007/JHEP07(2020)154

JHEP07(2020)154

Contents

JHEP07(2020)154

1 Introduction

The current cosmological observations are in significant agreement with the general concept of inflation paradigm [1–4] and several of its key predictions have been already confirmed by the cosmic microwave background (CMB) and large scale structure (LSS) data [5]. Besides, the upcoming ambitious missions, e.g., LiteBIRD [6, 7] and CMB Stage-4 [8], will soon provide us with even more data about the early Universe. However, our theoretical understanding of the particle content of inflation is still vague and incomplete in that sense. Given the fact that the energy scale of inflation can be as high as the GUT scale to a few TeV, it might provide an outstanding opportunity to explore the high energy physics beyond the standard model (BSM) and possibly breakthrough discoveries.

From the high-energy physics point of view, gauge fields and axions are very natural matter contents for high energy scales, e.g., the scale of inflation. Axion fields are abundant in theories BSM and hence well-motivated candidates for the inflaton field. Moreover, thanks to the isomorphy of the $su(2)$ and $so(3)$ algebras, any non-Abelian gauge field can acquire a homogeneous and isotropic vacuum field configuration (VEV) in its SU(2) subsector. In the presence of the effective interactions that break the conformal symmetry of the Yang-Mills theory, e.g., by coupling with the axion (to prevent its a^{-4} decay), the gauge field can enjoy a slow-roll dynamics with an almost constant energy density during inflation. The theoretically well-motivated and phenomenologically rich setting for SU(2) inflation models have been discovered in [9, 10] which showed that non-Abelian gauge fields can contribute to the physics of inflation. Followed by that, several more inflationary models with the SU(2) VEV have been proposed and studied in the literature. Despite their differences in details, all of the inflationary models with the SU(2) VEV share several key features as robust consequences of having non-Abelian gauge fields in the physics of inflation. The illustration in figure 1 summarizes some of them. For a review on gauge fields in inflation see [11], section 2 of [12] and the references therein.

The focus of the current work is the production of charged Dirac fermions by this primordial SU(2) gauge field in inflation (see figure 2). In [13], the fermionic backreaction to the SU(2) gauge field, J^{μ}_{a}, has been studied numerically for a small part of the parameter space, i.e., $m \sim H$. However, some key features, including the central rule of parity and CP violation, and most of the parameter space were missed in the previous analysis. The current work presents an extensive study of the setup and computes all of the non-vanishing fermionic induced currents analytically. We show that this setup naturally leads to a new (non-thermal) mechanism for generating massive fermions during inflation. More precisely, the SU(2)-axion vacuums spontaneously break P and CP during inflation [14] (see figure 3 for an illustration) and predict a *CP-violating* pre-Hot Big Bang physics.[1] That leads to a non-zero net fermion production in inflation, which otherwise would be missing. Comparing to the analysis of [13] in which the current integral is computed numerically by imposing a

[1]Since the seminal paper [15], it is well known that broken discrete symmetries cause cosmological domain wall problem, which can dominate the Universe if the symmetry is broken only spontaneously and happens after inflation [16]. Given the fact that in SU(2)-axion models, the scale of symmetry breaking is high, and prior to the Hot Big Bang, they avoid the domain wall problem.

JHEP07(2020)154

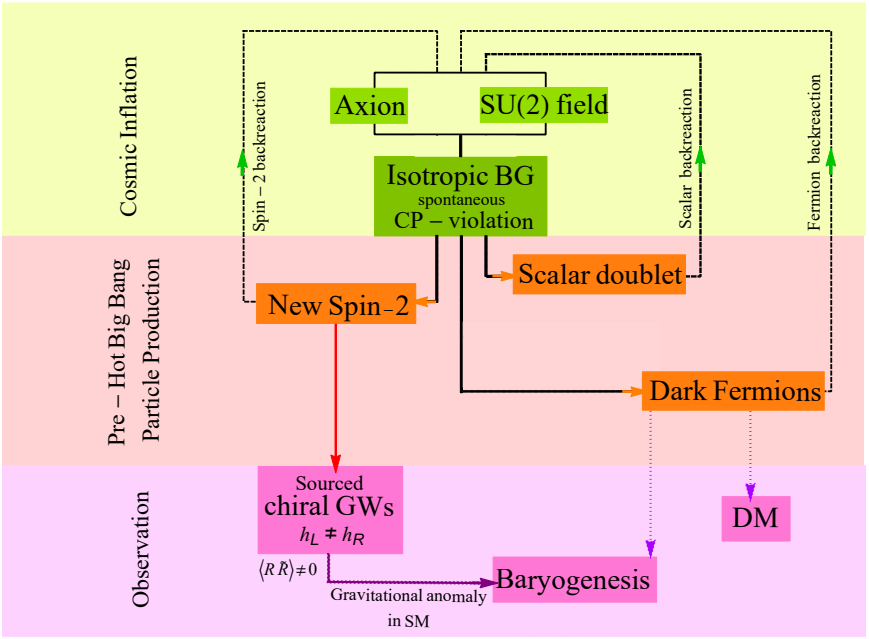

Figure 1. The SU(2)-axion inflation setup can be a complete beyond the standard model (BSM) which provides new mechanisms to explain and relate seemingly disparate phenomena in inflation and pre-Hot Big Bang (e.g., massive dark fermions, new spin-2 field, and chiral gravity waves) with late-time cosmological observations (dark matter, matter asymmetry, and primordial gravitational waves). Namely, the non-trivial CP-violating vacuum leads to distinctive features for the spin-2 and fermion fields coupled to it. The solid (dashed) black arrows show the particle production by (backreaction of the particles to) the vacuum. The colorful arrows show emerged phenomena due to the corresponding inflationary particle production. The distinctive features of the non-trivial VEV are as follows. 1) The perturbed gauge field has a new *chiral* tensorial mode (spin-2 field) which is linearly coupled to the gravitational waves (GW), and generates chiral GWs [9, 17, 18], parity-odd correlations of CMB, i.e., non-zero TB and EB [19], and a possible large tensor bispectrum [20, 21]. In [12], the backreaction of the spin-2 field on the background fields has been studied. 2) The production and backreaction of charged scalar (Higgs) doublets are studied in [22]. 3) Thanks to the SU(2)-axion vacuum, which spontaneously broke P and CP in inflation, this class of models provides a natural leptogenesis mechanism during inflation [14, 23, 24]. 4) It provides a new mechanism for the non-thermal generation of massive, self-interacting dark fermions during inflation, which is the focus of the current work.

hard UV cut-off, here we solve the integrals analytically. We regularize the UV divergent momentum integrals by the point-splitting regularization skim. As a result, for the limited cases that the comparison is possible, i.e., for J_a^μ with $m \sim H$, the two answers are not exactly equal. That is due to the miscalculation of the hard UV cut-off technique which is used in the numerical analysis of [13].

The paper is structured as follows. In section 2 we review the setup of a dark Dirac fermion charged under the gauge field in a generic SU(2)-axion inflation. In section 3, we discuss the symmetry structure of the SU(2)-axion vacuum and its consequences on the fermionic sector. In section 4, we solve for the mode functions in (quasi) de Sitter.

JHEP07(2020)154

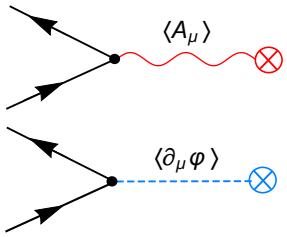

Figure 2. The processes underlying inflationary fermion production studied in this work. The gauge field vacuum naturally induces fermionic currents through $i\bar{\Psi}\not{D}\Psi \supset g_A\bar{\Psi}\gamma^\mu A_\mu\Psi$ (top). Moreover, fermions can possibly be coupled to the axion by effective interaction $\partial_\mu\varphi\bar{\Psi}\gamma^\mu\gamma^5\Psi$ (bottom).

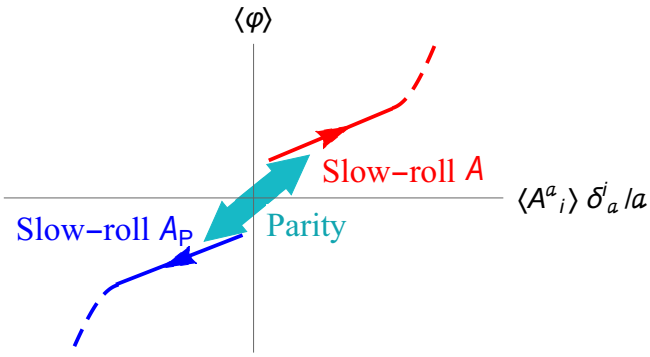

Figure 3. The SU(2)-axion vacuum structure. For each given parameter set and energy density, there are two SU(2)-axion field configuration vacuums, eqs. (2.7)–(2.8), which are related by the parity, i.e. slow-roll trajectories A and A_P. The two have identical background cosmologies; however, vacuum spontaneously breaks P at the level of perturbations of the fields with spin, e.g., fermions and spin-2 fields. For more details about the vacuum see section 2 of [12].

Next in section 5, we take a closer look at the solutions and investigate their generic features. Section 6 presents the analytical form of the fermionic currents after point-splitting regularization. Section 7 discusses the main results and compares the inflationary dark fermion production in different limits. In section 8, we take a quick view on the (non-thermal) dark fermion production mechanism naturally arises in our non-trivial vacuum. We finally conclude in 9. Technical details of the computations as well as the underlying mathematical tools are provided in appendices A–D. Readers interested in the main results may proceed directly to sections 7 and 8.

Notations and conventions. In this work, we adopt the notation introduced in [13] as much as possible. Although in some cases we use a more convenient notation to better capture the novel aspects of the setup. Here we deal with 8, 4 and 2-component spinors which are acted upon by 8×8, 4×4 and 2×2 matrices, respectively. We place a tilde ($\sim$) on top of 8 dimensional spinor and matrix. The 4-dimensional spinor and matrix remains unchanged, while the 2-dimensional ones are written in boldface. Moreover, $\mathrm{I_n}$ represents the $n\times n$ identity matrix and the gamma matrices are in the Dirac representation unless otherwise stated. We use the Einstein summation notation, i.e. repeated indices (one upper

JHEP07(2020)154

Representation	Isospin	$\rightarrow$	Weyl	$\rightarrow$	Color-spin helicity
Transformation		$\tilde{T}_1$		$\tilde{T}_2$	
$\tilde{\Psi} \equiv a^{\frac{3}{2}}\tilde{\Psi}$	$\begin{pmatrix}\Psi^1\\ \Psi^2\end{pmatrix}$		$\begin{pmatrix}\Psi_L\\ \Psi_R\end{pmatrix}$		$\begin{pmatrix}\Psi^+\\ \Psi^-\end{pmatrix}$

Table 1. The Dirac SU(2) doublet in three different representations.

and one lower) are summed. Greek letters starting from the middle of the alphabet, i.e. μ, ν, ..., are used for the space-time indices, whereas the starting ones, i.e. α, β, ..., present the indices of the tangent space (non-coordinate) bases. In particular, the tetrads are defined as $g^{\mu\nu} \equiv \eta^{\alpha\beta}\mathbf{e}^{\mu}{}_{\alpha}\mathbf{e}^{\nu}{}_{\beta}$. As a result, $\gamma^{\mu} = \mathbf{e}^{\mu}{}_{\alpha}\gamma^{\alpha}$. We recall that the FRW tetrads can be defined as $\mathbf{e}^{\mu}{}_{\alpha} = a^{-1}(\tau)\delta^{\mu}_{\alpha}$ and γ^{α} are the flat space Dirac matrices

$$\gamma^0 = \begin{pmatrix}\mathbf{I}_2 & \mathbf{0}\\ \mathbf{0} & -\mathbf{I}_2\end{pmatrix} \quad \text{and} \quad \gamma^i = \begin{pmatrix}\mathbf{0} & \boldsymbol{\sigma}^i\\ -\boldsymbol{\sigma}^i & \mathbf{0}\end{pmatrix},$$

which obey the Clifford algebra

$$\{\gamma^{\alpha}, \gamma^{\beta}\} = -2\eta^{\alpha\beta}\mathrm{I}_4,$$

where $\eta^{\alpha\beta}$ is the Minkowski metric with signature $(-+++)$. The indices of γ^{α} and $\boldsymbol{\sigma}^i$ are lowered as $\gamma_{\alpha} = \eta_{\alpha\beta}\gamma^{\beta}$ and $\boldsymbol{\sigma}_i = \delta_{ij}\boldsymbol{\sigma}^j$. The gamma matrices in the Weyl representation are presented as γ^{α}_{W}. The 4-dimensional Hermitian adjoint row spinor $\bar{\Psi}$ is given as $\bar{\Psi} \equiv \Psi^{\dagger}\gamma^0$. Besides, $\gamma^5 = i\gamma^0\gamma^1\gamma^2\gamma^3$. The 4×4 helicity operator, $h(k^{\alpha})$, is defined as

$$h(k^{\alpha}) \equiv \mathbf{I}_2 \otimes k^j.\boldsymbol{\sigma}_j. \tag{1.1}$$

$\mathbf{T}_a$ are the generators of the SU(2) group in the fundamental representation $[\mathbf{T}_a, \mathbf{T}_b] = i\epsilon^{c}{}_{ab}\mathbf{T}_c$, and we call the SU(2) index *color*. The generators of the SU(2) and the Pauli matrices are related as $\mathbf{T}_a = \frac{1}{2}\boldsymbol{\tau}^a$. As a mathematical tool to take care of the entanglement of the color and Lorentz indices in our setup, we define the color-spin helicity operator (c-helicity) as

$$\mathfrak{h}(k^{\alpha}) \equiv \frac{\delta_{ai}}{k^2}\ k^i.\boldsymbol{\tau}^a \otimes k^j.\boldsymbol{\sigma}_j, \tag{1.2}$$

in which k^{α} is the momentum of the mode with $k = |\vec{k}|$. Both $\boldsymbol{\sigma}^i$ and $\boldsymbol{\tau}^a$ are the Pauli matrices. However, $\boldsymbol{\sigma}^i$ represents the spin operator which carries a Lorentz index while $\boldsymbol{\tau}^a$ represents the generators of the gauge group and acts on color indices. Whenever convenient, we also use $\boldsymbol{\tau}^i = \delta^i_a\boldsymbol{\tau}^a$.

Throughout this work we will use three different representations of the doublet fermions, i.e. isospin, Weyl, and c-helicity frames which are related by two unitary operators, $\tilde{T}_1$ and $\tilde{T}_2$. We present these mappings in table 1.

Here, Ψ^1 and Ψ^2 are the eigenstates of the isopin, while Ψ_L and Ψ_R are chiral states which are the eigenstates of γ^5, i.e. $\gamma^5\Psi_{L,R} = \mp\Psi_{L,R}$. Finally, $\Psi^{\pm}$ are the eigenstates of the c-helicity operator defined in eq. (1.2). More precisely, we have $\mathfrak{h}(k^{\alpha})\Psi^{\pm} = \pm\Psi^{\pm}$.

JHEP07(2020)154

Moreover, the subscripts s and superscripts p are labels of the c-helicity frame. Throughout this work, the superscript $\pm$ denotes the plus/minus subspace, while the subscript $\pm$ denotes the corresponding 2d helicity polarization states, i.e.

$$\mathbf{E}_+ = \begin{pmatrix} 1 \\ 0 \end{pmatrix} \quad \text{and} \quad \mathbf{E}_- = \begin{pmatrix} 0 \\ 1 \end{pmatrix}, \tag{1.3}$$

besides, the subscripts C and P denote the charge conjugated and parity transformed quantities respectively.

In constructing physical observables associated with Grassmann variables and computing the expectation values, we use the antinormal ordering on the creation and annihilation operators of the spinors, $\vdots\,\vdots$, defined as

$$\vdots b_{\mathbf{k}} b^\dagger_{\mathbf{k}} \vdots \equiv b_{\mathbf{k}} b^\dagger_{\mathbf{k}} \quad \text{and} \quad \vdots b^\dagger_{\mathbf{k}} b_{\mathbf{k}} \vdots \equiv -b_{\mathbf{k}} b^\dagger_{\mathbf{k}}. \tag{1.4}$$

Finally, the point-splitting 4-vector which splits each point in the space-time into a forward and backward point is denoted by $\varepsilon^\mu = (\varepsilon, \boldsymbol{\varepsilon}^i)$. The forward/backward (physical) coordinates corresponding to X^μ and the splitting 4-vector ε^μ, are X^μ_f/ X^μ_b defined as

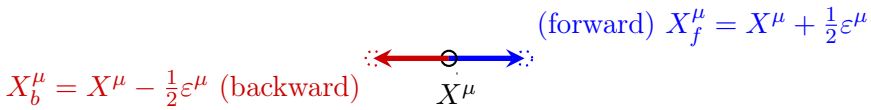

and we will eventually take ε^μ to zero. Notice that the slow-roll parameter is shown by $\epsilon = -\frac{\dot{H}}{H^2}$.

2 Setup

In this work, we consider an SU(2) doublet fermion in an SU(2)-axion inflation setting. This setup has been recently introduced in [13]. We consider a doublet of Dirac fermions

$$\tilde{\Psi} = \begin{pmatrix} \Psi^1 \\ \Psi^2 \end{pmatrix}, \tag{2.1}$$

charged under the gauge field of the SU(2)-axion model

$$S = \int \mathrm{d}^4x\sqrt{-g}\left[i\bar{\tilde{\Psi}}\not{D}\tilde{\Psi} - m\bar{\tilde{\Psi}}\tilde{\Psi}\right], \tag{2.2}$$

with mass m and $\not{D}$ as

$$\not{D} \equiv D_\mu \otimes \gamma^\mu = \mathbf{e}^\mu{}_\alpha\left[\mathbf{I}_2\nabla_\mu - ig_A A^a_\mu \mathbf{T}_a\right] \otimes \gamma^\alpha. \tag{2.3}$$

For the sake of completeness, we also consider the possible effective interaction of the axion with the fermion as

$$S_{\rm int} = \int \mathrm{d}^4x\sqrt{-g}\beta\frac{\lambda\varphi}{f}\nabla_\mu J^\mu_5, \tag{2.4}$$

JHEP07(2020)154

where φ is the axion field, f is the axion decay constant, λ is the dimensionless coefficient of the Chern-Simons interaction term of the axion, and β is a dimensionless parameter. Here, $\otimes$ is the Kronecker product. For definition of $\otimes$ see appendix A. Moreover, the quantity β can be of order unity or lower. Here, J_5^μ is the chiral current given as

$$J_5^\mu \equiv \bar{\tilde{\Psi}} \mathbf{I}_2 \otimes (\gamma^\mu \gamma^5) \tilde{\Psi}. \tag{2.5}$$

We assume slow-roll inflation with (quasi) de-Sitter metric

$$ds^2 = a^2(\tau)(-d\tau^2 + \delta_{ij} dx^i dx^j), \tag{2.6}$$

where τ is the conformal time, H is the (almost) constant Hubble parameter during inflation, $a(\tau)$ is the scale factor, and

$$\mathcal{H} \equiv aH.$$

Moreover, we assume a slowly-evolving homogeneous and isotropic SU(2) gauge field in the temporal gauge as [9][2]

$$A_0(\tau, \mathbf{x}) = A_0^a \mathbf{T}_a = 0 \quad \text{and} \quad \mathbf{A}_i(\tau, \mathbf{x}) = A_i^a \mathbf{T}_a = \frac{1}{2} a(t) \psi(\tau) \boldsymbol{\tau}^i, \tag{2.7}$$

and a homogeneous axion field

$$\varphi(\tau, \mathbf{x}) = \varphi(\tau), \tag{2.8}$$

where $\psi(\tau)$ and $\varphi(\tau)$ are two slow-varying pseudo-scalars during slow-roll inflation. Combination of the slow-varying SU(2) gauge field eq. (2.7) and axion eq. (2.8) make our SU(2)-*axion vacuum* (see figure 3). The class of inflationary models with such SU(2) VEV has several different realizations. See section 2 of [12] and the references therein for a recent comprehensive review on the models. In the perturbation sector, the SU(2)-axion vacuum appears in terms of the following dimensionless quantities[3]

$$\xi_A \equiv \frac{g_A \psi}{H}, \quad \xi_\varphi \equiv \beta \frac{\lambda \partial_\tau \varphi}{2af H}. \tag{2.9}$$

It is also useful to define a dimensionless parameter from the mass of the fermion as

$$\mu_{\rm m} \equiv \frac{m}{H}. \tag{2.10}$$

Moreover, it is more convenient to work with the canonically normalized field

$$\tilde{\Psi} \equiv a^{\frac{3}{2}} \tilde{\Psi}, \tag{2.11}$$

which is the comoving fermionic field. In the Fourier space, we can expand $\tilde{\Psi}(\tau, \mathbf{x})$ as

$$\tilde{\Psi}(\tau, \mathbf{x}) = \int \mathrm{d}^3 k e^{i\mathbf{k}.\mathbf{x}} \tilde{\Psi}_{\mathbf{k}}, \tag{2.12}$$

[2]The stability of this homogeneous-isotropic gauge field solution against initial stochastical anisotropies of the Bianchi cosmology has been studied in [25, 26]. Interestingly, although such systems can in principle acquires anisotropic hair [27, 28], the homogeneous-isotropic gauge field ansatz is the attractor solution (For the massive gauge field case see [29]).

[3]Notice that ξ_φ is different from $\xi \equiv \frac{\lambda \partial_\tau \varphi}{2af H}$ in the axion inflation backgrounds. In fact, ξ and ξ_φ are related as $\xi_\varphi = \beta \xi$, where β can be of order unity.

JHEP07(2020)154

and the fermion theory reads as

$$\mathcal{L}_\Psi = \bar{\tilde{\Psi}}_{\mathbf{k}}\left[i\mathbf{I}_2\otimes\gamma^0\partial_\tau - \left(k^i\mathbf{I}_2 - \frac{1}{2}\xi_A\mathcal{H}\boldsymbol{\tau}^i\right)\otimes\gamma_i - \mu_{\rm m}\mathcal{H}\mathrm{I}_8 - 2\xi_\varphi\mathcal{H}\mathbf{I}_2\otimes(\gamma^0\gamma^5)\right]\tilde{\Psi}_{\mathbf{k}}. \tag{2.13}$$

The above theory is in terms of 8-spinors wherein the color and spin indices are entangled. The reason is the homogenous-isotropic gauge field's VEV in eq. (2.7) in which the gauge group index associated with $su(2)$ and spatial Lorentz index associated with $so(3)$ has been identified to restore the rotational symmetry in the background (For a detailed discussion see [11]). The next step would be to find a frame in which the system is possibly reducible to lower dimension subspinors.

2.1 Ψ^+ and Ψ^- decomposition

Up to this point, we were in the isospin frame. However, the ideal frame, would be the one in which the three of $\mathbf{I}_2\otimes(\gamma^0\gamma^i)$, $\mathbf{I}_2\otimes k^i\gamma_i$, and $\boldsymbol{\tau}^i\otimes\gamma_i$ are diagonal. If exists, such a frame is made of two copies of the common eigenstates of $\mathbf{I}_2\otimes k^i.\boldsymbol{\sigma}_i$, and $\boldsymbol{\tau}^i\otimes\boldsymbol{\sigma}_i$. However, these two operators have only two common eigenstates. Thus, the theory is only block-diagonalizable and can be decomposed into two subspaces.

As a mathematical tool for any given 4-momentum k^α, we define the color-spin helicity operator (c-helicity) as

$$\mathfrak{h}(k^\alpha) \equiv \frac{1}{k^2}\; k^i.\boldsymbol{\tau}_i\otimes k^j.\boldsymbol{\sigma}_j, \tag{2.14}$$

in which the first Pauli matrix is the $su(2)$ generator while the second one is the spin operator. As we will show shortly, it is easier to expand the system in terms of the eigenstates of c-helicity, which automatically takes care of the entangled color and spin indices in the action (2.13). The orthonormal eigenstates of c-helicity satisfy in

$$\mathfrak{h}(k^\alpha)\; E^p{}_s(k^\alpha) = sp\; E^p{}_s(k^\alpha)\,, \tag{2.15}$$

where $p=\pm1$, $s=\pm1$, and $E^p{}_s(k^\alpha)$ are

$$\begin{aligned}
E^+{}_+(k^\alpha) &= \frac{\check{k}^\alpha\bar{\boldsymbol{\tau}}_\alpha\otimes\check{k}^\beta\bar{\boldsymbol{\sigma}}_\beta}{2k(k+k^3)}\begin{pmatrix}1\\0\\0\\0\end{pmatrix}, \qquad E^+{}_-(k^\alpha) = -\frac{\check{k}^\alpha\boldsymbol{\tau}_\alpha\otimes\check{k}^\beta\boldsymbol{\sigma}_\beta}{2k(k+k^3)}\begin{pmatrix}0\\0\\0\\1\end{pmatrix},\\
E^-{}_+(k^\alpha) &= -\frac{\check{k}^\alpha\boldsymbol{\tau}_\alpha\otimes\check{k}^\beta\bar{\boldsymbol{\sigma}}_\beta}{2k(k+k^3)}\begin{pmatrix}0\\0\\1\\0\end{pmatrix}, \qquad E^-{}_-(k^\alpha) = -\frac{\check{k}^\alpha\bar{\boldsymbol{\tau}}_\alpha\otimes\check{k}^\beta\boldsymbol{\sigma}_\beta}{2k(k+k^3)}\begin{pmatrix}0\\1\\0\\0\end{pmatrix},
\end{aligned} \tag{2.16}$$

in which $\boldsymbol{\sigma}^\alpha$ and $\bar{\boldsymbol{\sigma}}^\alpha$ are

$$\boldsymbol{\sigma}^\alpha = (\mathbf{I}_2, \boldsymbol{\sigma}^i) \quad \text{and} \quad \bar{\boldsymbol{\sigma}}^\alpha = (\mathbf{I}_2, -\boldsymbol{\sigma}^i), \tag{2.17}$$

and their indices are lowered with the Minkowski metric, i.e. $\boldsymbol{\sigma}_\alpha = \eta_{\alpha\beta}\boldsymbol{\sigma}^\beta$. In a similar way, we define $\boldsymbol{\tau}^\alpha$ and $\bar{\boldsymbol{\tau}}^\alpha$ from $\boldsymbol{\tau}^i$. Besides, $\check{k}^\alpha$ is a four vector given as

$$\check{k}^\alpha \equiv (k, \boldsymbol{k}), \tag{2.18}$$

JHEP07(2020)154

where $k = \sqrt{\mathbf{k}.\mathbf{k}}$. Notice that $\check{k}^\alpha$ is the four momentum of the massless field, but for the massive cases it is just a mathematical tool. It is straightforward to see that ${E^p}_s(k^\alpha)$ are eigenstates of helicity operator as well

$$\mathbf{I}_2 \otimes k^i.\boldsymbol{\sigma}_i {E^p}_s(k^\alpha) = s\ k {E^p}_s(k^\alpha)\,, \tag{2.19}$$

and satisfy the orthonormality condition

$$E^{p\dagger}_s(k^\alpha) \cdot {E^{p'}}_{s'}(k^\alpha) = \delta_{ss'}\delta^{pp'}\,. \tag{2.20}$$

The $p = +1$ elements are also eigenvectors of $\boldsymbol{\tau}^i \otimes \boldsymbol{\sigma}_i$ in eq. (B.6)

$$\boldsymbol{\tau}^i \otimes \boldsymbol{\sigma}_i {E^+}_s(k^\alpha) = {E^+}_s(k^\alpha)\,. \tag{2.21}$$

However, the $p = -1$ elements does not satisfy eigenstate equations with $\boldsymbol{\tau}^i \otimes \boldsymbol{\sigma}_i$ operator. Thus, the system is not fully, but only block diagonalizable.

The ${E^p}_s(k^\alpha)$ 4-vectors make an orthonormal basis and two copies of them define a 8×8 frame, i.e c-helicity frame. As it is implies by the form of ${E^p}_s(k^\alpha)$s, the color and spin are totally mixed in this frame. It is shown in [13] by the author that the system is decomposed into two independent subsystems. For self-sufficiency, we provide the details in appendix B.1 and here we only present the final forms. The plus subspace is made of two copies of ${E^+}_s(k^\alpha)$, and the minus subspace is made of two copies of ${E^-}_s(k^\alpha)$, i.e.

$$\tilde{\Psi}^\pm_{\mathbf{k}} = \Psi^+_{\mathbf{k}} \oplus \Psi^-_{\mathbf{k}} = \begin{pmatrix} \Psi^+_{\mathbf{k}} \\ \Psi^-_{\mathbf{k}} \end{pmatrix}, \tag{2.22}$$

such that the theory is given as

$$S[\tilde{\Psi}] = S^+[\Psi^+] + S^-[\Psi^-],$$

where $S^+[\Psi^+]$ and $S^-[\Psi^-]$ are[4]

$$S^+ = \int \mathrm{d}\tau \mathrm{d}^3k \bar{\Psi}^+_{\boldsymbol{k}} \left[i\gamma^0\partial_\tau - \gamma^3 k - \left(2\xi_\varphi - \frac{\xi_A}{2}\right)\mathcal{H}\gamma^0\gamma^5 - \mu_{\mathrm{m}}\mathcal{H}\mathrm{I}_4 \right] \Psi^+_{\boldsymbol{k}}\,, \tag{2.23}$$

$$S^- = \int \mathrm{d}\tau \mathrm{d}^3k \bar{\Psi}^-_{\boldsymbol{k}} \left[i\gamma^0\partial_\tau - \gamma^3 k - \left(2\xi_\varphi + \frac{\xi_A}{2}\right)\mathcal{H}\gamma^0\gamma^5 - \mu_{\mathrm{m}}\mathcal{H}\mathrm{I}_4 + \gamma^1\xi_A\mathcal{H} \right] \Psi^-_{\boldsymbol{k}}\,. \tag{2.24}$$

The system is reducible into two 4-Dirac spinors, Ψ^+ and Ψ^-, thanks to the isospin symmetry as well as the isotropic-homogeneous configuration of the gauge field's VEV which identifies the $su(2)$ gauge index and $so(3)$ rotation index. In particular, in case that the mass term breaks the isospin symmetry, i.e., the isospinors have different masses, the $\Psi^+_{\mathbf{k}}$ and $\Psi^-_{\mathbf{k}}$ fields would be coupled by terms proportional to the difference of the isospinor masses. Hence the reduction is not possible in the absence of the isospin symmetry.

[4]Notice that our notation in defining the c-helicity frame is slightly different than [13] so that the sign of $k\gamma^3$ term be the same in both subspaces.

JHEP07(2020)154

Our Dirac fields can be expanded as

$$\Psi^{\pm}_{\mathbf{k}} = \sum_{s=\pm} \begin{pmatrix} \psi^{\pm\uparrow}_{s}(\tau,k)\mathbf{E}_s \\ \\ s\psi^{\pm\downarrow}_{s}(\tau,k)\mathbf{E}_s \end{pmatrix}, \tag{2.25}$$

where $\psi^{\pm\uparrow}_{s}(\tau,k)$ and $\psi^{\pm\downarrow}_{s}(\tau,k)$ are mode functions and $\mathbf{E}_s$ with $s=\pm1$ are the two-spinor polarization states

$$\mathbf{E}_{+} = \begin{pmatrix} 1 \\ 0 \end{pmatrix} \quad \text{and} \quad \mathbf{E}_{-} = \begin{pmatrix} 0 \\ 1 \end{pmatrix}. \tag{2.26}$$

Note 1: the superscript $\pm$ denotes the plus/minus subspace, while the subscript $\pm$ denotes the corresponding 2d helicity polarization states, $\mathbf{E}_{\pm}$. Note 2: being already in the helicity frame for the given momentum, the 2-spinor polarization states are k-independent. As a result, the plus spinor is decoupled in terms of the polarization spinor $\mathbf{E}_s$ and it is makes two pairs of coupled field equations for each polarization. On the other hand, the minus spinor is not diagonalizable due to the extra (time dependent) term proportional to γ^1 in the action (2.24). As a result, the minus subsystem includes four coupled field equations. In the limit of either well inside the horizon, i.e. $k \gg \mathcal{H}$, or $\xi_A/\mu_{\rm m} \ll 1$, this term is negligible and the minus system approximately decoupled into two pairs of coupled field equations.

Our fermionic sector generates the fermion current and isospin current as

$$J^{\mu} = \bar{\tilde{\Psi}}\mathbf{I}_2 \otimes \gamma^{\mu}\tilde{\Psi} \quad \text{and} \quad J^{\mu a} = g_A \bar{\tilde{\Psi}}\mathbf{T}^a \otimes \gamma^{\mu}\tilde{\Psi}, \tag{2.27}$$

as well as axial current, J^{μ}_5, in eq. (2.5) and axial isospin current

$$J^{\mu a}_5 = g_A \bar{\tilde{\Psi}}\mathbf{T}^a \otimes \gamma^{\mu}\gamma^5\tilde{\Psi}. \tag{2.28}$$

Among them, $J^{\mu a}$ backreacts on the background equation of the gauge field as[5]

$$\frac{1}{3a}\delta^a_i \frac{\delta \mathcal{L}_{\rm inf}}{\delta A^a_i}\bigg|_{BG} = \mathcal{J} \equiv \frac{1}{3a}\delta^i_a \langle J^a_i \rangle\,, \tag{2.29}$$

where the left hand side is the background field equation of the SU(2) gauge field and $\mathcal{L}_{\rm inf}$ is the specific theory of the SU(2)-axion inflation model. Moreover, the axial current backreacts on the axion background equation as

$$-\frac{\delta \mathcal{L}}{\delta \varphi}\bigg|_{BG} = \beta \frac{\lambda}{2f}\nabla_{\mu}J^{\mu}_5 \equiv \mathcal{B}\,, \tag{2.30}$$

where the left hand side is the background field equation of the axion, and the $\nabla_{\mu}J^{\mu}_5$ is given as

$$\nabla_{\mu}J^{\mu}_5 = -\frac{2im}{a^3}\bar{\tilde{\Psi}}\gamma_5\tilde{\Psi} - \frac{2g^2_A}{16\pi^2}F^{a\mu\nu}\tilde{F}_{a\mu\nu}\,. \tag{2.31}$$

In the right-hand side, the first term is the tree-level effect of explicite breaking of the chiral symmetry by the mass term, while the second term is the loop effect due to the well-known chiral (Adler-Bell-Jackiw) anomaly [30, 31].

[5]For the explicit form of the background equations in different realizations of SU(2)-axion inflationary models see section 2 of [12].

JHEP07(2020)154

3 Non-trivial vacuum structure and fermions

To gain more insight on the nature of our dark fermions and capture some of the novel aspects of the vacuum, here we explore the action of the discrete symmetries C, P and CP, as well as the continuous chiral symmetry on fermions. Here, just by using the symmetry structure of the system, we extract the general features of the observable quantities. Later in section 6, we explicitly compute these quantities and confirm this qualitative analysis. The chiral charge and the fermion backreaction to the background gauge field equation, eqs. (2.5) and (2.29), in the Weyl frame can be written as[6]

$$Q_5 \equiv \langle a J_5^0 \rangle = Q_R - Q_L, \tag{3.1}$$

$$\mathcal{J} = \frac{1}{3a}\delta_a^i \langle J_{iL}^a + J_{iR}^a \rangle, \tag{3.2}$$

in which the R/L subscription denotes the contribution of the right-/left-handed fields to that quantity. The net fermion number eq. (2.27) is given as

$$Q \equiv \langle a J^0 \rangle = Q_R + Q_L, \tag{3.3}$$

and the axial isospin current can be written as

$$J_5^{\mu a} = J_R^{\mu a} - J_L^{\mu a}. \tag{3.4}$$

The left- and right-handed isospin currents are

$$J_L^{\mu a} \equiv g_A \Psi_L^\dagger \mathbf{T}^a \otimes \bar{\boldsymbol{\sigma}}^\mu \Psi_L \quad \text{and} \quad J_R^{\mu a} \equiv g_A \Psi_R^\dagger \mathbf{T}^a \otimes \boldsymbol{\sigma}^\mu \Psi_R. \tag{3.5}$$

3.1 C-symmetry, P- and CP-violation

As showed in eq. (C.1), our fermion theory in eq. (2.13) is invariant under the action of the charge conjugation operator, $\tilde{C}$, defined as

$$\tilde{C} = \mathbf{I}_2 \otimes C \quad \text{where} \quad C = i\gamma^2\gamma^0. \tag{3.6}$$

In other words, both $\tilde{\Psi}$, and its charge conjugated field

$$\tilde{\Psi}_c \equiv \tilde{C}\bar{\tilde{\Psi}},$$

obey the same theory (see eq. (C.8)) and the theory is C-symmetric. The 4×4 operator C is the charge conjugation operator of each plus and minus subsystems.

However, parity is different since both φ (axion) and ψ (the effective field value of the SU(2) gauge field) in eqs. (2.7) and (2.8), are pseudo-scalars. As a result, parity is spontaneously broken in the action (2.13). Under the action of parity, this theory goes to its parity conjugate with (see figure 3)

$$\xi_A \xrightarrow{P} -\xi_A \quad \text{and} \quad \xi_\varphi \xrightarrow{P} -\xi_\varphi. \tag{3.7}$$

[6] Notice that the chiral charge is defined in terms of $J_5^t = \frac{\partial t}{\partial \tau} J_5^0$ which justifies the extra factor of a inside the integral eq. (3.1).

JHEP07(2020)154

As a result, both P and CP are spontaneously broken by the vacuum of the SU(2)-axion, i.e., the vacuum is CP-violating with non-vanishing $\tilde{R}R$ and $F\tilde{F}$ [14, 23]. Violation of CP is the essential condition in any matter-antimatter asymmetric scenario. Then the out of thermal equilibrium state which is guaranteed by inflation ensures that the production of matter by one mechanism is not immediately compensated by its disappearance through the inverse reaction. This robust aspect of SU(2)-axion models make them natural settings for inflationary leptogenesis [14, 23]. In the current fermionic sector with C-symmetry and CP-violation, we expect a vanishing net fermion number, $J^0 = 0$ and a non-zero chiral charge, $J_5^0 \neq 0$ which will be confirmed by the exact computation in section 6. There we will show that both $\mathcal{J}$ and Q_5 are directly proportional to the sources of the CP-violation, i.e., ξ_A and ξ_φ.

3.2 Chiral anomaly and conserved currents

In the massless limit, the fermionic sector enjoys the chiral symmetry in the classical level under the unitary chiral transformation

$$\tilde{\Psi} \to e^{i\alpha^a(x)\mathbf{t}_a\otimes\gamma_5}\ \tilde{\Psi}, \tag{3.8}$$

where $\mathbf{t}_a$ is the isospin matrix (equals to $\mathbf{T}_a$ for isospin doublet and $\mathbf{I}_2$ for isospin singlet), and $\alpha^a(x)$ is the parameter of the transformation. All four fermionic currents are classically conserved under the above unitary transformation. At the quantum level, the left- and right-handed isospin currents in eq. (3.5) satisfy the following equalities by the non-Abelian chiral anomaly

$$D_\mu J^{\mu a}_{L,R} = \pm\frac{g_A^2}{24\pi^2}\nabla_\mu\left(\epsilon^{\mu\nu\lambda\sigma}\mathrm{tr}\left[\boldsymbol{T}^a\left(A_\nu\partial_\lambda A_\sigma - \frac{g_A}{2}A_\nu A_\lambda A_\sigma\right)\right]\right), \tag{3.9}$$

which implies that the (vector) isospin current satisfies

$$D_\mu J^{\mu a} = 0, \tag{3.10}$$

and the axial isospin current satisfies

$$D_\mu J_5^{\mu a} = -\frac{g_A^2}{12\pi^2}\nabla_\mu\left(\epsilon^{\mu\nu\lambda\sigma}\mathrm{tr}\left[\boldsymbol{T}^a\left(A_\nu\partial_\lambda A_\sigma - \frac{g_A}{2}A_\nu A_\lambda A_\sigma\right)\right]\right). \tag{3.11}$$

Thus, the fermion vector current and isospin current remain anomaly free at the quantum level. In particular, eq. (3.10) consistency condition for the gauge theory [32]. However, the axial vector and axial isospin currents receives corrections according to the Adler-Bell-Jackiw anomaly [30, 31] respectively as

$$\nabla_\mu J_5^\mu = -\frac{g_A^2}{16\pi^2}\epsilon^{\mu\nu\lambda\sigma}F^b_{\mu\nu}F^c_{\lambda\sigma}\mathrm{tr}\big[\{\mathbf{T}_b,\mathbf{T}_c\}\big] = -\frac{2g_A^2}{16\pi^2}F\tilde{F}, \tag{3.12}$$

and the chiral isospin current anomaly in eq. (3.11) can be written as

$$D_\mu J_5^{\mu a} = -\frac{g_A^2}{16\pi^2}\epsilon^{\mu\nu\lambda\sigma}F^b_{\mu\nu}F^c_{\lambda\sigma}\mathrm{tr}\big[\mathbf{T}_a\{\mathbf{T}_b,\mathbf{T}_c\}\big] = 0. \tag{3.13}$$

JHEP07(2020)154

Therefore, in this setup the axial isospin current is not affected by the chiral anomaly and remains conserved.

In the zero mass limit, the only fermionic effect is the Abelian chiral anomaly in eq. (3.12), $\frac{g_A^2}{16\pi^2}F\tilde{F}$ which backreacts to the axion field as well as the spatial component of the chiral isospin current, $J_5^{ai} \simeq \frac{g_A^2}{6\pi^2}\psi^2 H = \frac{\xi_A^2}{6\pi^2}H^3$. Massive fermions, however, break chiral symmetry explicitly and have non-zero $\mathcal{J}$ as well. Recalling (3.2), it should be directly proportional to the mass of the fermions, i.e.

$$\mathcal{J} \propto \mu_{\rm m}, \tag{3.14}$$

since $\mu_{\rm m} = \frac{m}{H}$ quantifies the deviation from chiral symmetry.

4 Fermions in SU(2)-axion inflation

Now we turn to solve the field equations and find $\Psi_{\boldsymbol{k}}^{\pm}$ specified by the actions in the eqs. (2.23) and (2.24). The $\Psi_{\boldsymbol{k}}^{p}$ spinors with $p = \pm 1$ can be decomposed as

$$\Psi_{\boldsymbol{k}}^{p} = \sum_{s=\pm}\left[U_{s,\mathbf{k}}^{p}(\tau)a_{s,\boldsymbol{k}}^{p} + V_{s,-\mathbf{k}}^{p}(\tau)b_{s,-\boldsymbol{k}}^{p\dagger}\right], \tag{4.1}$$

where $a_{s,\boldsymbol{k}}^{p}$ and $b_{s,\boldsymbol{k}}^{p}$ are creation and annihilation operators obey

$$\{a_{s,\boldsymbol{k}}^{p}, a_{s',\boldsymbol{k}'}^{p\dagger}\} = \delta_{ss'}\delta^{(3)}(\boldsymbol{k}-\boldsymbol{k}') \quad \text{and} \quad \{b_{s,\boldsymbol{k}}^{p}, b_{s',\boldsymbol{k}'}^{p\dagger}\} = \delta_{ss'}\delta^{(3)}(\boldsymbol{k}-\boldsymbol{k}')\,. \tag{4.2}$$

Note that the superscript $p = \pm$ denotes the plus/minus subspace, while the subscript $s = \pm$ denotes the corresponding 2d helicity polarization states, $\mathbf{E}_{\pm}$. Moreover, the charge conjugation relates the field to its charge conjugated field as (see section C.1)

$$\Psi_{C\mathbf{k}}^{p} = i\gamma^2\Psi_{-\mathbf{k}}^{p*}, \tag{4.3}$$

which gives

$$V_{s,\mathbf{k}}^{p} = i\gamma^2 U_{s,\mathbf{k}}^{p*}. \tag{4.4}$$

The 4-spinor fields, $\Psi_{\boldsymbol{k}}^{p}$, are govern by first order differential equations. Therefore, they are each made of four linearly independent solutions. We will solve them by setting the Bunch-Davies vacuum as the initial condition for the fields

$$\lim_{\tau\to-\infty} U_{s,\mathbf{k}}^{p}(\tau) = \frac{e^{-ik\tau}}{(2\pi)^3}\begin{pmatrix}\mathbf{E}_s\\ s\mathbf{E}_s\end{pmatrix}. \tag{4.5}$$

Here, we define the rescaled physical momentum as

$$\tilde{\tau} \equiv \frac{k}{aH} = -k\tau. \tag{4.6}$$

Since the plus and minus spinors are decoupled, we study them individually.

JHEP07(2020)154

4.1 Ψ^+ fermions

As we discussed in section 2.1, the $\Psi^+_{\mathbf{k}}$ spinors are defined to be diagonalizable in terms of the c-helicity. The $\Psi^+_{\boldsymbol{k}}$ spinors are described by the linear differential equation specified by the action (2.23). Therefore, $U^+_{s,\mathbf{k}}(\tau)$ and $V^+_{s,\mathbf{k}}(\tau)$ in eq. (4.1) can be decomposed in terms of the 2d helicity polarization states, $\mathbf{E}_\pm$, defined in eq. (1.3) as

$$U^+_{s,\mathbf{k}}(\tau)=\frac{1}{\sqrt{2}}\begin{pmatrix}\mathbf{E}_s u^{\uparrow}_s(k,\tau)\\ s\mathbf{E}_s u^{\downarrow}_s(k,\tau)\end{pmatrix}\quad\text{and}\quad V^+_{s,-\mathbf{k}}(\tau)=\frac{1}{\sqrt{2}}\begin{pmatrix}\mathbf{E}_s v^{\uparrow}_s(k,\tau)\\ s\mathbf{E}_s v^{\downarrow}_s(k,\tau)\end{pmatrix}. \tag{4.7}$$

Moreover, using eq. (4.4), we can read $V^+_{s,-\mathbf{k}}(\tau)$ as

$$V^+_{s,-\mathbf{k}}(\tau)=-\frac{1}{\sqrt{2}}\begin{pmatrix}\mathbf{E}_s u^{\downarrow *}_{-s}(k,\tau)\\ s\mathbf{E}_s u^{\uparrow *}_{-s}(k,\tau)\end{pmatrix}. \tag{4.8}$$

Using (4.7) in the action (2.23), we arrive at two sets of coupled field equations for $u^{\uparrow}_s$ and $u^{\downarrow}_s$ as

$$(i\partial_\tau-\mu_{\rm m}\mathcal{H})u^{\uparrow}_s-\left[k+s\left(2\xi_\varphi-\frac{\xi_A}{2}\right)\mathcal{H}\right]u^{\downarrow}_s=0\,, \tag{4.9}$$

$$(i\partial_\tau+\mu_{\rm m}\mathcal{H})u^{\downarrow}_s-\left[k+s\left(2\xi_\varphi-\frac{\xi_A}{2}\right)\mathcal{H}\right]u^{\uparrow}_s=0\,. \tag{4.10}$$

The above coupled set of equations can be decoupled in terms of the following decomposition

$$u^{\uparrow}_s=\frac{1}{\sqrt{2\tilde\tau}}\left(Y_s+Z_s\right)\quad\text{and}\quad u^{\downarrow}_s=\frac{1}{\sqrt{2\tilde\tau}}\left(Y_s-Z_s\right). \tag{4.11}$$

The coupled set of first order differential equations (4.9) and (4.10) can be decoupled into two second order differential equations for Y_s and Z_s as

$$\partial^2_{\tilde\tau}Y_s+\left[1-\frac{2i\kappa^+_s}{\tilde\tau}+\frac{1/4-(\mu^+)^2}{\tilde\tau^2}\right]Y_s=0\,, \tag{4.12}$$

$$\partial^2_{\tilde\tau}Z_s+\left[1-\frac{2i\tilde\kappa^+_s}{\tilde\tau}+\frac{1/4-(\mu^+)^2}{\tilde\tau^2}\right]Z_s=0\,, \tag{4.13}$$

where κ^+_s, and $\tilde\kappa^+_s$ are

$$\kappa^+_s=\frac{1}{2}+is\left(2\xi_\varphi-\frac{\xi_A}{2}\right)\quad\text{and}\quad\tilde\kappa^+_s=-\frac{1}{2}+is\left(2\xi_\varphi-\frac{\xi_A}{2}\right), \tag{4.14}$$

and μ^+ is

$$\mu^+=i\left[\mu^2_{\rm m}+\left(2\xi_\varphi-\frac{\xi_A}{2}\right)^2\right]^{\frac{1}{2}}. \tag{4.15}$$

The general solutions for eqs. (4.12) and (4.13) are W and M Whittaker functions. Setting the Bunch-Davies vacuum as the initial condition for $u^{\uparrow}_s$ and $u^{\downarrow}_s$ and using eqs. (A.9) and (A.10), we find Y_s and Z_s as

$$\begin{aligned}Y_s&=\frac{1}{(2\pi)^{\frac{3}{2}}}e^{s(\xi_A/4-\xi_\varphi)\pi}W_{\kappa^+_s,\mu^+}(-2i\tilde\tau),\\ Z_s&=-\frac{i\mu_{\rm m}}{(2\pi)^{\frac{3}{2}}}e^{s(\xi_A/4-\xi_\varphi)\pi}W_{\tilde\kappa^+_s,\mu^+}(-2i\tilde\tau).\end{aligned} \tag{4.16}$$

JHEP07(2020)154

4.2 Ψ^- fermions

Next, we turn to $\Psi^-_{\boldsymbol{k}}$ modes, described by the action (2.24). The theory of the minus subspace is not diagonalizable in a time independent frame. Hence, the helicity eigenstates are only the eigenstates of the Lagrangian in the asymptotic past limit. Therefore, we use the ansatz

$$U^-_{s,k}(\tau) = \frac{1}{\sqrt{2}}\begin{pmatrix}\mathbf{E}_s u^{\uparrow}_{s,+}(k,\tau)\\ s\mathbf{E}_s u^{\downarrow}_{s,+}(k,\tau)\end{pmatrix} + \frac{1}{\sqrt{2}}\begin{pmatrix}\mathbf{E}_{-s} u^{\uparrow}_{s,-}(k,\tau)\\ -s\mathbf{E}_{-s} u^{\downarrow}_{s,-}(k,\tau)\end{pmatrix}, \tag{4.17}$$

where $\mathbf{E}_s$ are the 2-spinor polarization states defined in eq. (1.3). Since in the asymptotic past limit the system is diagonalized in this particular basis, we have

$$\lim_{\tilde\tau\to\infty} u^{\uparrow}_{s,-}(k\tau) = \lim_{\tilde\tau\to\infty} u^{\downarrow}_{s,-}(k\tau) = 0. \tag{4.18}$$

Moreover, using the charge conjugation relation, we can read $V^-_{s,-\mathbf{k}}(\tau)$ as

$$V^-_{s,k}(\tau) = -\frac{1}{\sqrt{2}}\begin{pmatrix}\mathbf{E}_s u^{\downarrow *}_{-s,+}(k,\tau)\\ s\mathbf{E}_s u^{\uparrow *}_{-s,+}(k,\tau)\end{pmatrix} - \frac{1}{\sqrt{2}}\begin{pmatrix}\mathbf{E}_{-s} u^{\downarrow *}_{-s,-}(k,\tau)\\ -s\mathbf{E}_{-s} u^{\uparrow *}_{-s,-}(k,\tau)\end{pmatrix}. \tag{4.19}$$

Using the ansatz eq. (4.17) in the action (2.24), we arrive at the field equations below

$$(i\partial_\tau - \mu_{\rm m}\mathcal{H})u^{\uparrow}_{s,s'} - \left[k + ss'\left(2\xi_\varphi + \frac{\xi_A}{2}\right)\mathcal{H}\right]u^{\downarrow}_{s,s'} - ss'\xi_A\mathcal{H}u^{\downarrow}_{s,-s'} = 0\,, \tag{4.20}$$

$$(i\partial_\tau + \mu_{\rm m}\mathcal{H})u^{\downarrow}_{s,s'} - \left[k + ss'\left(2\xi_\varphi + \frac{\xi_A}{2}\right)\mathcal{H}\right]u^{\uparrow}_{s,s'} + ss'\xi_A\mathcal{H}u^{\uparrow}_{s,-s'} = 0\,. \tag{4.21}$$

Note that for each given s and s', the equations with $s' = +$ and $s' = -$ are coupled. We make the decompositions

$$u^{\uparrow}_{s,s'} = \frac{1}{\sqrt{2\tilde\tau}}\left(Y_{s,s'} + Z_{s,s'}\right) \quad \text{and} \quad u^{\downarrow}_{s,s'} = \frac{1}{\sqrt{2\tilde\tau}}\left(Y_{s,s'} - Z_{s,s'}\right), \tag{4.22}$$

which gives

$$\begin{aligned} &i\partial_{\tilde\tau}Y_{s,s'} + \left[1 + \frac{ss'(4\xi_\varphi+\xi_A) - i}{2\tilde\tau}\right]Y_{s,s'} + \frac{\mu_{\rm m}}{\tilde\tau}Z_{s,s'} - \frac{ss'\xi_A}{\tilde\tau}Z_{s,-s'} = 0\,,\\ &i\partial_{\tilde\tau}Z_{s,s'} - \left[1 + \frac{ss'(4\xi_\varphi+\xi_A) + i}{2\tilde\tau}\right]Z_{s,s'} + \frac{\mu_{\rm m}}{\tilde\tau}Y_{s,s'} + \frac{sp\xi_A}{\tilde\tau}Y_{s,-s'} = 0\,. \end{aligned} \tag{4.23}$$

We can reduce the above coupled first order equations to pairs of coupled second order equations

$$\begin{aligned} &\partial^2_{\tilde\tau}Y_{s,s'} + \left[1 - \frac{2is'[\kappa^-_s + \frac{1}{2}(s'-1)]}{\tilde\tau} + \frac{1/4-(\mu^-)^2}{\tilde\tau^2}\right]Y_{s,s'} - \frac{2\xi_A(2\xi_\varphi+\xi_A/2)}{\tilde\tau^2}Z_{s,-s'} = 0\,,\\ &\partial^2_{\tilde\tau}Z_{s,s'} + \left[1 - \frac{2is'[\tilde\kappa^-_s - \frac{1}{2}(s'-1)]}{\tilde\tau} + \frac{1/4-(\mu^-)^2}{\tilde\tau^2}\right]Z_{s,s'} - \frac{2\xi_A(2\xi_\varphi+\xi_A/2)}{\tilde\tau^2}Y_{s,-s'} = 0\,, \end{aligned} \tag{4.24}$$

where κ^-_s, and $\tilde\kappa^-_s$ are

$$\kappa^-_s = \frac{1}{2} + is\left(2\xi_\varphi + \frac{\xi_A}{2}\right) \quad \text{and} \quad \tilde\kappa^-_s = -\frac{1}{2} + is\left(2\xi_\varphi + \frac{\xi_A}{2}\right), \tag{4.25}$$

JHEP07(2020)154

while μ^- is

$$\mu^- = i\left[\mu_{\rm m}^2 + \left(2\xi_\varphi + \frac{\xi_A}{2}\right)^2 + \xi_A^2\right]^{\frac{1}{2}}. \tag{4.26}$$

Unlike the plus spinors, the set of equations in minus system is still coupled and cannot be solved analytically. However, since the coupling term becomes relevant around and after horizon crossing, it is possible to solve the system analytically in the limit that the coupling is negligible, i.e. $k\tau \gg 1$ and/or $\xi_A/\mu_{\rm m} \ll 1$. More precisely, we can decompose the fields as[7]

$$\begin{aligned} Y_{s,+}(\tilde\tau) &= y_{s,+}(\tilde\tau)Y_s(\tilde\tau) \qquad \text{and} \qquad Y_{s,-}(\tilde\tau) = y_{s,-}(\tilde\tau)Y_{-s}(\tilde\tau), \\ Z_{s,+}(\tilde\tau) &= z_{s,+}(\tilde\tau)Z_s(\tilde\tau) \qquad \text{and} \qquad Z_{s,-}(\tilde\tau) = -\frac{s\xi_A}{\mu_{\rm m}} z_{s,-}(\tilde\tau)Z_{-s}(\tilde\tau), \end{aligned} \tag{4.27}$$

where Y_s, and Z_s are analytically solvable while the other four functions, $y_{s,p}(\tilde\tau)$ and $z_{s,p}(\tilde\tau)$, should be solved numerically. In the asymptotic past, we have

$$\lim_{\tilde\tau\to\infty} y_{s,+}(\tilde\tau) = 1 \tag{4.28}$$

$$\lim_{\tilde\tau\to\infty} z_{s,+}(\tilde\tau) = 1, \tag{4.29}$$

$$\lim_{\tilde\tau\to\infty} y_{s,-}(\tilde\tau) = 0, \tag{4.30}$$

and $z_{s,-}(\tilde\tau)$ up to a phase, $(2\tilde\tau_0)^{2is\kappa_I}$, is

$$\lim_{\tilde\tau\to\infty} z_{s,-}(\tilde\tau) = 1. \tag{4.31}$$

Notice that at $\tilde\tau \to \infty$, $Z_s(\tilde\tau) \sim \tilde\tau^{-1}Y_s(\tilde\tau)$ (see eq. (4.33)). The fields Y_s and Z_s satisfy

$$\begin{aligned} \partial_{\tilde\tau}^2 Y_s + \left[1 - \frac{2i\kappa_s^-}{\tilde\tau} + \frac{1/4-\mu_-^2}{\tilde\tau^2}\right] Y_s = 0\,, \\ \partial_{\tilde\tau}^2 Z_s + \left[1 - \frac{2i\tilde\kappa_s^-}{\tilde\tau} + \frac{1/4-\mu_-^2}{\tilde\tau^2}\right] Z_s = 0\,. \end{aligned} \tag{4.32}$$

The above differential equations can be solved analytically in terms of Whittaker functions and setting the Bunch-Davies vacuum as the initial condition for $u_{s,+}^{\uparrow}$ and $u_{s,+}^{\downarrow}$, Y_s and Z_s are given as

$$Y_s = e^{-s(\xi_A/4+\xi_\varphi)\pi} W_{\kappa_s^-,\mu^-}(-2i\tilde\tau) \quad \text{and} \quad Z_s = -i\mu_{\rm m} e^{-s(\xi_A/4+\xi_\varphi)\pi} W_{\tilde\kappa_s^-,\mu^-}(-2i\tilde\tau). \tag{4.33}$$

Next, using the ansatz eq. (4.27), as well as the first order differential equations of Y_s and Z_s in eq. (4.23), we find a set of coupled first order differential equations for $y_{s,s'}$ and $z_{s,s'}$. Given the analytical forms of Y_s and Z_s in eq. (4.33) and the initial condition eqs. (4.28)–(4.31), we solve the above coupled linear differential equations numerically. The results are presented in section 5.2 (figures 8–15). In order to have a better insightful vision of the minus subsystem, next we discuss the qualitative behavior of $\Psi_{\mathbf{k}}^-$ and the $y_{s,s'}$ and $z_{s,s'}$ functions.

[7] The prefactor $-\frac{s\xi_A}{\mu_{\rm m}}$ of $Z_{s,-}(\tilde\tau)$ in eq. (4.27) is chosen such that the initial value of $z_{s,-}$ is one.

JHEP07(2020)154

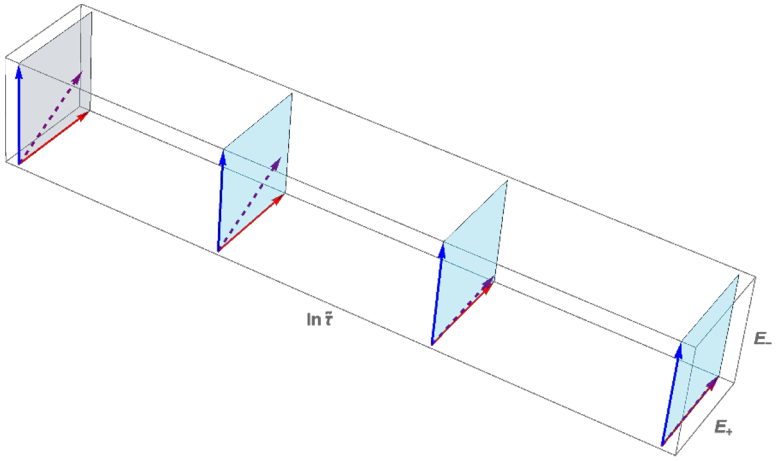

Figure 4. Schematic time evolution of the Ψ^- polarization states, $\mathbf{E}^Y_+(\tilde{\tau})$ (and $\mathbf{E}^Z_+(\tilde{\tau})$). The (purple) dashed vectors show $\mathbf{E}^Y_+(\tilde{\tau})$ (and $\mathbf{E}^Z_+(\tilde{\tau})$) while the helicity polarization vectors, $\mathbf{E}_+$ and $\mathbf{E}_-$ are shown in red and blue respectively. The direction of time is from right to left, and the gray plane presents the horizon crossing, i.e. $\tilde{\tau} = 1$.

Geometry of the minus subspace. Unlike the plus subspace, helicity is not a good quantum number in the minus subspace. That is because of the off-diagonal term proportional to ξ_A in its action in eq. (2.24). Therefore, although both Ψ^+ and Ψ^- spinors have similar asymptotic past limits, but the more minus spinors are stretched and approach the horizon, the more they experience the off diagonal time-dependent term. As a result, a minus fermion with a given initial polarization state $\mathbf{E}_s$, gradually rotates in the helicity space and turns to a mixed state of $\mathbf{E}_s$ and $\mathbf{E}_{-s}$, i.e.

$$Y_s(\tilde{\tau}) \begin{pmatrix} \mathbf{E}_s \\ s\mathbf{E}_s \end{pmatrix} \longrightarrow \left(|Y_{s,+}(\tilde{\tau})|^2 + |Z_{s,-}(\tilde{\tau})|^2\right)^{\frac{1}{2}} \begin{pmatrix} \mathbf{E}^{\mathrm{Y}}_s(\tilde{\tau}) \\ s\mathbf{E}^{\mathrm{Y}}_s(\tilde{\tau}) \end{pmatrix}, \tag{4.34}$$

$$Z_s(\tilde{\tau}) \begin{pmatrix} \mathbf{E}_s \\ -s\mathbf{E}_s \end{pmatrix} \longrightarrow \left(|Z_{s,+}(\tilde{\tau})|^2 + |Y_{s,-}(\tilde{\tau})|^2\right)^{\frac{1}{2}} \begin{pmatrix} \mathbf{E}^{\mathrm{Z}}_s(\tilde{\tau}) \\ -s\mathbf{E}^{\mathrm{Z}}_s(\tilde{\tau}) \end{pmatrix}, \tag{4.35}$$

where the time dependent polarization states, $\mathbf{E}^{\mathrm{Y}}_s(\tilde{\tau})$ and $\mathbf{E}^{\mathrm{Z}}_s(\tilde{\tau})$, can be read off in terms of the helicity eigenstates, $\mathbf{E}_\pm$, as

$$\mathbf{E}^{\mathrm{Y}}_s(\tilde{\tau}) = \frac{Y_{s,+}(\tilde{\tau})}{\left(|Y_{s,+}(\tilde{\tau})|^2 + |Z_{s,-}(\tilde{\tau})|^2\right)^{\frac{1}{2}}}\mathbf{E}_s + \frac{Z_{s,-}(\tilde{\tau})}{\left(|Y_{s,+}(\tilde{\tau})|^2 + |Z_{s,-}(\tilde{\tau})|^2\right)^{\frac{1}{2}}}\mathbf{E}_{-s}, \tag{4.36}$$

$$\mathbf{E}^{\mathrm{Z}}_s(\tilde{\tau}) = \frac{Z_{s,+}(\tilde{\tau})}{\left(|Z_{s,+}(\tilde{\tau})|^2 + |Y_{s,-}(\tilde{\tau})|^2\right)^{\frac{1}{2}}}\mathbf{E}_s + \frac{Y_{s,-}(\tilde{\tau})}{\left(|Z_{s,+}(\tilde{\tau})|^2 + |Y_{s,-}(\tilde{\tau})|^2\right)^{\frac{1}{2}}}\mathbf{E}_{-s}. \tag{4.37}$$

All $\mathbf{E}^Y_s(\tilde{\tau})$ and $\mathbf{E}^Z_s(\tilde{\tau})$ polarization states start from $\mathbf{E}_s$ at asymptotic past. Then, around and at horizon crossing, they make most of their rotation in the $\mathbf{E}_+ - \mathbf{E}_-$ plane. Here, for more insight, figure 4 shows schematic rotation of $\mathbf{E}^Y_+(\tilde{\tau})$ (and $\mathbf{E}^Z_+(\tilde{\tau})$) in $\mathbf{E}_+ - \mathbf{E}_-$ plane.

JHEP07(2020)154

Before going any further and numerically solve the minus subsystem in section 5.2 (figures 8–15), let us discuss the qualitative behavior of these functions.

- The $y_{s,+}(\tilde{\tau})$, and $z_{s,+}(\tilde{\tau})$ start from one at asymptotic past and after a fast transition phase each reduces to another constant number after horizon crossing, i.e. y_{0s+} and z_{0s+}. Their behavior can be roughly described as $\big(\tanh[\alpha_s\tilde{\tau}-\tilde{\tau}_{0s}]+\beta_s\big)/(1+\beta_s)$ with $\tilde{\tau}_{0s}\gtrsim 1$, $\alpha_s\lesssim 1$, while for $y_{s,+}(\tilde{\tau})$ we have $\beta_s=\frac{1+y_{0s+}}{1-y_{0s+}}$, and for $z_{s,+}(\tilde{\tau})$ we get $\beta_s=\frac{1+z_{0s+}}{1-z_{0s+}}$.
- The $y_{s,-}(\tilde{\tau})$ starts from zero at asymptotic past and after a quick transition phase increases to a constant number less than one after horizon crossing, i.e. y_{0s-}. Its behavior can be roughly described by $\frac{1}{2}y_{0s-}\big(-\tanh[\alpha_s\tilde{\tau}-\tilde{\tau}_{0s}]+1\big)$ with $y_{0s-}\lesssim 1$.
- The $z_{s,-}(\tilde{\tau})$ starts from one at asymptotic past and after horizon crossing approach a constant value either less or more (but of the order of) one. Yet it also follows a tanh-type behavior.

5 Mode functions, a closer look

In this part, first, we discuss the generic features of the analytical solutions Y_s and Z_s, which are in common between the plus and minus subsystems. Next, we present the numerical study of the four functions, $y_{s,p}$ and $z_{s,p}$, which we introduced in the minus subspace to take care of the rotation of its mode functions in the helicity plane.

5.1 $\Psi^{\pm}$ spinors: Y_s and Z_s

Here, we consider Y_s and Z_s mode functions which are in common between the plus and minus sub-sectors. In fact, in both subsystems, μ is pure imaginary, i.e. (see eqs. (4.15) and (4.26))

$$\mu^{\pm}=i|\mu^{\pm}|, \tag{5.1}$$

while $\kappa_s^{\pm}$ and $\tilde{\kappa}_s^{\pm}$ in eqs. (4.14) and (4.25), can be written as

$$\kappa_s^{\pm}=\frac{1}{2}+is\kappa_I^{\pm}\quad\text{and}\quad\tilde{\kappa}_s^{\pm}=-\frac{1}{2}+is\kappa_I^{\pm}, \tag{5.2}$$

where $\kappa_I^{\pm}$ is the absolute value of the imaginary parts of $\kappa_s^{\pm}$ (and $\tilde{\kappa}_s^{\pm}$) and $\mu^{\pm}$ can be decomposed as

$$\mu^{\pm}=i\left[(m_{\rm eff}^{\pm})^2+(\kappa_I^{\pm})^2\right]^{\frac{1}{2}}, \tag{5.3}$$

where $m_{\rm eff}^{\pm}$ is

$$m_{\rm eff}^{+}=\mu_m\quad\text{and}\quad m_{\rm eff}^{-}=(\mu_m^2+\xi_A^2)^{\frac{1}{2}}. \tag{5.4}$$

Here, $|\mu^{\pm}|$, $m_{\rm eff}^{\pm}$, and $\kappa_I^{\pm}$ are real parameters in terms of ξ_A, ξ_φ, and $\frac{m}{H}$. As a result, we can present the analytical solutions in both subspaces, eqs. (4.16) and (4.33), in a unified form and in terms of three independent parameters, ξ_A, κ_I, and $m_{\rm eff}$ as

$$\begin{aligned}Y_s(\tilde{\tau})&=\frac{1}{(2\pi)^{\frac{3}{2}}}e^{-s\kappa_I\pi/2}W_{\frac{1}{2}+is\kappa_I,\mu}(-2i\tilde{\tau}),\\ Z_s(\tilde{\tau})&=-\frac{i\mu_{\rm m}}{(2\pi)^{\frac{3}{2}}}e^{-s\kappa_I\pi/2}W_{-\frac{1}{2}+is\kappa_I,\mu}(-2i\tilde{\tau}).\end{aligned} \tag{5.5}$$

JHEP07(2020)154

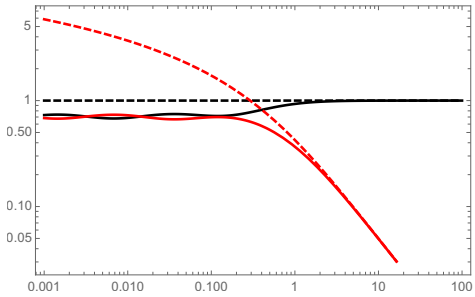

Figure 5. The evolution of absolute values of $(2\pi)^{\frac{3}{2}}\frac{Y_{\pm}(\tilde{\tau})}{\sqrt{2\tilde{\tau}}}$ (black) and $(2\pi)^{\frac{3}{2}}\frac{Z_{\pm}(\tilde{\tau})}{\sqrt{2\tilde{\tau}}}$ (red) for trivial vacuum with $\kappa_I = 0$ with respect to $\tilde{\tau}$. The dashed lines shows $\mu_m = 0$, and the solid lines presents $\mu_m = 1$.

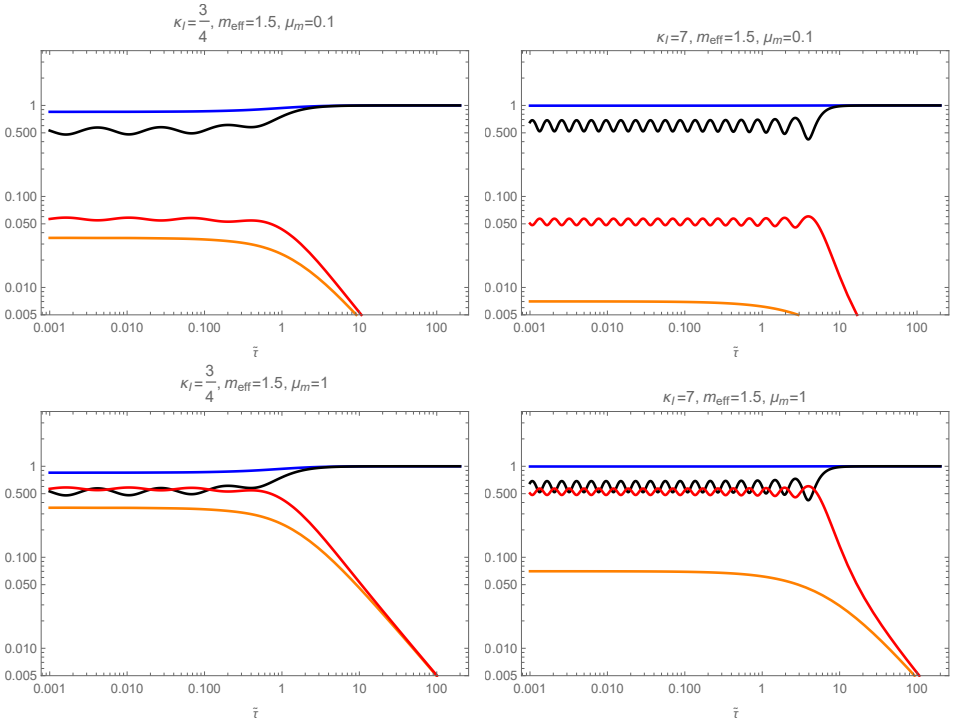

Figure 6. The evolution of absolute values of $(2\pi)^{\frac{3}{2}}\frac{Y_{\pm}(\tilde{\tau})}{\sqrt{2\tilde{\tau}}}$ and $(2\pi)^{\frac{3}{2}}\frac{Z_{\pm}(\tilde{\tau})}{\sqrt{2\tilde{\tau}}}$ with respect to $\tilde{\tau}$ for different values of κ_I, $m_{\rm eff}$, and μ_m. The blue shows $(2\pi)^{\frac{3}{2}}\frac{Y_{+}(\tilde{\tau})}{\sqrt{2\tilde{\tau}}}$, orange is $(2\pi)^{\frac{3}{2}}\frac{Z_{+}(\tilde{\tau})}{\sqrt{2\tilde{\tau}}}$, black is $(2\pi)^{\frac{3}{2}}\frac{Y_{-}(\tilde{\tau})}{\sqrt{2\tilde{\tau}}}$, and red shows $(2\pi)^{\frac{3}{2}}\frac{Z_{-}(\tilde{\tau})}{\sqrt{2\tilde{\tau}}}$.

Figure 5 shows the mode functions for trivial vacuum with $\kappa_I = 0$. As we see, in the absence of the source of CP violation, the mode functions are parity symmetric and their after horizon amplitude decreases with the mass of the fermion. In figure 6, we present $\frac{Y_s}{\sqrt{x}}$ and $\frac{Z_s}{\sqrt{x}}$ with $s = \pm$ in terms of $\tilde{\tau}$ for several values of parameters. Moreover, figure 7 shows the same quantities as well as $\frac{Y_+(\tilde{\tau})-Z_-(\tilde{\tau})}{\sqrt{2\tilde{\tau}}}$ and $\frac{Y_-(\tilde{\tau})-Z_+(\tilde{\tau})}{\sqrt{2\tilde{\tau}}}$ in the large mass limit.

JHEP07(2020)154

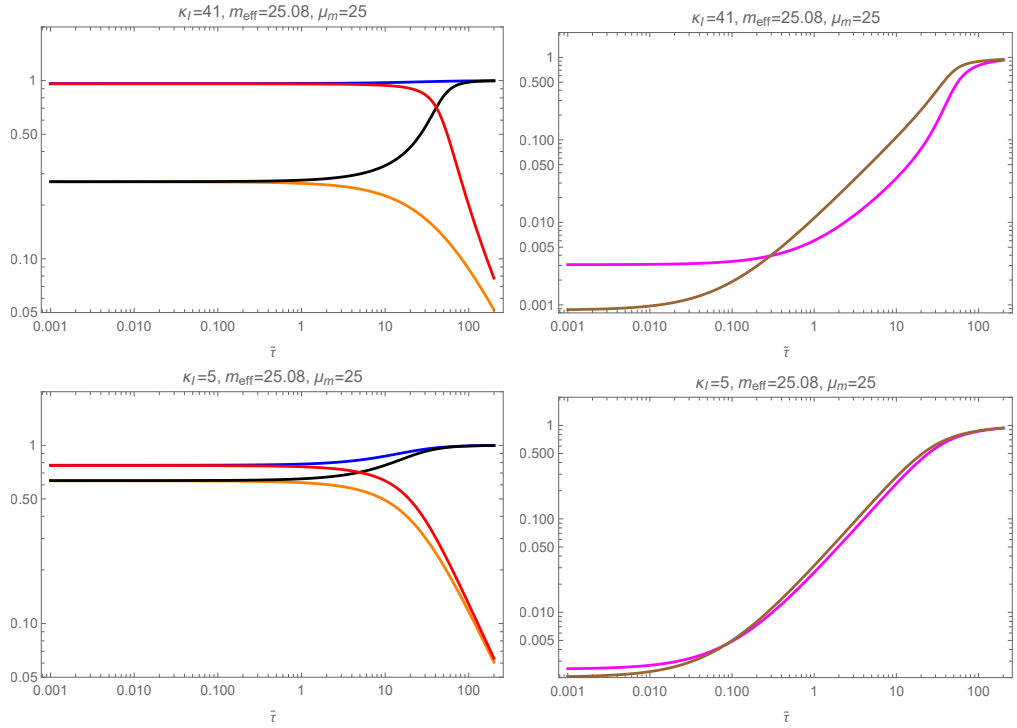

Figure 7. Large mass limit behavior of $(2\pi)^{\frac{3}{2}}\frac{Y_{\pm}(\tilde{\tau})}{\sqrt{2\tilde{\tau}}}$ and $(2\pi)^{\frac{3}{2}}\frac{Z_{\pm}(\tilde{\tau})}{\sqrt{2\tilde{\tau}}}$. The left panels show absolute values of $(2\pi)^{\frac{3}{2}}\frac{Y_{+}(\tilde{\tau})}{\sqrt{2\tilde{\tau}}}$ (blue), $(2\pi)^{\frac{3}{2}}\frac{Z_{+}(\tilde{\tau})}{\sqrt{2\tilde{\tau}}}$ (orange), $(2\pi)^{\frac{3}{2}}\frac{Y_{-}(\tilde{\tau})}{\sqrt{2\tilde{\tau}}}$ (black), and $(2\pi)^{\frac{3}{2}}\frac{Z_{-}(\tilde{\tau})}{\sqrt{2\tilde{\tau}}}$ (red) respectively with respect to $\tilde{\tau}$. The right panels show the absolute values of $(2\pi)^{\frac{3}{2}}\frac{Y_{+}(\tilde{\tau})-Z_{-}(\tilde{\tau})}{\sqrt{2\tilde{\tau}}}$ (magenta) and $(2\pi)^{\frac{3}{2}}\frac{Y_{-}(\tilde{\tau})-Z_{+}(\tilde{\tau})}{\sqrt{2\tilde{\tau}}}$ (brown) respectively with respect to $\tilde{\tau}$.

Here we summarize the generic behavior of these mode functions.

- After horizon crossing, the mode functions $Y_{\pm}/\sqrt{\tilde{\tau}}$ and $Z_{\pm}/\sqrt{\tilde{\tau}}$, oscillate like $\tilde{\tau}^{i|\mu|}$ around a constant value.
- The frequency of these oscillations as well as the amplitude of $Y_{\pm}$ increase with the increase of κ_I. However, the amplitude of $Z_{\pm}$ decreases with κ_I.
- Increasing m_{eff} without changing μ_m, which is possible in the minus subspace, decreases Y_{-} and Z_{-}, while has negligible effect on Y_{+} and Z_{+}.
- Increasing μ_m has negligible effect on Y_s while it linearly increases Z_s, i.e. $Z_s \propto \mu_m$.
- In the large mass limit, $\mu_m \gg \xi_\phi, \xi_A$ and for each $s = \pm$, Z_s increases to a constant value very close to (but less than) Y_{-s}. See the right panels of figure 7.
- The mode functions of the comoving plus fermion, i.e. $u^{\uparrow}_{\pm}(\tilde{\tau})$ and $u^{\downarrow}_{\pm}(\tilde{\tau})$, and hence $\Psi^{+}_{\mathbf{k}}$ are freezed out after horizon crossing.
- For the $\Psi^{-}_{\mathbf{k}}$, one needs $y_{s,s'}(\tilde{\tau})$ and $z_{s,s'}(\tilde{\tau})$ functions in addition to the Y_s and Z_s to fully identify this subsystem. That is the task of section 5.2.

JHEP07(2020)154

5.2 Ψ^- spinors: $y_{s,s'}$ and $z_{s,s'}$

In eq. (4.27) we decomposed the fermion mode functions of the minus subspace in terms of the analytical functions, Y_s and Z_s, as well as four unknown functions, $y_{s,\pm}$ and $z_{s,\pm}$ which should be solved numerically. In this part, we present the numerical solutions of these functions in terms of $\tilde{\tau}$ and for several values of $\mu_{\rm m}$, ξ_A, and ξ_φ parameters. Moreover, for later use, here we also present $|y_{s,+}|^2+|y_{-s,-}|^2$, and $|z_{s,+}|^2+\frac{\xi_A^2}{\mu_{\rm m}^2}|z_{-s,-}|^2$. Later we will see that these are the combinations which appearers in the currents of the minus spinors.

- *Neutral fermions.* In this limit the fermion is not charged under the SU(2) gauge field, and is only derivatively coupled to the axion. In eqs. (4.27) which formulate the deviation of the minus spinors from the plus one, we have $y_{s,+}(\tilde{\tau})=z_{s,+}=1$, and $y_{s,-}(\tilde{\tau})=\frac{\xi_A}{\mu_{\rm m}}z_{s,-}(\tilde{\tau})=0$. For the fermions which are coupled to the gauge field through ξ_A, this limit is the same as going to $\xi_A=0$. See the $\xi_A=0$ (gray) curves in figures 8–15. Therefore, the minus subspace is simply another copy of the plus subspace.

- *Large mass limit.* Two different regimes with large mass limit are presented in figures 8–11. Figures 8 and 9 show systems with $\mu_{\rm m}=25$ and $\xi_\varphi=\xi_A$, while figures 10 and 11 present systems with $\mu_{\rm m}=10$ and $\xi_\varphi=8$ for different values of ξ_A. The generic features of the system at this limit is as follows. The $y_{s,+}(\tilde{\tau})$, and $z_{s,+}(\tilde{\tau})$ ($y_{s,-}(\tilde{\tau})$) start from one (zero) at asymptotic past and after a fast transition phase each reduces (increases) to another constant number less than one after horizon crossing. The $z_{s,-}(\tilde{\tau})$ starts from one at asymptotic past and after horizon crossing approach a constant value of the order of $\frac{\mu_{\rm m}}{\xi_A}$. All of the curves roughly follows a tanh-type behavior. Furthermore, in the very massive fermion limit, the combinations $|y_{s,+}|^2+|y_{-s,-}|^2$, and $|Z_{s,+}|^2+\frac{\xi_A^2}{\mu_{\rm m}^2}|Z_{-s,-}|^2$ ($s=\pm$) start from one at asymptotic past and remain very close to it throughout the mode's evolution.

- *Large ξ_A limit.* A system with large values of ξ_A and relatively small values of $\mu_{\rm m}$ and ξ_φ, i.e. $\mu_{\rm m}=0.1$ and $\xi_\varphi=0.05$ is presented in figures 12 and 13.

- SU(2) *Schwinger process.* The system with no axion coupling, $\xi_\varphi=0$, is presented in figures 14 and 15. This limit is simply the SU(2) Schwinger process during a (quasi) de-Sitter expansion.

6 Fermionic currents: point-splitting regularization

Working out the fermion fields in the previous section, we are now ready to compute the induced currents. The three currents induced by our fermions are presented in eqs. (2.5) and (2.27). However, those expressions for currents are in their classical forms. Given the Graussman nature of the fermion fields, i.e. $\tilde{\Psi}^\dagger_\alpha$ and $\tilde{\Psi}_\beta$ do not commute, the quantum currents are given by the anti-symmetrization of the fermionic fields. Therefore, the physical fermion (vector) current is given as [33]

$$\langle J^\mu\rangle=\frac{1}{a}\delta^\mu_\alpha\left\langle 0\left|[\bar{\tilde{\Psi}},\mathbf{I}_2\otimes\gamma^\alpha\tilde{\Psi}]\right|0\right\rangle. \tag{6.1}$$

JHEP07(2020)154

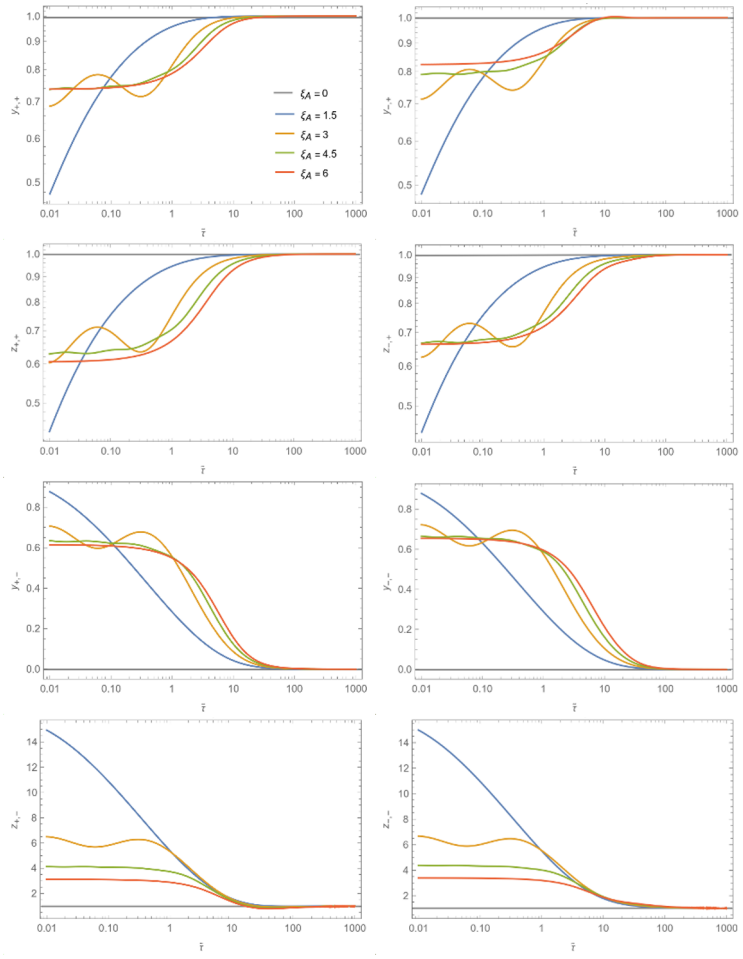

Figure 8. $y_{s,s'}(\tilde{\tau})$ and $z_{s,s'}(\tilde{\tau})$ with respect to $\tilde{\tau}$ for $\mu_m = 25$, $\xi_\varphi = \xi_A$, and different values of ξ_A.

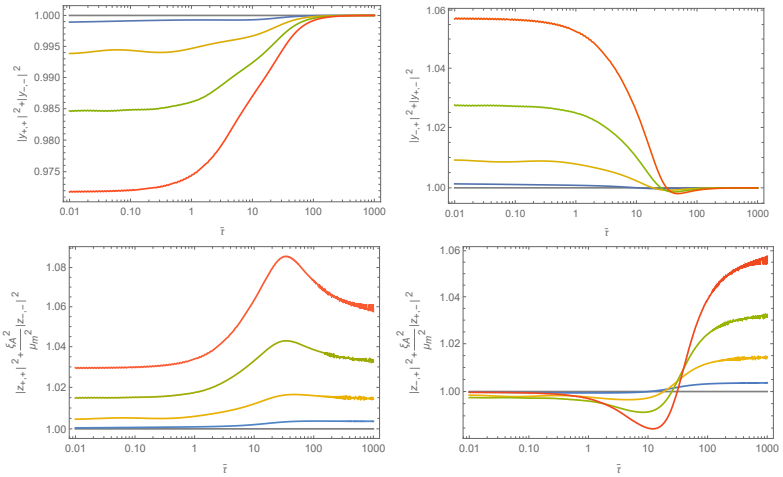

Figure 9. $|y_{s,+}|^2 + |y_{-s,-}|^2$, and $|Z_{s,+}|^2 + \frac{\xi_A^2}{\mu_m^2}|Z_{-s,-}|^2$ for the same parameters of figure 8.

JHEP07(2020)154

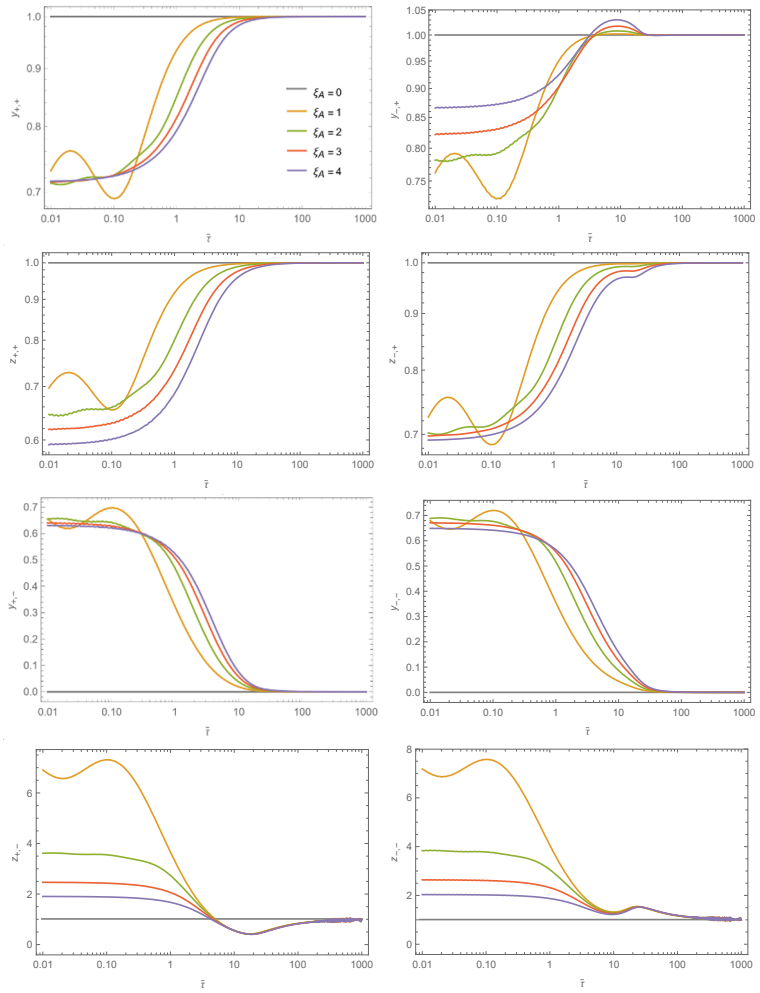

Figure 10. $y_{s,s'}(\tilde{\tau})$ and $z_{s,s'}(\tilde{\tau})$ with respect to $\tilde{\tau}$ for $\mu_m = 10$, $\xi_\varphi = 8$, and different values of ξ_A.

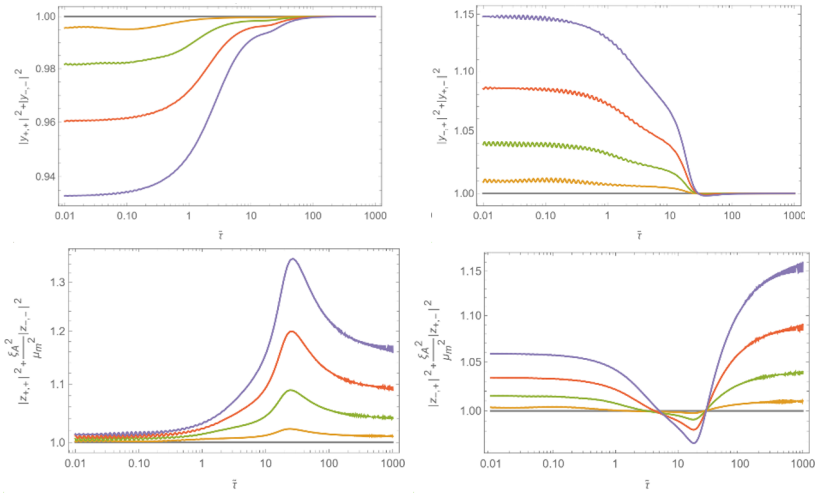

Figure 11. $|y_{s,+}|^2 + |y_{-s,-}|^2$, and $|Z_{s,+}|^2 + \frac{\xi_A^2}{\mu_m^2}|Z_{-s,-}|^2$ for the same parameters of figure 10.

JHEP07(2020)154

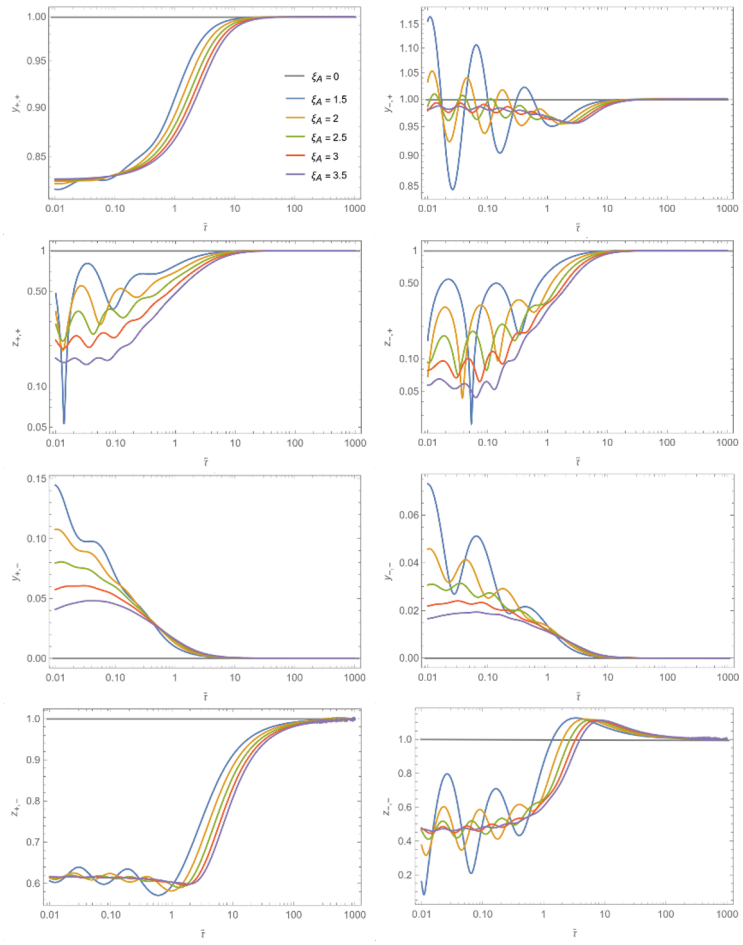

Figure 12. $y_{s,s'}(\tilde{\tau})$ and $z_{s,s'}(\tilde{\tau})$ with respect to $\tilde{\tau}$ for $\mu_m = 0.1$, $\xi_\varphi = 0.05$.

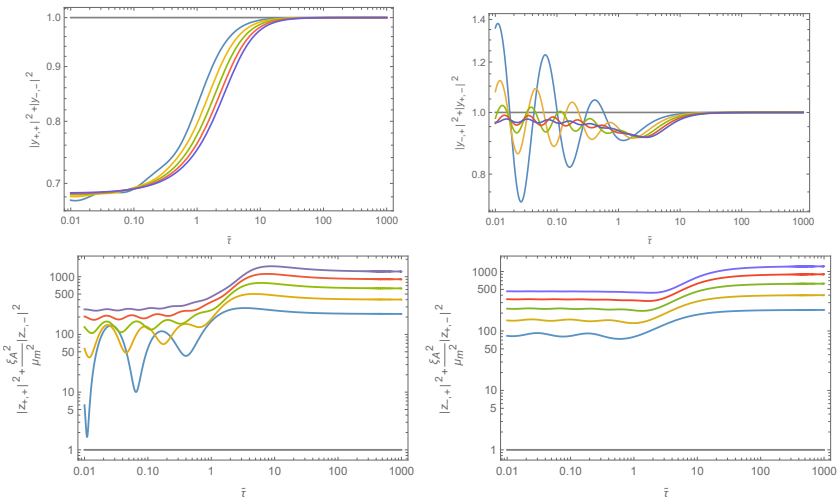

Figure 13. $|y_{s,+}|^2 + |y_{-s,-}|^2$, and $|Z_{s,+}|^2 + \frac{\xi_A^2}{\mu_m^2}|Z_{-s,-}|^2$ for the same parameters of figure 12.

JHEP07(2020)154

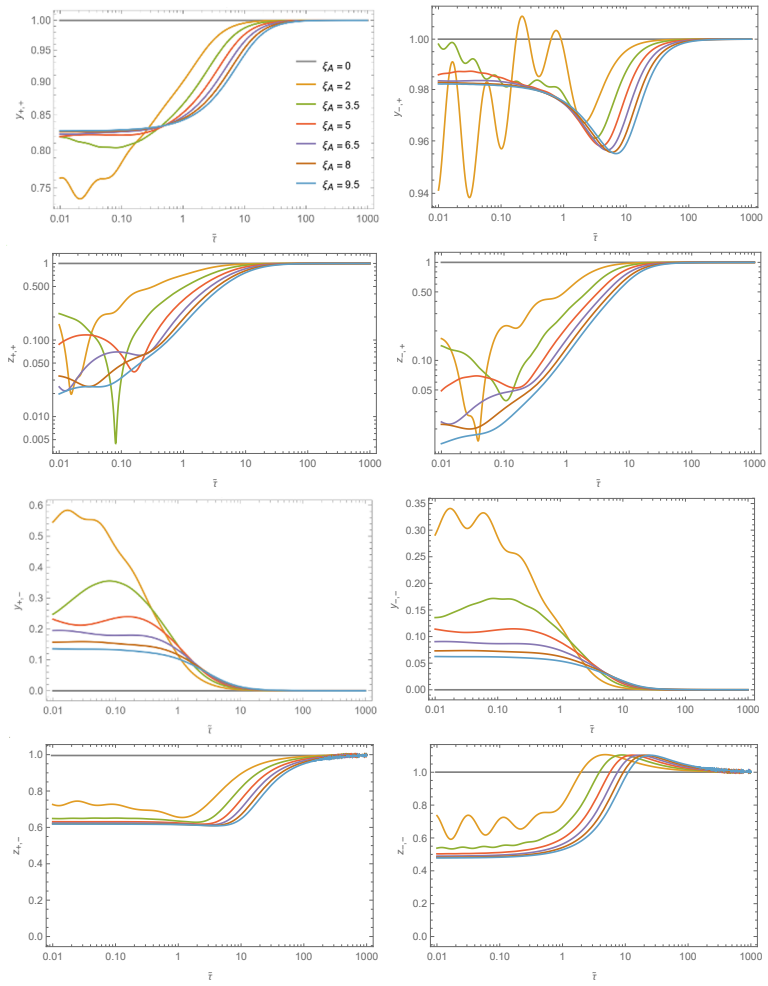

Figure 14. $y_{s,s'}(\tilde{\tau})$ and $z_{s,s'}(\tilde{\tau})$ with respect to $\tilde{\tau}$ for $\mu_m = 1$, $\xi_\varphi = 0$, and different values of ξ_A.

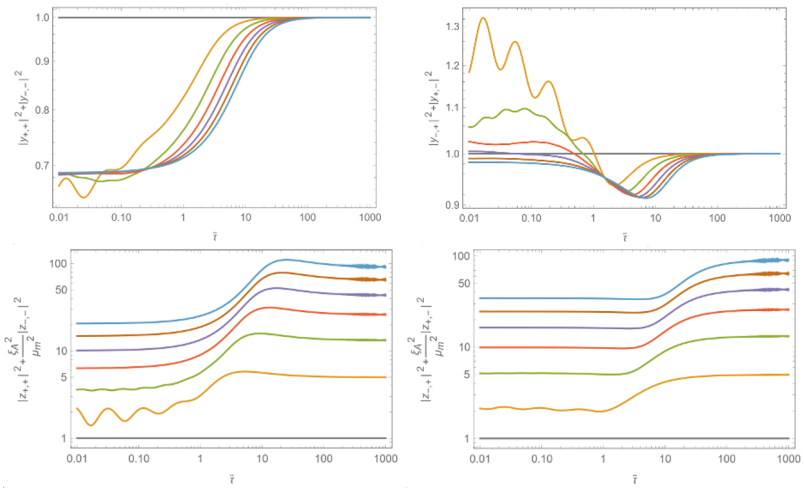

Figure 15. $|y_{s,+}|^2 + |y_{-s,-}|^2$, and $|Z_{s,+}|^2 + \frac{\xi_A^2}{\mu_m^2}|Z_{-s,-}|^2$ for the same parameters as figure 14.

JHEP07(2020)154

It is more convenient to replace the commutation on operators with the antinormal ordering on the creation and annihilation operators, $\vdots$, defined as

$$\vdots b_{\mathbf{k}} b_{\mathbf{k}}^{\dagger} \vdots \equiv b_{\mathbf{k}} b_{\mathbf{k}}^{\dagger} \quad \text{and} \quad \vdots b_{\mathbf{k}}^{\dagger} b_{\mathbf{k}} \vdots \equiv -b_{\mathbf{k}} b_{\mathbf{k}}^{\dagger}. \tag{6.2}$$

Therefore, the physical fermion current can be written as

$$\langle J^{\mu} \rangle = \frac{1}{a} \delta_{\alpha}^{\mu} \left\langle 0 \middle| \vdots \bar{\tilde{\Psi}} \mathbf{I}_2 \otimes \gamma^{\alpha} \tilde{\Psi} \vdots \middle| 0 \right\rangle. \tag{6.3}$$

Similarly, we can find the physical isospin current and chiral current from their classical forms in eqs. (2.27) and (2.5).

6.1 Fermion number

Here we compute the net fermion number, J^0. From eq. (6.3), we find the contribution of the plus fermions to the net fermion number as

$$\langle J^{0+} \rangle = \frac{1}{a^4} \sum_{s=\pm} \int \mathrm{d}^3 k \left[(v_s^{\uparrow *} v_s^{\uparrow} + v_s^{\downarrow *} v_s^{\downarrow}) - (u_s^{\uparrow *} u_s^{\uparrow} + u_s^{\downarrow *} u_s^{\downarrow}) \right] = 0, \tag{6.4}$$

where in the last equality we used eq. (4.8). Similarly, the contribution of the minus fermions to the net fermion number is

$$\langle J^{0-} \rangle = \frac{1}{a^4} \sum_{s,s'=\pm} \int \mathrm{d}^3 k \left[(v_{s,s'}^{\uparrow *} v_{s,s'}^{\uparrow} + v_{s,s'}^{\downarrow *} v_{s,s'}^{\downarrow}) - (u_{s,s'}^{\uparrow *} u_{s,s'}^{\uparrow} + u_{s,s'}^{\downarrow *} u_{s,s'}^{\downarrow}) \right] = 0. \tag{6.5}$$

As a result, the net fermion number vanishes

$$\langle J^0 \rangle = \langle J^{0+} \rangle + \langle J^{0-} \rangle = 0, \tag{6.6}$$

which is a consequence of the C-symmetry in the fermionic sector.

6.2 Isospin current and chiral charge

At this part, we compute the isospin current, $J^{\mu a}$, and the chiral current, J_5^{μ}. The corresponding momentum integrals are UV divergent and need to be renormalized for which we will use the point-splitting regularization skim. The gauge invariant isospin and chiral currents with symmetric point separation are respectively given as

$$\langle J^{\mu a}(x^{\nu}; \varepsilon^{\nu}) \rangle \equiv \mathrm{symm} \lim_{\varepsilon \to 0} g_A \left\langle 0 \middle| \vdots \bar{\tilde{\Psi}}(x_f^{\nu}) \mathcal{W}(x, x_f) \mathbf{T}^a \otimes \gamma^{\mu} \mathcal{W}(x_b, x) \tilde{\Psi}(x_b^{\nu}) \vdots \middle| 0 \right\rangle, \tag{6.7}$$

and

$$\langle J_5^{\mu}(x^{\nu}; \varepsilon^{\nu}) \rangle \equiv \mathrm{symm} \lim_{\varepsilon \to 0} \left\langle 0 \middle| \vdots \bar{\tilde{\Psi}}(x_f^{\nu}) \mathcal{W}(x_b, x_f) \mathbf{I}_2 \otimes (\gamma^{\mu} \gamma_5) \tilde{\Psi}(x_b^{\nu}) \vdots \middle| 0 \right\rangle, \tag{6.8}$$

in which $\mathcal{W}(y, z)$ is the Wilson line defined as

$$\mathcal{W}(y, z) \equiv \mathcal{P} \left[\exp \left(-i g_A \int_y^z A_{\lambda} \mathrm{d}x^{\lambda} \right) \right], \tag{6.9}$$

JHEP07(2020)154

which is required to maintain the gauge invariance and trace is over the fundamental representation of the gauge group, $\mathcal{P}$ stands for path ordering, and x_f^μ and x_b^μ are the *forward* and *backward* point-splitting points, corresponding to the point-splitting *physical* points[8]

$$X_f^\mu \equiv \left(t + \frac{\varepsilon}{2}, \mathbf{X}^i + \frac{\boldsymbol{\varepsilon}^i}{2}\right) \quad \text{and} \quad X_b^\mu \equiv \left(t - \frac{\varepsilon}{2}, \mathbf{X}^i - \frac{\boldsymbol{\varepsilon}^i}{2}\right), \tag{6.10}$$

respectively and ε^μ is a constant 4-vector which we will eventually take to zero. Using the slow-roll inflation relations, $Ha(\tau) \simeq -\frac{1}{\tau}$ and $a(\tau) \simeq e^{Ht}$, we can read off the forward and backward point-splitting conformal times as

$$\tau_f = \left(1 - \frac{\varepsilon}{2}\right)\tau \quad \text{and} \quad \tau_b = \left(1 + \frac{\varepsilon}{2}\right)\tau, \tag{6.11}$$

and the spatial comoving coordinates as

$$\mathbf{x}_f = \mathbf{x} + \frac{\boldsymbol{\varepsilon}}{2a} \quad \text{and} \quad \mathbf{x}_b = \mathbf{x} - \frac{\boldsymbol{\varepsilon}}{2a}. \tag{6.12}$$

In terms of the comoving fields and using the plus and minus decomposition, the chiral charge in eq. (3.1) can be written as

$$Q_5 = \langle a J_5^0 \rangle = Q_5^+ + Q_5^-, \tag{6.13}$$

where Q_5^+ and Q_5^- are the contribution of the plus and minus fermions to Q_5 respectively. Similarly, the fermionic backreaction to the gauge field's equation in eq. (2.29) can be written as

$$\mathcal{J} \equiv \frac{a}{3}\delta_a^i \langle J^{ai} \rangle = \mathcal{J}^+ + \mathcal{J}^-, \tag{6.14}$$

where $\mathcal{J}^\pm$ are the contributions of the plus and minus spinors to $\mathcal{J}$.

Taking the ε^μ goes to zero limit and using eq. (B.31), $Q_5^\pm(x^\nu;\varepsilon)$ can be written as

$$Q_5^\pm(x^\nu;\varepsilon) = -\frac{H^3\xi_A^3}{(2\pi)^2} + \frac{a}{(a_f a_b)^2}\left\langle 0\left|:\bar{\Psi}^\pm(x_f^\nu)\gamma^0\gamma^5\Psi^\pm(x_b^\nu):\right|0\right\rangle, \tag{6.15}$$

where a_f and a_b are the forward and backward scale factors, i.e.

$$a_f(\tau) \equiv a(\tau_f) \quad \text{and} \quad a_b(\tau) \equiv a(\tau_b). \tag{6.16}$$

Moreover, using eq. (B.32), $\mathcal{J}^\pm(x^\nu;\varepsilon)$ is[9]

$$\mathcal{J}^\pm(x^\nu;\varepsilon) = \text{symm}\lim_{\varepsilon\to 0}\frac{\pm a g_A}{2(a_f a_b)^2}\left\langle 0\left|:\bar{\Psi}^\pm(x_f^\nu)\gamma^0\gamma^5\Psi^\pm(x_b^\nu):\right|0\right\rangle. \tag{6.17}$$

[8]It is noteworthy to mention that in the expanding universe, the point-splitting, i.e. $X^\mu \to \{X_f^\mu, X_b^\mu\}$ with $X_f^\mu = X_b^\mu + \varepsilon^\mu$, should be done to the physical coordinates and not the comoving ones. Otherwise, the UV divergent terms would be powers of $\frac{\tau}{\varepsilon}$, not $\frac{1}{\varepsilon}$. Such a mistake leads to an unphysical term of the form $\ln(a)$ in the currents which fakes an IR divergence.

[9]More precisely, the explicate form of $\mathcal{J}^-(x^\nu;\varepsilon)$ is

$$\mathcal{J}^-(x^\nu;\varepsilon) = -\text{symm}\lim_{\varepsilon\to 0}\frac{1}{2}\frac{a g_A}{(a_f a_b)^2}\left\langle 0\left|:\bar{\Psi}^-(x_f^\nu)\left(\gamma^0\gamma^5 - 2\gamma^1\right)\Psi^-(x_b^\nu):\right|0\right\rangle.$$

However, from the combination of the charge conjugation eq. (4.4), as well as antinormal ordering in eq. (1.4), we find that $\text{symm}\lim_{\varepsilon\to 0}\left\langle 0\left|:\bar{\Psi}^-(x_f^\nu)\gamma^1\Psi^-(x_b^\nu):\right|0\right\rangle = 0$. Therefore, up to a total sign difference, the expectation value of $\mathcal{J}^-(x^\nu;\varepsilon)$ takes the form of $\mathcal{J}^+(x^\nu;\varepsilon)$.

JHEP07(2020)154

It is noteworthy to mention that the first term in eq. (6.15) is the contribution of $\boldsymbol{\varepsilon}^i$ terms in the presence of the gauge field and the Wilson line. This term is the zeroth element of the Chern-Simons current and the result of the Abelian Adler-Bell-Jackiw anomaly [30, 31] (see eq. (3.12)). In the momentum integrals on the right hand sides of eq. (6.15) and (6.17), all the divergent terms are given in terms of the temporal separation. That is due to the spatial isotropy of our setup. Therefore, from now on, we set $\boldsymbol{\varepsilon}^i$ to zero and only keep the separation in time parameter, i.e. ε.

Interestingly, both the isospin backreactions, $\mathcal{J}^{\pm}$, and chiral charges, $Q_5^{\pm}$, are specified in term of the following dimensionless quantity

$$\mathcal{K}^{\pm}(x^\mu;\varepsilon) \equiv \text{symm} \lim_{\varepsilon\to 0} \frac{a}{2(a_f a_b)^2} \frac{(2\pi)^2}{H^3} \left\langle 0 \left| :\Psi^{\pm\dagger}(x_f^\nu)\gamma^5 \Psi^{\pm}(x_b^\nu): \right| 0 \right\rangle. \tag{6.18}$$

More precisely, the currents can be written as

$$\mathcal{J}^{\pm}(x^\mu;\varepsilon) = \pm \frac{g_A H^3}{(2\pi)^2} \mathcal{K}^{\pm}(x^\mu;\varepsilon) \quad \text{and} \quad Q_5^{\pm}(x^\mu;\varepsilon) = \frac{2H^3}{(2\pi)^2}\left(-\frac{1}{2}\xi_A^3 + \mathcal{K}^{\pm}(x^\mu;\varepsilon)\right). \tag{6.19}$$

Besides, the fermionic backreaction to the axion background in eq. (2.30) can be written as

$$\mathcal{B}(x^\mu;\varepsilon) = \frac{\beta\lambda}{2f}\left(\partial_t Q_5 + 3HQ_5\right). \tag{6.20}$$

In the following, we compute $\mathcal{K}^{+}(x^\mu;\varepsilon)$ and $\mathcal{K}^{-}(x^\mu;\varepsilon)$ which are the contributions of the plus and minus fermions respectively.

$\boldsymbol{\Psi^+}$ fermions. In the plus subspace and after using eqs. (4.8) and (6.18), $\mathcal{K}^{+}$ can be written as

$$\mathcal{K}^{+}(x^\mu;\varepsilon) = -\text{symm} \lim_{\varepsilon\to 0} \sum_{s=\pm} s \, \frac{a(2\pi)^2/H^3}{2(a_f a_b)^2} \int \mathrm{d}^3k \left[u_s^{\uparrow *}(k,\tau_f) u_s^{\downarrow}(k,\tau_b) + u_s^{\downarrow *}(k,\tau_f) u_s^{\uparrow}(k,\tau_b)\right]. \tag{6.21}$$

This momentum integral is UV divergent and we use the point-splitting skim to regularize it. Here, we present the final results and the details of the computations are presented in appendix D. We find that $\mathcal{K}^{+}(\tau,\varepsilon)$ has a log divergent term and can be written as

$$\mathcal{K}^{+}(\tau;\varepsilon) = 4\kappa_{+,I}\mu_{\rm m}^2 \ln\left(\frac{\varepsilon}{2}\right) + \mathcal{K}^{+}_{\rm reg}(\tau), \tag{6.22}$$

where $\mathcal{K}^{+}_{\rm reg}(\tau;\varepsilon)$ is the regularized current, given as

$$\begin{aligned}
&\mathcal{K}^{+}_{\rm reg} = \\
&\kappa_I^+ \left\{ \frac{2}{3}(1-2(\kappa_I^+)^2)\left(1 - \frac{|\mu^+|}{\kappa_I^+}\frac{\sinh(2\kappa_I^+\pi)}{\sinh(2|\mu^+|\pi)}\right) + \mu_{\rm m}^2\left(-4\psi^{(0)}(1) + 2 - \frac{8|\mu^+|}{3\kappa_I^+}\frac{\sinh(2\kappa_I^+\pi)}{\sinh(2|\mu^+|\pi)}\right) + \right. \\
&\left. \mu_{\rm m}^2 \sum_{s=\pm} \mathrm{Re}\left[\frac{e^{2|\mu^+|\pi} - e^{-2s\kappa_I^+\pi}}{\sinh(2|\mu^+|\pi)}\psi^{(0)}(-is\kappa_I^+ - i|\mu^+|) - \frac{e^{-2|\mu^+|\pi} - e^{-2s\kappa_I^+\pi}}{\sinh(2|\mu^+|\pi)}\psi^{(0)}(i|\mu^+| - is\kappa_I^+)\right]\right\},
\end{aligned} \tag{6.23}$$

in which $\psi^{(0)}(z) \equiv \frac{d\Gamma(z)}{dz}$ is the digamma function and κ_I^+ is the imaginary part of κ^+, i.e. $\kappa_I^+ = 2\xi_\varphi - \frac{1}{2}\xi_A$, and $|\mu^+| = [\mu_{\rm m}^2 + (\kappa_I^+)^2]^{\frac{1}{2}}$. Notice that $\mathcal{K}^{+}_{\rm reg}$ is proportional to κ_I^+ and the quantity inside the curly brackets is even under parity.

JHEP07(2020)154

Ψ^- fermions. For the minus subspace and after using eq. (4.19), we obtain $\mathcal{K}^-(\tau,\varepsilon)$ as

$$\mathcal{K}^-(\tau;\varepsilon)=-\text{symm}\lim_{\varepsilon\to 0}\frac{a(2\pi)^2/H^3}{2(a_f a_b)^2}\sum_{s,s'=\pm}ss'\int \mathrm{d}^3k\Big[u^{\uparrow *}_{s,s'}(k,\tau_f)u^{\downarrow}_{s,s'}(k,\tau_b)+u^{\downarrow *}_{s,s'}(k,\tau_f)u^{\uparrow}_{s,s'}(k,\tau_b)\Big], \tag{6.24}$$

which by decomposition defined by eq. (4.27), it can be simplified to

$$\mathcal{K}^-=-\text{symm}\lim_{\varepsilon\to 0}\frac{a(2\pi)^2/H^2}{2(a_f a_b)^{\frac{3}{2}}}\sum_{s=\pm}s\int\frac{\mathrm{d}^3k}{k}\Big[(|y_{s,+}|^2+|y_{-s,-}|^2)|Y_s|^2-\Big(|z_{s,+}|^2+\frac{\xi_A^2}{\mu_{\rm m}^2}|z_{-s,-}|^2\Big)|Z_s|^2\Big]. \tag{6.25}$$

Since we only have $y_{s,s'}(\tilde{\tau})$ and $z_{s,s'}(\tilde{\tau})$ functions numerically, we can not work out the current analytically. However, as it is expected from eqs. (4.23) and is showed in section 5.2, in the limit $\xi_A/\mu_{\rm m}\ll 1$, the combinations $\big(|y_{s,+}(\tilde{\tau})|^2+|y_{-s,-}(\tilde{\tau})|^2\big)$, and $\big(|z_{s,+}(\tilde{\tau})|^2+\frac{\xi_A^2}{\mu_{\rm m}^2}|z_{-s,-}(\tilde{\tau})|^2\big)$ are always close to one. As a result, we can approximate $\mathcal{K}^-(\tau;\varepsilon)$ in this limit as

$$\mathcal{K}^-(\tau;\varepsilon)\simeq-\text{symm}\lim_{\varepsilon\to 0}\frac{a(2\pi)^2/H^2}{2(a_f a_b)^{\frac{3}{2}}}\sum_{s=\pm}s\int\frac{\mathrm{d}^3k}{k}\big(|Y_s|^2-|Z_s|^2\big). \tag{6.26}$$

Following the corresponding analysis in the plus subspace, we find the regularized current in the minus subspace, $\mathcal{K}^-_{\rm reg}$, as

$$\begin{aligned}&\mathcal{K}^-_{\rm reg}\simeq\\&\kappa_I^-\Big\{\frac{2}{3}(1-2(\kappa_I^-)^2)\Big(1-\frac{|\mu^-|}{\kappa_I^-}\frac{\sinh(2\kappa_I^-\pi)}{\sinh(2|\mu^-|\pi)}\Big)+\mu_{\rm m}^2\Big(-4\psi^{(0)}(1)+2-\frac{8|\mu^-|}{3\kappa_I^-}\frac{\sinh(2\kappa_I^-\pi)}{\sinh(2|\mu^-|\pi)}\Big)+\\&\mu_{\rm m}^2\sum_{s=\pm}\text{Re}\Big[\frac{e^{2|\mu^-|\pi}-e^{-2s\kappa_I^-\pi}}{\sinh(2|\mu^-|\pi)}\psi^{(0)}(-is\kappa_I^--i|\mu^-|)-\frac{e^{-2|\mu^-|\pi}-e^{-2s\kappa_I^-\pi}}{\sinh(2|\mu^-|\pi)}\psi^{(0)}(i|\mu^-|-is\kappa_I^-)\Big]\Big\},\end{aligned} \tag{6.27}$$

where κ_I^- is the imaginary part of κ^-, i.e. $\kappa_I^-=2\xi_\varphi+\frac{1}{2}\xi_A$, and $|\mu^-|=[\mu_{\rm m}^2+(\kappa_I^-)^2+\xi_A^2]^{\frac{1}{2}}$. As we mentioned earlier, is only valid in the limit $\xi_A/\mu_{\rm m}\ll 1$.

To summarize, we worked out the induced currents analytically by using the point-splitting regularization skim. In the minus subspace, our analytical solution for $\mathcal{J}^-$ and Q_5^- (given in terms of $\mathcal{K}^-$) are approximations which are valid in $\xi_A/\mu_{\rm m}\ll 1$ limit. To find $\mathcal{K}^-_{\rm reg}(\tau)$ in other parts of the parameter space, one needs a full numerical analysis, e.g. [13]. The two approaches are only in agreement when the source of the particle production, $\kappa_I^\pm$ is large. The reason is in the use of a hard cut-off in the numerical computation of the momentum integrals carried out in [13]. As a result, the numerical approach subtracts the divergences correctly but misses the finite terms which appear by the regularization process.

7 Dirac fermions in (quasi) de Sitter

In the previous section, we worked out the analytic form of the fermionic currents sourced by an SU(2) gauge field and possibly derivatively coupled to the axion field in de Sitter. In

JHEP07(2020)154

this section, we take a closer look at the results and make a detailed comparison with other cases of fermions generated in different setups in de Sitter, i.e., neutral fermions coupled to axion, and Abelian fermions. We also compare the non-Abelian fermion Schwinger effect with its scalar counterpart.

7.1 Charged SU(2) fermions

This setup of Dirac fermion doublet is reducible into two subspaces of Dirac fermions in the c-helicty frame (section 2)

$$\tilde{\Psi}_{\mathbf{k}} = \Psi^{+}_{\mathbf{k}} \oplus \Psi^{-}_{\mathbf{k}},$$

where the supercript $+/-$ denotes the plus/minus subspace, and $\Psi^{\pm}_{\mathbf{k}}$ are two 4-spinors. In section 6, we showed that our non-Abelian fermions have vanishing fermion number, i.e.

$$\langle J^0 \rangle = 0.$$

as a consequence of C-symmetry in our setup. Then, we showed that the isospin current backreacts to the (background) SU(2) gauge field, $\mathcal{J} \equiv \frac{a}{3}\delta^i_a \langle J^{ai} \rangle = \mathcal{J}^+ + \mathcal{J}^-$, and also has a non-zero chiral charge, $Q_5 \equiv \langle a J^0_5 \rangle = Q^+_5 + Q^-_5$. We regularized both of these quantities in section D and found

$$\mathcal{J}_{\rm reg} = \pm \frac{g_A H^3}{(2\pi)^2}\big(\mathcal{K}^+_{\rm reg} - \mathcal{K}^-_{\rm reg}\big) \quad \text{and} \quad Q_{5\rm reg} = \frac{2H^3}{(2\pi)^2}\big(\mathcal{K}^+_{\rm reg} + \mathcal{K}^-_{\rm reg} - \xi^3_A\big), \tag{7.1}$$

where $\mathcal{K}^{\pm}_{\rm reg}$ is a momentum integral which we computed analytically for the plus subspace in eqs. (6.23) (and for minus subspace in $\xi_A/\mu_{\rm m} \ll 1$ in eq. (6.27)). During slow-roll, they are almost constant quantities in terms of the (slow-varying and CP-breaking) vacuum quantities ξ_A, ξ_φ in eqs. (2.9), as well as the mass of the fermion $\mu_{\rm m} = \frac{m}{H}$. Thus, the backreaction to the axion background, $\mathcal{B} \equiv \frac{\beta\lambda}{2f}\nabla_\mu J^\mu_5$, is given as

$$\mathcal{B}_{\rm reg} \simeq \frac{3\beta\lambda}{f}\frac{H^4}{(2\pi)^2}\big(\mathcal{K}^+_{\rm reg} + \mathcal{K}^-_{\rm reg} - \xi^3_A\big). \tag{7.2}$$

The $\mathcal{K}^{\pm}_{\rm reg}$ are directly proportional to (and an odd function of) $\kappa^{\pm}_I = (2\xi_\varphi \mp \xi_A/2)$ which is the source of CP-violation and increase with the mass of the fermion, $\mu_{\rm m}$, which is the source of chiral symmetry breaking. Thus, $\mathcal{K}^{\pm}_{\rm reg}$ vanishes in the massless limit where the system has classical chiral symmetry. Moreover, in the absence of the SU(2) gauge field and the axion interactions which are the sources of CP-breaking, the fermion fields are unpolarized and all the currents vanish. That is in agreement with our qualitative discussion based on symmetries in section 3. In the large and small mass limits $\mathcal{K}^+_{\rm reg}$ is

$$\mathcal{K}^+_{\rm reg} = \begin{cases} 4\kappa^+_I \mu^2_{\rm m}\Big[\ln\mu_{\rm m} - \psi^{(0)}(1) + \frac{1}{2}\Big] + \kappa^+_I(1 - \frac{4}{3}(\kappa^+_I)^2) & \text{where} \quad \mu_{\rm m} \gg 1, \\ -\frac{4\pi}{3}\kappa^+_I \mu^2_{\rm m}|\kappa^+_I| & \text{where} \quad \mu_{\rm m} \ll 1. \end{cases} \tag{7.3}$$

In the limit that $\kappa^+_I \gg \mu_{\rm m}$, the $\mathcal{K}^+_{\rm reg}(\tau)$ takes the following asymptotic form

$$\mathcal{K}^+_{\rm reg}(\tau) \simeq -\frac{4(\kappa^+_I)^2|\kappa^+_I|}{3}\left(1 - e^{-\frac{\mu^2_{\rm m}\pi}{\kappa^+_I}}\right) \simeq -\frac{4\pi}{3}\mu^2_{\rm m}\kappa^+_I|\kappa^+_I|. \tag{7.4}$$

JHEP07(2020)154

In figure 16, we plot $\mathcal{K}^{\pm}_{\rm reg}$ for fermion fields coupled both to the gauge field and axion which $\xi_\varphi = 2$. Figure 17 shows $\mathcal{K}^{\pm}_{\rm reg}$ for fermions coupled to the isotropic SU(2) gauge field but in the absence of the derivative coupling with the axion, i.e. $\beta = 0$ and $\xi_\varphi = 0$.

Light fermions. In the massless limit, $\mathcal{K}^{\pm}_{\rm reg} = 0$, and the chiral charge is

$$Q_{5\rm reg} = -\frac{2H^3\xi_A^3}{(2\pi)^2}, \tag{7.5}$$

and the fermion backreaction to the background axion field

$$\mathcal{B}_{\rm reg} = -\frac{3\beta\lambda}{f}\frac{H^4\xi_A^3}{(2\pi)^2}. \tag{7.6}$$

Namely, the only non-zero effect is the Abelian chiral anomaly (see section 3.2).

Heavy fermions. The mass of the fermion and the energy scale of inflation cannot exceed the decay constant of the axion, f, which is the UV cutoff of the theory. Apart from that, the size of the fermion backreactions on the background gauge field and axion put upper bounds on it. Note that unlike the non-perturbative tunneling effects in Minkowski space, our current analysis is perturbative and relays on assuming a classical background with infinite energy that sources the fermions. That approximation is broken once the fermion backreaction becomes large. Following [12], here we constrain the parameter space of the system based on the size of the fermion backreaction.

I) Backreaction to the background SU(2) *gauge field.* The validity of the perturbation theory and slow-roll dynamics requires that the backreaction to the gauge field should utmost be as small as slow-roll suppressed terms. Demanding that condition, we find

$$\frac{g_A H^3}{(2\pi)^2}\mathcal{K}^{\pm}_{\rm reg} \ll H^2\psi, \tag{7.7}$$

which in the large mass limit, and requiring the r.h.s. be smaller than $10^{-2}H^2\psi$, gives

$$m \lesssim \frac{\pi}{10g_A}\left(\frac{\xi_A}{\kappa_I^+}\right)^{\frac{1}{2}} H, \tag{7.8}$$

which for typical values of κ_I^+ and ξ_A of order one and $g_A \sim 10^{-2} - 10^{-3}$ gives $m \lesssim 100H$.

II) Backreaction to the background axion field. Demanding that the femrion backreaction to the axion field equation should utmost be as small as slow-roll suppressed terms implies

$$\frac{\lambda\beta}{f}\frac{H^4}{(2\pi)^2}\left(\mathcal{K}^{+}_{\rm reg} + \mathcal{K}^{-}_{\rm reg} + \xi_A^3\right) \lesssim H\dot{\varphi}. \tag{7.9}$$

In SU(2)-axion models during slow-roll inflation, we have $\xi_A \sim \xi$ [12] which using in the above, it gives

$$\xi_A \lesssim \frac{2\pi f}{H} \quad \text{and} \quad m \lesssim 2\pi f. \tag{7.10}$$

For instance, for $f/H \sim 10^2$ we have $\xi_A \sim \frac{m}{H} < 600$.

JHEP07(2020)154

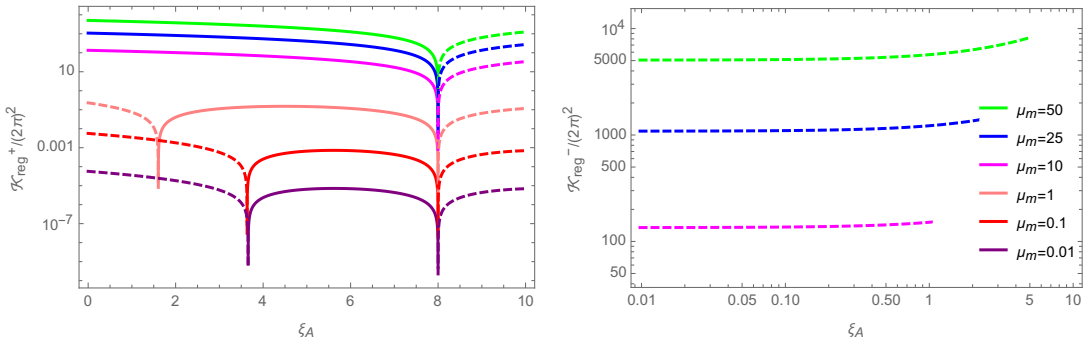

Figure 16. The absolute values of $\mathcal{K}^{+}_{\rm reg}/(2\pi)^2$ (left panel) and $\mathcal{K}^{-}_{\rm reg}/(2\pi)^2$ (right panel) for Dirac fermions coupled to the SU(2) gauge field with $\xi_\varphi = 2$ in terms of ξ_A and for different values of $\mu_{\rm m}$. The solid (dashed) lines denote positive (negative) values of current. The $\mathcal{K}^{-}_{\rm reg}$ lines are only plotted at the regime of the validity of our analytical approximation for this subspace, i.e. $\xi_A/\mu_{\rm m} < 0.1$.

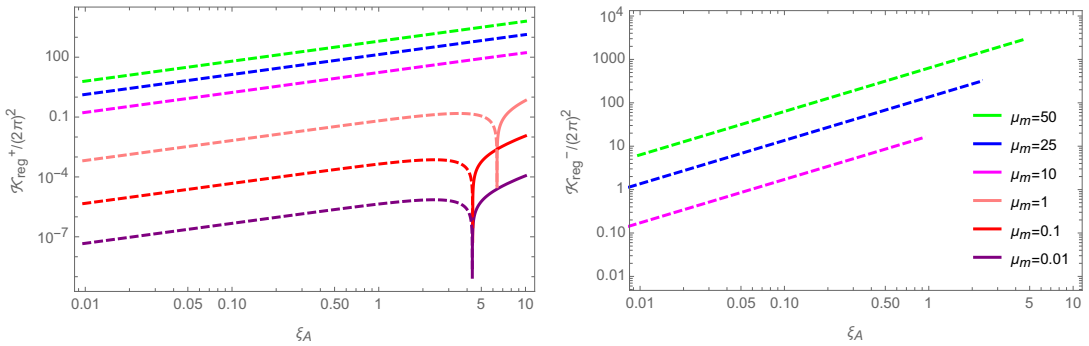

Figure 17. $\mathcal{K}^{+}_{\rm reg}/(2\pi)^2$ (left panel) and $\mathcal{K}^{-}_{\rm reg}/(2\pi)^2$ (right panel) for Dirac fermions coupled to the SU(2) gauge field but in the absence of the axion coupling, i.e. $\xi_\varphi = 0$. The solid (dashed) lines denote positive (negative) values. Notice that the $\mathcal{K}^{-}_{\rm reg}$ are only plotted at the regime of the validity of our analytical approximation for this subspace.

7.1.1 Charged scalars vs charged fermions

Here we compare the scalar and fermion backreactions to the background SU(2) gauge field. As for the backreaction of the charged scalars, we use the analytical formula worked out in [22]. In figure 18, we show the regularized scalar and fermion backreactions. Interestingly, our vacuum produces more fermions than scalars in i) large ξ_A and ii) large mass $\mu_{\rm m} > 1$, i.e. $m > H$ limits. More precisely, the asymptotic form of $\mathcal{J}_{\rm reg}$ in the large ξ_A for the scalars decreases like $1/\xi_A$ while for the Dirac fermions increase as ξ_A^2. That is because the SU(2) gauge field VEV adds an additional mass term to the spin-0 field in such a way that the charged scalar has negligible particle production in the strong field limit [22]. Moreover, by the increase of their mass, the scalar current decreases like $1/\mu_{\rm m}$ while the fermionic one increases like $\mu_{\rm m}^2$. As a result, the SU(2)-axion inflationary models can efficiently produce massive fermions.

JHEP07(2020)154

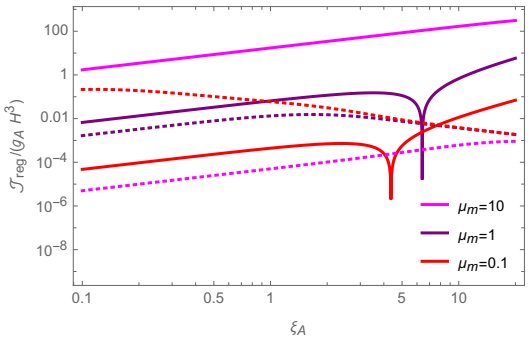

Figure 18. Comparing the scalar and fermion backreactions to the background SU(2) gauge field. The solid lines denotes $\mathcal{J}^{+}_{\rm reg}$ for charged Dirac fermions (with $\xi_\varphi = 0$) and the dotted lines represent the corresponding backreaction of the charged scalar fields worked out analytically in [22].

7.2 Neutral fermions coupled to axion

As a limit in our setup, here we focus on neutral Dirac fermions coupled derivative to the axion.[10] In the absence of the interaction with the gauge field, the minus subsystem is simply a second copy of the plus subsystem, hence $\mathcal{K}^{-}_{\rm reg} = \mathcal{K}^{+}_{\rm reg} = \mathcal{K}_{\rm reg}$. Thus from eq. (7.1), its backreaction to the gauge field vanishes, i.e.

$$\mathcal{J}_{\rm reg} = \mathcal{J}^{+}_{\rm reg} + \mathcal{J}^{-}_{\rm reg} = 0.$$

Moreover, the fermion number is zero, i.e.

$$\langle J^0 \rangle = 0. \tag{7.11}$$

However, it still has a non-zero chiral charge

$$Q_{5\rm reg} = \frac{4H^3}{(2\pi)^2}\mathcal{K}_{\rm reg},$$

while the backreaction to the axion field equation is given as

$$\mathcal{B} = \frac{6\beta\lambda}{f}\frac{H^4}{(2\pi)^2}\mathcal{K}_{\rm reg}, \tag{7.12}$$

where $\mathcal{K}_{\rm reg}$ is

$$\mathcal{K}_{\rm reg} = \kappa_I\Bigg\{\frac{2}{3}(1-2\kappa_I^2)\left(1-\frac{|\mu|}{\kappa_I}\frac{\sinh(2\kappa_I\pi)}{\sinh(2|\mu|\pi)}\right)+\mu_{\rm m}^2\left(2-4\psi^{(0)}(1)-\frac{8|\mu|}{3\kappa_I}\frac{\sinh(2\kappa_I\pi)}{\sinh(2|\mu|\pi)}\right)$$
$$+\mu_{\rm m}^2\sum_{s=\pm}{\rm Re}\left[\frac{e^{2|\mu|\pi}-e^{-2s\kappa_I\pi}}{\sinh(2|\mu|\pi)}\psi^{(0)}(-is\kappa_I-i|\mu|)-\frac{e^{-2|\mu|\pi}-e^{-2s\kappa_I\pi}}{\sinh(2|\mu|\pi)}\psi^{(0)}(i|\mu|-is\kappa_I)\right]\Bigg\},$$

[10] Neutral Dirac fermions derivatively coupled to the axion, its backreaction to the axion $\nabla_\mu J_5^\mu = -2im\bar{\Psi}\gamma_5\Psi$, and the fermionic effects on the curvature perturbations have been extensively studied in [34]. The UV divergent momentum integrals are regularized using adiabatic regularization for fermions. The authors reported a singularity in the massless limit and used a change of basis to remove it. In this work, we did not find any singularities. In the massless limit in particular, we realize that the neutral fermions acquire conformal and chiral symmetry and all the observable currents vanish.

JHEP07(2020)154

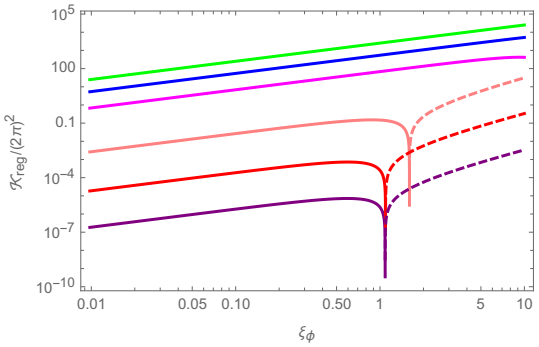

Figure 19. $\mathcal{K}_{\rm reg}/(2\pi)^2$ for uncharged Dirac fermions coupled to the axion in terms of ξ_φ and for different values of $\mu_{\rm m}$. The colors correspond to the values similar to figure 17. The solid (dashed) lines denote positive (negative) values.

in which $\kappa_I = 2\xi_\varphi$ and $|\mu| = (\mu_{\rm m}^2 + \kappa_I^2)^{\frac{1}{2}}$. The chiral charge increases with the mass of the fermion like $\mu_{\rm m}^2$ and the axion parameter like ξ_φ^2. The $\mathcal{K}_{\rm reg}$ in this case is presented in figure 19.

7.3 Abelain fermions, small mass limit

For the sake of completeness, let us now consider the case of a Dirac fermion coupled to an Abelian gauge field in the small mass limit in de Sitter. The aim is to explore the relation of the mass of the fermion and its backreaction in the U(1) gauge field case qualitatively to explore if it also shows the increase with m behavior which we found for the other cases. Consider a U(1) gauge field in the temporal gauge, with a constant electric field as

$$A_\mu = (0, 0, 0, A_3(\tau)) \quad \text{where} \quad A_3(\tau) = \frac{E_3}{H^2\tau}, \tag{7.13}$$

and a Dirac fermion which is charged under it with the theory

$$\sqrt{-g}\mathcal{L}_\Psi = \bar{\Psi}\big(i\gamma^\alpha\partial_\alpha - eA_3\gamma^3 - m\big)\Psi, \tag{7.14}$$

where Ψ is the canonical Dirac field (for which the spin connection disappears), and m is the mass of the fermion. In this case, the Noether current is

$$J^\mu = -\frac{e}{a^4}\delta^\mu_\alpha\langle\bar{\Psi}\gamma^\alpha\Psi\rangle = -\frac{e}{a^4}\Big(\Psi_L^\dagger\bar{\boldsymbol{\sigma}}^\mu\Psi_L + \Psi_R^\dagger\boldsymbol{\sigma}^\mu\Psi_R\Big), \tag{7.15}$$

and the fermion backreaction to the U(1) gauge field is given as

$$\mathcal{J}_{\rm reg} = \langle J^3\rangle = \frac{e}{a^4}\Big(\Psi_L^\dagger\boldsymbol{\sigma}^3\Psi_L - \Psi_R^\dagger\boldsymbol{\sigma}^3\Psi_R\Big). \tag{7.16}$$

Moreover, in this case $\langle F\tilde{F}\rangle = 0$, and hence both the vector and axial vector currents are conserved. Namely, the massless fermions have chiral symmetry, hence their backreaction to the gauge field should vanish. It implies that the backreaction should be directly related

JHEP07(2020)154

to the mass of the fermion which is the source of the chiral symmetry breaking[11]

$$\mathcal{J}_{\rm reg} \propto \frac{m}{H}. \tag{7.17}$$

As a result, our simple argument implies that even in the U(1) gauge field case, the fermionic backreaction should increase with the mass of the fermion.

8 Fermion dark matter, a quick view

Up to this point, we analytically studied the (dark) Dirac fermions charged under the SU(2) VEV in a generic SU(2)-axion inflationary model. We realized that the spontaneous *CP*-violating vacuum structure of this class of models leads to a new and efficient mechanism to generate non-thermal massive dark fermions with a preferred helicity state, *h-asymmetric*, during inflation. Moreover, the generated dark fermions can be very massive, which depending on the efficiency of their possible feebly interactions with the visible and lighter dark sectors, may decay to leptons and baryons or other dark particles after inflation. In other words, these Dirac fermions may replace the right-handed neutrinos in the standard thermal leptogenesis scenario and hence provide a novel natural scenario to explain the observed matter asymmetry in the Universe. However, this possibility, as well as the late time macroscopic properties of the produced dark fermions as a dark matter sector, are all highly model-dependent. They depend on the value of the gauge coupling, g_A, the possible mass of the gauge field at some symmetry breaking scale after inflation, and the details of the possible feebly interactions of the dark fermions with the visible and dark sectors which is beyond the scope of the current work. We leave these important questions for future exhaustive study. However, let us here roughly estimate the gist of the simplest possible scenario for fermio-genesis in this setup.

The three necessary Sakharov conditions to generate an imbalance of baryonic matter are i) C-symmetry and CP-symmetry violation, ii) interactions out of thermal equilibrium, and iii) baryon number, B, violation [37]. One can generalize it for any form of matter by replacing the third condition by the violation of its corresponding fermion number. The fermion doublets charged under our SU(2) gauge field which we studied so far are C-symmetric. That, however, can be easily and naturally violated by the mass term, nonperturbative effects, and especially interactions with the SM fermions, which is beyond the scope of the current work. In the absence of these effects, the generated fermions are not asymmetric in the standard sense but fermions with h-asymmetry.

For simplicity, we assume that the dark sector is made of one generation of massive dark fermion doublets, $\tilde{\Psi}$. We also assume that they are only gravitationally coupled to the visible sector. Thus, dark fermions are stable. The dark fermion has a constant energy density during inflation

$$\rho_{df}^{\rm inf} \sim m^2 H^2 \left({\kappa_I^+}^2 + {\kappa_I^-}^2 \right), \tag{8.1}$$

[11] The fermion theory in eq. (7.14) and its fermion production in de Sitter is studied analytically using adiabatic regularization skim in [35], and later with a different regularization condition in [36] which led to another result. However, the results of both of these studies disagree with our observation based on the symmetries of $\mathcal{J}$ in eq. (7.17).

JHEP07(2020)154

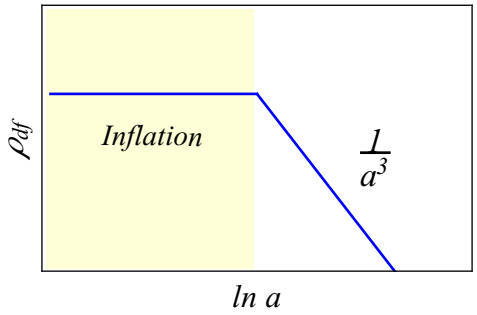

Figure 20. The time evolution of the energy density of the dark fermions which are gravitationally coupled to the rest of the matter fields.

where H is the Hubble parameter during inflation. Notice that the contribution of the $\pm$ spinors into ρ_{df} (which is positive definite) should be directly proportional and an even function of $\kappa_I^{\pm}$ which is the source of the particle production. After the end of inflation, the source of fermion production (gauge field and axion) disappears and therefore ρ_{df} decays like ordinary matter, i.e. (see figure 20)

$$a^3\rho_{df}(a) = a_{\rm inf}^3\rho_{df}^{\rm inf}. \tag{8.2}$$

Here, in order to estimate the energy density of the reheating, we consider the phenomenological reheating model below

$$\rho^{\rm reh} = \sigma\left(\frac{a_{\rm inf}}{a_{\rm reh}}\right)^4\rho^{\rm inf} \tag{8.3}$$

where σ is the efficiency of the reheating process and relates $\rho^{\rm reh}$ and the energy density at the end of inflation, $\rho^{\rm inf}$. From that, one can read the number density of photons during reheating as

$$n_\gamma^{\rm reh} = \frac{6\sqrt{3}\zeta(3)}{\pi^2}\left(\frac{\sigma}{g_{\rm eff}}\right)^{\frac{3}{4}}\left(\frac{a_{\rm inf}}{a_{\rm reh}}\right)^3(HM_{\rm Pl})^{\frac{3}{2}}, \tag{8.4}$$

where $g_{\rm eff} = 427/4$ is the number of relativistic degrees of freedom at the time of reheating, and $\zeta(z)$ is the Riemann zeta function, $\zeta(3) = 1.2$. Now, we define the parameter θ_{df} as the ratio of the dark fermion energy density to the number density of photons as

$$\theta_{df}(a) \equiv \frac{\rho_{df}(a)}{n_\gamma(a)}, \tag{8.5}$$

which has the dimension of mass and gives

$$\theta_{df}^0 \simeq \theta_{df}^{\rm reh} \sim 24\frac{m^2}{M_{\rm Pl}}\sigma^{-\frac{3}{4}}\left(\frac{H}{M_{\rm Pl}}\right)^{\frac{1}{2}}\left(\kappa_I^{+\,2} + \kappa_I^{-\,2}\right), \tag{8.6}$$

where we assume that the dark fermions are only gravitationally coupled to the visible (and other extra dark) sectors.

JHEP07(2020)154

Given the fact that the dark matters energy fraction and the visible one are related as $\Omega_D \simeq 5\Omega_B$ and $\Omega_{df} < \Omega_D$ gives

$$\theta^0_{df} \lesssim 5 m_p \eta^0_B, \tag{8.7}$$

in which $m_p \simeq 10^{-19} M_{\rm Pl}$ is the mass of proton and η^0_B is the baryon asymmetry observed today, i.e. $\eta^0_B = 6 \times 10^{-10}$ [38]. From the combination of eqs. (8.6) and (8.7), we find the upper value of the dark fermion as

$$\frac{m}{M_{\rm Pl}} \sim 10^{-1} \left(\frac{m_p}{M_{\rm Pl}} \eta^0_B\right)^{\frac{1}{2}} \sigma^{\frac{3}{8}} \left(\frac{H}{M_{\rm Pl}}\right)^{-\frac{1}{4}}. \tag{8.8}$$

For a scale of inflation as high as GUT scales, $H \sim 10^{-6} M_{\rm Pl}$, and σ of order one, that gives $m \sim 10\,\text{TeV}$. Notice that it is much lower than the upper bound imposed by the size of the backreaction in eq. (7.8) and higher than the electroweak scale, $E_{\rm EW} \sim 246\,\text{GeV}$.

9 Discussion

Models of inflation with an axion and SU(2) gauge field have very rich phenomenology. In this class of models, the SU(2) gauge field has a (slow-varying) homogeneous and isotropic VEV with an almost constant energy density during inflation. Both of the axion and effective VEV of the gauge field are pseudo-scalars (see eqs. (2.7)–(2.8) and figure 3). As a result, both P and CP are spontaneously broken by the vacuum. Although the background evolution is insensitive to that symmetry breaking, cosmic perturbations with spin, e.g., fermions, and spin-2 fields notice that and become chiral (see figure 1). In particular, the P-violation leads to (a short phase of tachyonic) production of the spin-2 field of the perturbed gauge field which produces chiral primordial gravitational waves. Fermions are even more sensitive to the structure of the vacuum as a consequence of the celebrated Atiyah-Singer index theorem. As first pointed out in [14, 23, 24], the spontaneous CP-violation and non-trivial topology of this vacuum with $\langle R\tilde{R}\rangle \neq 0$, provides a natural leptogenesis setting via the gravitational anomaly in SM. In this work, we unveiled yet another unique aspect of such SU(2)-axion vacuum for fermions which might open a new window toward particle cosmology.

In the context of SU(2)-axion inflation models, we considered a (dark) massive Dirac fermion doublet charged under the SU(2) gauge field and (for the sake of completeness, possibly) derivatively coupled to the axion. This setup has been recently introduced in [13] in which the fermion backreaction to the gauge field background has been numerically computed for a small part of the parameter space, i.e., $m \sim H$. Here, we extensively and analytically studied the system and using the point-splitting regularization skim computed the induced currents (eqs. (6.19), (6.23), and (6.27)). The net fermion number vanishes due to the C-symmetry. However, the isospin current, $J^{\mu a}\mathbf{T}_a$, and the chiral current, J^μ_5, are non-zero. We found that the dark fermion's backreaction, $\mathcal{J} = \frac{1}{3a}\delta^i_a \langle J^a_i\rangle$, and its chiral charge, $Q_5 = \langle J^t_5\rangle$, are almost constant during inflation. They are both proportional to the scale of inflation as H^3, the two sources of CP-violation ξ_A and ξ_φ (corresponding to the VEV of the gauge field and axion), and both increases with the mass of the fermion which explicitly

JHEP07(2020)154

breaks the chiral symmetry in the fermionic sector (section 7.1). In fact, the massless Dirac fermions enjoy conformal and chiral symmetries and have zero (tree-level) induced currents. The massless fermions only have a non-zero chiral charge and therefore backreacts to axion field according to the celebrated Adler-Bell-Jackiw anomaly. Besides, the currents vanish in the absence of the CP-breaking the vacuum. We compared the production of charged scalars with fermions of this setup in section 7.1.1. Interestingly, the vacuum produces more fermions than scalars in two limits; i) when the mass of the corresponding field is higher than Hubble during inflation, i.e., $m > H$, and ii) in large ξ_A limit. Apart from explicit computation for the SU(2)-axion vacuum in section 6, based on symmetries in sections 3 and 7, we explained why the fermion currents should increase with the mass regardless of the source, whether it is the VEV of a SU(2), U(1), or an axion. At first glance, this behavior seems counter-intuitive. However, the present and similar studies which were carried out in de Sitter, are perturbative computations based on assuming a classical background with infinite energy that can always source and support the particle production. However, once the size of backreaction becomes sizable, that approximation is not valid anymore.

We realized that the spontaneous CP-violation during inflation naturally leads to a new and efficient mechanism to generate non-thermal massive dark fermions during inflation. That is regardless of the details of the specific SU(2)-axion model. The size of the fermionic backreaction as well as the present-day density fraction of dark matter put upper bounds on the fermion's mass respectively as $10^2\ H$ (eq. (7.8)) and $(10^{10}\frac{M_{\rm Pl}}{H})^{\frac{1}{4}}$ GeV (eq. (8.8)). In deriving the latter, we assumed that the heavy fermions are only gravitationally coupled to the rest of the visible and dark sectors. For a GUT scale inflation, the dark fermions can be as heavy as 10 TeV.

The generated dark fermions can be very massive, which depending on the efficiency of their possible feebly interactions with the visible sector, may decay to the visible and lighter dark sectors once the temperature drops below their mass. In other words, these Dirac fermions may replace the right-handed neutrinos in the standard thermal leptogenesis scenario and hence provide a novel natural scenario to explain the observed matter asymmetry in the Universe. However, this possibility, as well as the late time macroscopic properties of the produced (self-interacting) dark fermions as a dark matter sector, are all highly model-dependent. These promising possibilities depend on the value of the gauge coupling, g_A, the possible mass of the gauge field after inflation, and the details of the possible feebly interactions of the dark fermions with themselves and the visible sector which is beyond the scope of the current work and we leave for future exhaustive study.

Acknowledgments

Special thanks go to Eiichiro Komatsu for stimulating discussions over the years and bringing the importance of Schwinger effect in the early universe into my attention which led to a series of papers including the current work. I appreciate Kaloian Lozanov for his collaboration in the early stage of the project. I am grateful to David Curtin, Gia Dvali, Elisa Ferreira, Mohammad Khorrami, Yuki Watanabe, and Fabian Schmidt for valuable discussions.

JHEP07(2020)154

A Mathematical tools

For the sake of self-sufficiency, this appendix reviews mathematical tools that we use throughout this work. This overview includes the definition of the direct sum and product, the spinor covariant derivative, and Whittaker functions, respectively.

A.1 Direct sum and product

The vector space $\mathbf{V}$, is the direct sum of two subspaces, $\mathbf{U_1}$ and $\mathbf{U_2}$, as

$$\mathbf{V} = \mathbf{U_1} \oplus \mathbf{U_2}, \tag{A.1}$$

if and only if $\mathbf{V} = \mathbf{U_1} + \mathbf{U_2}$, and $\mathbf{U_1}$ and $\mathbf{U_2}$ are independent. The Kronecker product of two matrices, $\mathbf{A}_{m\times n}$ and $\mathbf{B}_{q\times p}$, is defined as a $mp \times nq$ block matrix given by

$$\mathbf{A} \otimes \mathbf{B} = \begin{pmatrix} A_{11}\mathbf{B} & \dots & A_{1n}\mathbf{B} \\ & \ddots & \\ A_{m1}\mathbf{B} & \dots & A_{mn}\mathbf{B} \end{pmatrix}. \tag{A.2}$$

A.2 Spinor covariant derivative

The 8-spinor covariant derivative in (2.3) is

$$D_\mu \otimes \gamma^\alpha \tilde{\psi} \equiv (\mathbf{I}_2 \nabla_\mu - i g_A \mathbf{A}_\mu) \otimes \gamma^\alpha \tilde{\psi}\,, \tag{A.3}$$

where the spin covariant derivative is

$$\nabla_\mu \tilde{\psi} = [\mathrm{I}_4 \partial_\mu + \omega_\mu]\tilde{\psi}, \tag{A.4}$$

with ω_μ being the spin-connections

$$\omega_\mu = -\frac{i}{2}\omega_\mu{}^{\alpha\beta}\sigma_{\alpha\beta}, \tag{A.5}$$

and $\sigma_{\alpha\beta} = \frac{i}{4}[\gamma_\alpha, \gamma_\beta]$ being the spinor generators of the Lorentz algebra. The elements of the spin-connection $\omega_\mu{}^{\alpha\beta}$ are given by

$$\omega_\mu{}^{\alpha\beta} = \mathbf{e}_\nu{}^\alpha \nabla_\mu \mathbf{e}^{\nu\beta}. \tag{A.6}$$

In FLRW spacetime using the conformal time, the verbeins are

$$\mathbf{e}^\mu{}_\alpha = a(\tau)^{-1}\delta^\mu_\alpha, \tag{A.7}$$

and the only non-zero components of the spin connection coefficients are

$$\omega_\mu{}^{i0} = -\omega_\mu{}^{0i} = -\mathcal{H}\delta^i_\mu. \tag{A.8}$$

JHEP07(2020)154

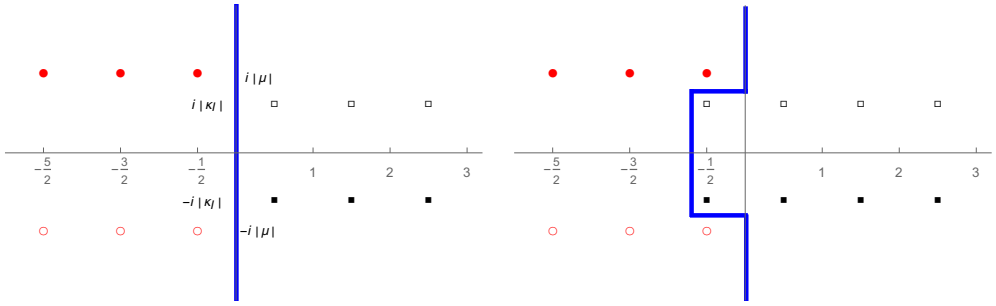

Figure 21. Positions of poles $\alpha_{n,\pm}$ (circles) and $\tilde{\alpha}_{n,s}$ (squares) and the possible contouring for the validity of the Mellin-Barnes integral representation in (A.12) are shown where κ_I is the imaginary part of κ and $m \neq 0$. In the left panel, we show the locations of poles for $\mathrm{Re}\kappa = -\frac{1}{2}$ and in the right panel we have the poles for $Re\kappa = \frac{1}{2}$. The Mellin-Barnes integral is valid for any closed contour as far as it separates the circle poles from the square poles and it runs from $-i\infty$ to $+i\infty$.

A.3 Whittaker functions

Whittaker functions $W_{\kappa,\mu}(z)$ and $M_{\kappa,\mu}(z)$ take the following aymptotic forms in the limit $|\, z \,| \to \infty$

$$W_{\kappa,\mu}(z) \to z^{\kappa} e^{-z/2}, \tag{A.9}$$

$$M_{\kappa,\mu}(z) \to \Gamma(2\mu+1)\left(\frac{i(-1)^{\mu-\kappa} z^{\kappa} e^{-z/2}}{\Gamma(-\kappa+\mu+\frac{1}{2})} + \frac{z^{-\kappa} e^{z/2}}{\Gamma(-\kappa+\mu+\frac{1}{2})}\right), \tag{A.10}$$

where $|\arg z| < \frac{3}{2}\pi$. Thus, for a complex κ, we have

$$\lim_{\tau \to -\infty} (2\tilde{\tau})^{-\kappa_{\mathrm{R}}} e^{-\kappa_{\mathrm{I}}\pi/2} W_{\kappa,\mu}(-2i\tilde{\tau}) = e^{-ik\tau}, \tag{A.11}$$

where κ_{R} and κ_{I} are the real and imaginary parts of κ.

The Mellin-Barnes integral representation of the Whittaker functions is [39]

$$W_{\kappa,\mu}(z) = \frac{e^{-\frac{z}{2}}}{2i\pi} \int_{\mathcal{C}_\alpha} \frac{\Gamma(\frac{1}{2}+\mu+\alpha)\Gamma(\frac{1}{2}-\mu+\alpha)\Gamma(-\kappa-\alpha)}{\Gamma(\frac{1}{2}+\mu-\kappa)\Gamma(\frac{1}{2}-\mu-\kappa)} z^{-\alpha} d\alpha \quad \text{where} \quad |\arg(z)| < \frac{3}{2}\pi, \tag{A.12}$$

which holds when

$$\frac{1}{2} \pm \mu - \kappa \neq 0, -1, -2, \ldots,$$

and the contour of the integration, $\mathcal{C}_\alpha$, separates the poles of $\Gamma(\frac{1}{2}+\mu+\alpha)\Gamma(\frac{1}{2}-\mu+\alpha)$ at

$$\alpha_{n,\pm} = -\frac{1}{2} - n \pm \mu \quad \forall n \in \mathbb{N}, \tag{A.13}$$

and the poles of $\Gamma(-\kappa-\alpha)$ at

$$\tilde{\alpha}_n = -\kappa + n \quad \forall n \in \mathbb{N}, \tag{A.14}$$

from each other as we show in figure 21. In our setup, $\mu^p = i|\mu^p|$ is pure imaginary and κ_s^p is a complex number with a real part equal to $|\mathrm{Re}\kappa| = \frac{1}{2}$.

JHEP07(2020)154

B Color-spin helicity

This appendix gives a self-contained derivation of the split of our setup as $\Psi^+ \oplus \Psi^-$. It is a brief review of appendix B of [13] by the author, which generalized the $2d$ helicity representation to the $4d$ color-spin helicity frame (c-helicity).

B.1 $\Psi^+ \oplus \Psi^-$

At this point, it is more insightful to go to the Fourier space and write the system in the Weyl frame. The 8-spinor in the isospin frame can be written in the Weyl frame as

$$\tilde{T}_1 \begin{pmatrix} \Psi^1 \\ \Psi^2 \end{pmatrix} = \begin{pmatrix} \Psi_L \\ \Psi_R \end{pmatrix},$$

where $\tilde{T}_1$ is the following 8×8 unitary matrix

$$\tilde{T}_1 = \frac{1}{\sqrt{2}} \begin{pmatrix} \mathbf{I}_2 & -\mathbf{I}_2 & \mathbf{0} & \mathbf{0} \\ \mathbf{0} & \mathbf{0} & \mathbf{I}_2 & -\mathbf{I}_2 \\ \mathbf{I}_2 & \mathbf{I}_2 & \mathbf{0} & \mathbf{0} \\ \mathbf{0} & \mathbf{0} & \mathbf{I}_2 & \mathbf{I}_2 \end{pmatrix}. \tag{B.1}$$

Moreover, the $\mathbf{I}_2 \otimes \gamma^\alpha$ operators transform as

$$\tilde{T}_1.(\mathbf{I}_2 \otimes \gamma^\alpha).\tilde{T}_1^{-1} = \begin{pmatrix} \mathbf{0} & \mathbf{0} & \boldsymbol{\sigma}^\alpha & \mathbf{0} \\ \mathbf{0} & \mathbf{0} & \mathbf{0} & \boldsymbol{\sigma}^\alpha \\ \bar{\boldsymbol{\sigma}}^\alpha & \mathbf{0} & \mathbf{0} & \mathbf{0} \\ \mathbf{0} & \bar{\boldsymbol{\sigma}}^\alpha & \mathbf{0} & \mathbf{0} \end{pmatrix}, \tag{B.2}$$

where $\boldsymbol{\sigma}^\alpha$ and $\bar{\boldsymbol{\sigma}}^\alpha$ are

$$\boldsymbol{\sigma}^\alpha = (\mathbf{I}_2, \boldsymbol{\sigma}^i) \quad \text{and} \quad \bar{\boldsymbol{\sigma}}^\alpha = (\mathbf{I}_2, -\boldsymbol{\sigma}^i), \tag{B.3}$$

and their indices are lowered with the Minkowski metric, i.e. $\boldsymbol{\sigma}_\alpha = \eta_{\alpha\beta}\boldsymbol{\sigma}^\beta$. In the Weyl frame, the action (2.13) takes the following form

$$S_\Psi = \int \mathrm{d}\tau \mathrm{d}k^3 (\Psi^\dagger_{R,\mathbf{k}} \Psi^\dagger_{L,\mathbf{k}}) \,.\, \tilde{\mathrm{L}}_\mathbf{k}(\tau) \,.\, \begin{pmatrix} \Psi_{L,\mathbf{k}} \\ \Psi_{R,\mathbf{k}} \end{pmatrix}, \tag{B.4}$$

where $\tilde{\mathrm{L}}_\mathbf{k}(\tau)$ is a 8×8 operator given as

$$\tilde{\mathrm{L}}_\mathbf{k}(\tau) \equiv i \begin{pmatrix} i\mu_\mathrm{m}\mathcal{H}\mathrm{I}_4 & \mathrm{I}_4\partial_\tau + i\Sigma_4(\tau, \boldsymbol{k}) \\ \mathrm{I}_4\partial_\tau - i\Sigma_4(\tau, \boldsymbol{k}) & i\mu_\mathrm{m}\mathcal{H}\mathrm{I}_4 \end{pmatrix}, \tag{B.5}$$

and Σ_4 is the following 4×4 operator

$$\Sigma_4(\tau, \boldsymbol{k}) = \mathbf{I}_2 \otimes k^i.\boldsymbol{\sigma}_i + \mathcal{H}\left(2\xi_\varphi \mathrm{I}_4 - \frac{\xi_A}{2}\boldsymbol{\tau}^i \otimes \boldsymbol{\sigma}_i\right). \tag{B.6}$$

As we see in eq. (B.5), in the absence of μ_m, massless case, the system in eq. (B.4) is decomposed into two independent sub-sectors in terms of the L- and R-handed fields. However, in the massive case, we need to take one step further.

JHEP07(2020)154

The ideal frame would be the one in which Σ_4 is diagonalized. Such frame, if exists, must be made of the common eigenstates of the helicity operator, $\mathbf{I}_2 \otimes k^i.\boldsymbol{\sigma}_i$, and $\boldsymbol{\tau}^i \otimes \boldsymbol{\sigma}_i$. However, these two operators have only two common eigenstates. Thus, Σ_4 is only block-diagonalizable and reducible up to two subspaces.

As a mathematical tool, we define the color-spin helicity operator for any given 4-momentum k^α, as

$$\mathfrak{h}(k^\alpha) \equiv \frac{\delta_{ia}}{k^2}\; k^i.\boldsymbol{\tau}^a \otimes k^j.\boldsymbol{\sigma}_j, \tag{B.7}$$

in which the first Pauli matrix is a $su(2)$ generator while the second one is the spin operator. The orthonormal eigenstates of this operator are

$$\begin{aligned}
E^+{}_+(k^\alpha) &= \frac{\check{k}^\alpha \bar{\boldsymbol{\tau}}_\alpha \otimes \check{k}^\beta \bar{\boldsymbol{\sigma}}_\beta}{2k(k+k^3)} \begin{pmatrix} 1\\0\\0\\0 \end{pmatrix}, \qquad E^+{}_-(k^\alpha) = -\frac{\check{k}^\alpha \boldsymbol{\tau}_\alpha \otimes \check{k}^\beta \boldsymbol{\sigma}_\beta}{2k(k+k^3)} \begin{pmatrix} 0\\0\\0\\1 \end{pmatrix}, \\
E^-{}_+(k^\alpha) &= -\frac{\check{k}^\alpha \boldsymbol{\tau}_\alpha \otimes \check{k}^\beta \bar{\boldsymbol{\sigma}}_\beta}{2k(k+k^3)} \begin{pmatrix} 0\\0\\1\\0 \end{pmatrix}, \qquad E^-{}_-(k^\alpha) = -\frac{\check{k}^\alpha \bar{\boldsymbol{\tau}}_\alpha \otimes \check{k}^\beta \boldsymbol{\sigma}_\beta}{2k(k+k^3)} \begin{pmatrix} 0\\1\\0\\0 \end{pmatrix},
\end{aligned} \tag{B.8}$$

where $\check{k}^\alpha$ is a four vector given as

$$\check{k}^\alpha \equiv (k, \boldsymbol{k}) \quad \text{where} \quad k = \sqrt{k^i.k^i}. \tag{B.9}$$

Thus, $\check{k}^\alpha$ is the four momentum of the massless field. The c-helicity $\mathfrak{h}(k^\alpha)$, and helicity $\mathbf{I}_2 \otimes k^i\boldsymbol{\sigma}_i$, have 4 eigenstates in common. However, $\mathfrak{h}(k^\alpha)$ and $\boldsymbol{\tau}^i \otimes \boldsymbol{\sigma}_i$ have only two common eigenstates. More precisely, $E^p{}_s(k^\alpha)$ with $p = \pm$ and $s = \pm$ satisfies the eigenstate equations

$$\mathbf{I}_2 \otimes k^i.\boldsymbol{\sigma}_i \; E^p{}_s(k^\alpha) = s \; kE^p{}_s(k^\alpha)\,, \tag{B.10}$$

and the orthonormality condition

$$E^{p\dagger}_s(k^\alpha) \cdot E^{p'}{}_{s'}(k^\alpha) = \delta_{ss'}\delta^{pp'}\,. \tag{B.11}$$

However, only $p = +$ elements of $E^p{}_s(k^\alpha)$ are eigenstates of $\boldsymbol{\tau}^i \otimes \boldsymbol{\sigma}_i$ as well

$$\boldsymbol{\tau}^i \otimes \; \boldsymbol{\sigma}_i E^+{}_s(k^\alpha) = E^+{}_s(k^\alpha). \tag{B.12}$$

The $E^p{}_s(k^\alpha)$ make an orthonormal basis and hence the following unitary matrix

$$R_{\mathbf{k}} = \left[E^+{}_+(k^\alpha)\; E^+{}_-(k^\alpha)\; E^-{}_+(k^\alpha)\; E^-{}_-(k^\alpha)\right] = \begin{pmatrix} e^+{}_{+1} & e^+{}_{-1} & e^-{}_{+1} & e^-{}_{-1} \\ e^+{}_{+2} & e^+{}_{-2} & e^-{}_{+2} & e^-{}_{-2} \\ e^+{}_{+3} & e^+{}_{-3} & e^-{}_{+3} & e^-{}_{-3} \\ e^+{}_{+4} & e^+{}_{-4} & e^-{}_{+4} & e^-{}_{-4} \end{pmatrix}, \tag{B.13}$$

where $e^p{}_{si}$ is the ith element of the $E^p{}_s(k^\alpha)$. For each given momentum k^α, $R_{\mathbf{k}}$ takes the Weyl spinors to their c-helicity frame. Notice that the definition of $R_{\mathbf{k}}$ is a bit different than

JHEP07(2020)154

the corresponding matrix in [13]. More precisely, comparing with [13], here we switched the orders of 3rd and 4th columns.

The 8-spinor in the Weyl representation can transformed to the c-helicity state as

$$\tilde{R}_{\mathbf{k}}\begin{pmatrix}\Psi_{L,\mathbf{k}}\\ \Psi_{R,\mathbf{k}}\end{pmatrix}=\begin{pmatrix}\mathbf{\Psi}^{+}_{L,\mathbf{k}}\\ \mathbf{\Psi}^{-}_{L,\mathbf{k}}\\ \mathbf{\Psi}^{+}_{R,\mathbf{k}}\\ \mathbf{\Psi}^{-}_{R,\mathbf{k}}\end{pmatrix}, \tag{B.14}$$

where $\tilde{R}_{\mathbf{k}}$ is the following 8×8 unitary operator

$$\tilde{R}_{\mathbf{k}}\equiv \mathbf{I}_2\otimes R^{-1}_{\mathbf{k}}. \tag{B.15}$$

This split would be clearer if we take another unitary transformation

$$\tilde{S}=\begin{pmatrix}\mathbf{I}_2 & 0 & 0 & 0\\ 0 & 0 & \mathbf{I}_2 & 0\\ 0 & \mathbf{I}_2 & 0 & 0\\ 0 & 0 & 0 & \mathbf{I}_2\end{pmatrix}. \tag{B.16}$$

In fact, $\tilde{S}\tilde{R}_{\mathbf{k}}$ takes the 8-spinor transforms in Weyl frame to the c-helicity frame

$$\tilde{S}\tilde{R}_{\mathbf{k}}\begin{pmatrix}\Psi_{L,\mathbf{k}}\\ \Psi_{R,\mathbf{k}}\end{pmatrix}=\begin{pmatrix}\Psi^{+}_{\mathbf{k},W}\\ \Psi^{-}_{\mathbf{k},W}\end{pmatrix}=\begin{pmatrix}\mathbf{\Psi}^{+}_{L,\mathbf{k}}\\ \mathbf{\Psi}^{+}_{R,\mathbf{k}}\\ \mathbf{\Psi}^{-}_{L,\mathbf{k}}\\ \mathbf{\Psi}^{-}_{R,\mathbf{k}}\end{pmatrix}. \tag{B.17}$$

As a result, the Lagrangian operator becomes the following block diagonal 8×8 matrix

$$L_{\mathbf{k},W}(\tau)=\tilde{S}\tilde{R}_{\mathbf{k}}\,.\,\tilde{L}_{\mathbf{k},W}(\tau)\,.\,(\tilde{S}\tilde{R}_{\mathbf{k}})^{-1}=\begin{pmatrix}L^{+}_{\mathbf{k},W}(\tau) & 0\\ 0 & L^{-}_{\mathbf{k},W}(\tau)\end{pmatrix}, \tag{B.18}$$

where $L^{\pm}_{\mathbf{k},W}(\tau)$ are the following 4×4 operations

$$L^{\pm}_{\mathbf{k},W}(\tau)\equiv i\begin{pmatrix}i\mu_{\mathrm{m}}\mathcal{H}\mathbf{I}_2 & \mathbf{I}_2\partial_\tau+i\check{\mathbf{\Sigma}}^{\pm}(\tau,\boldsymbol{k})\\ \mathbf{I}_2\partial_\tau-i\check{\mathbf{\Sigma}}^{\pm}(\tau,\boldsymbol{k}) & i\mu_{\mathrm{m}}\mathcal{H}\mathbf{I}_2\end{pmatrix}. \tag{B.19}$$

Here, $\check{\mathbf{\Sigma}}^{\pm}(\tau,\boldsymbol{k})$ are given as

$$\check{\mathbf{\Sigma}}^{+}\equiv k\boldsymbol{\sigma}^3+\left(2\xi_\varphi-\frac{\xi_A}{2}\right)\mathcal{H}\mathbf{I}_2\quad\text{and}\quad\check{\mathbf{\Sigma}}^{-}\equiv k\boldsymbol{\sigma}^3+\left(2\xi_\varphi+\frac{\xi_A}{2}\right)\mathcal{H}\mathbf{I}_2-\xi_A\mathcal{H}\boldsymbol{\sigma}^1\,. \tag{B.20}$$

Therefore, the theory in eq. (B.4) splits into two subsectors as

$$S_\Psi[\tilde{\Psi}]=S_+[\Psi^{+}_{W}]+S_-[\Psi^{-}_{W}], \tag{B.21}$$

where

$$S_\pm=\int\frac{\mathrm{d}\tau\mathrm{d}k^3}{(2\pi)^3}\bar{\Psi}^{\pm}_{\mathbf{k},W}\,.\,\tilde{\mathrm{L}}^{\pm}_{\mathbf{k},W}(\tau)\,.\Psi^{\pm}_{\mathbf{k},W}. \tag{B.22}$$

JHEP07(2020)154

The $\tilde{\mathrm{L}}^{\pm}_{\mathbf{k},W}(\tau)$ operators are given as

$$\tilde{\mathrm{L}}^{+}_{\mathbf{k},W}(\tau) \equiv \left[i\gamma^0_{\mathrm{W}}\partial_\tau - k\gamma^3_{\mathrm{W}} - \left(2\xi_\varphi - \frac{\xi_A}{2}\right)\mathcal{H}\gamma^0_{\mathrm{W}}\gamma^5_{\mathrm{W}} - \mu_{\mathrm{m}}\mathcal{H}\mathrm{I}_4 \right], \tag{B.23}$$

$$\tilde{\mathrm{L}}^{-}_{\mathbf{k},W}(\tau) \equiv \left[i\gamma^0_{\mathrm{W}}\partial_\tau - k\gamma^3_{\mathrm{W}} + \gamma^1_{\mathrm{W}}\xi_A\mathcal{H} - \left(2\xi_\varphi + \frac{\xi_A}{2}\right)\mathcal{H}\gamma^0_{\mathrm{W}}\gamma^5_{\mathrm{W}} - \mu_{\mathrm{m}}\mathcal{H}\mathrm{I}_4 \right], \tag{B.24}$$

where $\gamma^\alpha_{\mathrm{W}}$s are the gamma matrices in the Weyl representation and notice that

$$\gamma^0_{\mathrm{W}}\gamma^5_{\mathrm{W}} = \gamma^0\gamma^5 = \begin{pmatrix} 0 & \mathbf{I}_2 \\ -\mathbf{I}_2 & 0 \end{pmatrix}. \tag{B.25}$$

Up to now, we split the 8-spinor system into two 4-spinor systems each in a Weyl representation (see eq. (B.17)). For the quantization purposes, it is more convenient to write the 4-d fields in the Dirac frame. The Weyl 4-spinors can be transformed to their Dirac representation as

$$\Psi^{\pm}_{\mathrm{D}} = \mathcal{D}\,\Psi^{\pm}, \tag{B.26}$$

where

$$\mathcal{D} = \frac{1}{\sqrt{2}}\begin{pmatrix} \mathbf{I}_2 & \mathbf{I}_2 \\ -\mathbf{I}_2 & \mathbf{I}_2 \end{pmatrix} \quad \text{and} \quad \tilde{\mathcal{D}} = \mathbf{I}_2 \otimes \mathcal{D}. \tag{B.27}$$

The gamma matrices in the Weyl representation, $\gamma^\alpha_{\mathrm{W}}$, and Dirac representation, γ^α, are related as $\gamma^\alpha = \mathcal{D}\gamma^\alpha_{\mathrm{W}}\mathcal{D}^{-1}$. Therefore, the operator $\tilde{T}_{2,\mathbf{k}}$ defined as

$$\tilde{T}_{2,\mathbf{k}} \equiv \tilde{\mathcal{D}}\tilde{S}\tilde{R}_{\mathbf{k}}, \tag{B.28}$$

transforms the 8-spinor in the Weyl frame to the final Dirac frame as

$$\tilde{T}_{2,\mathbf{k}}\begin{pmatrix} \Psi_{L,\mathbf{k}} \\ \Psi_{R,\mathbf{k}} \end{pmatrix} = \begin{pmatrix} \Psi^{+}_{\mathbf{k}} \\ \Psi^{-}_{\mathbf{k}} \end{pmatrix}, \tag{B.29}$$

where now $\Psi^{\pm}_{\mathbf{k}}$ are each in a Dirac frame. The matrix operators from the isospin to this final extended helicity representation are transformed as

$$\tilde{T}_{2,\mathbf{k}}\ \mathbf{I}_2 \otimes \gamma^0\ \tilde{T}^{-1}_{2,\mathbf{k}} = \mathbf{I}_2 \otimes \gamma^0, \tag{B.30}$$

$$\tilde{T}_{2,\mathbf{k}}\ \mathbf{I}_2 \otimes \gamma^0\gamma^5\ \tilde{T}^{-1}_{2,\mathbf{k}} = \mathbf{I}_2 \otimes \gamma^0\gamma^5, \tag{B.31}$$

and

$$\delta^\alpha_a\tilde{T}_{2,\mathbf{k}}\ \mathbf{T}^a \otimes \gamma^\alpha\ \tilde{T}^{-1}_{2,\mathbf{k}} = \begin{pmatrix} \frac{1}{2}\gamma^0\gamma^5 & 0 \\ 0 & -\frac{1}{2}\gamma^0\gamma^5 + \gamma^1 \end{pmatrix}. \tag{B.32}$$

Finally, the theory in eq. (B.4) splits into two subsectors in terms of the plus and minus spinors as

$$S_\Psi[\tilde{\Psi}] = S^{+}[\Psi^{+}] + S^{-}[\Psi^{-}], \tag{B.33}$$

where

$$S^{\pm} = \int \frac{\mathrm{d}\tau \mathrm{d}k^3}{(2\pi)^3}\bar{\Psi}^{\pm}_{\mathbf{k}}\ .\ \tilde{\mathrm{L}}^{\pm}_{\mathbf{k},}(\tau)\ .\Psi^{\pm}_{\mathbf{k}}, \tag{B.34}$$

JHEP07(2020)154

with $\tilde{\mathrm{L}}^{\pm}_{\mathbf{k}}(\tau)$ as

$$\tilde{\mathrm{L}}^{+}_{\mathbf{k}}(\tau) \equiv \left[i\gamma^0\partial_\tau - k\gamma^3 - \left(2\xi_\varphi - \frac{\xi_A}{2}\right)\mathcal{H}\gamma^0\gamma^5 - \mu_{\mathrm{m}}\mathcal{H}\mathrm{I}_4 \right], \tag{B.35}$$

$$\tilde{\mathrm{L}}^{-}_{\mathbf{k}}(\tau) \equiv \left[i\gamma^0\partial_\tau - k\gamma^3 - \left(2\xi_\varphi + \frac{\xi_A}{2}\right)\mathcal{H}\gamma^0\gamma^5 - \mu_{\mathrm{m}}\mathcal{H}\mathrm{I}_4 + \gamma^1\xi_A\mathcal{H} \right]. \tag{B.36}$$

This completed the proof that our theory splits into two irreducible representations as

$$\tilde{\Psi}_{\mathbf{k}} = \Psi^{+}_{\mathbf{k}} \oplus \Psi^{-}_{\mathbf{k}}. \tag{B.37}$$

C Charge conjugation and parity

In this appendix, we focus on the discrete symmetries, charge conjugation, and parity. Sections C.1 and C.2 investigate the action of the charge conjugation and parity on the theory, respectively.

C.1 Charge conjugation

At this point, we work out the charge conjugation operator and will show it is a symmetry of the theory in eq. (2.13), i.e.

$$\mathcal{L}_\Psi = i\bar{\tilde{\Psi}}\left[\mathbf{I}_2\partial_\tau \otimes \gamma^0 + \left(\mathbf{I}_2\partial_i - \frac{i}{2}\xi_A\mathcal{H}\boldsymbol{\tau}^i\right)\otimes\gamma_i + i\mu_{\mathrm{m}}\mathcal{H}\mathrm{I}_8 + 2i\xi_\varphi\mathcal{H}\mathbf{I}_2\otimes(\gamma^0\gamma^5)\right]\tilde{\Psi}. \tag{C.1}$$

Notice that the action above is presented in the real space and isospin frame. We define the charge conjugated field as

$$\tilde{\Psi}_C \equiv \tilde{C}\ \bar{\tilde{\Psi}}^T, \tag{C.2}$$

where $\tilde{C}$ is the charge conjugation operator, and T superscript stands for transpose with respect to Lorentz indices. Under the action of the charge conjugation the fermion charge g_A will go to $g_{A,C} = -g_A$ which implies

$$\xi_{A,C} = \frac{g_{A,C}\psi}{H} = -\xi_A. \tag{C.3}$$

Moreover, $\tilde{C}$ is a 8×8 matrix which satisfies

$$\tilde{C}^{-1}\mathbf{I}_2\otimes\gamma^\alpha\tilde{C} = -\mathbf{I}_2\otimes\gamma^{\alpha T}. \tag{C.4}$$

The $\tilde{C}$ matrix can be written as

$$\tilde{C} = \mathbf{I}_2\otimes C \quad \text{where} \quad C = i\gamma^2\gamma^0, \tag{C.5}$$

and $\tilde{C}^{-1} = \mathbf{I}_2\otimes C^{-1}$. Then it is straightforward to check the following equalities

$$\tilde{C}^{-1}\boldsymbol{\tau}^i\otimes\gamma_i\tilde{C} = -\boldsymbol{\tau}^i\otimes\gamma_i^T, \tag{C.6}$$

$$\tilde{C}^{-1}\mathbf{I}_2\otimes(\gamma^0\gamma^5)\tilde{C} = \mathbf{I}_2\otimes(\gamma^0\gamma^5)^T. \tag{C.7}$$

JHEP07(2020)154

Now lets $\tilde{C}$ acts on action in eq. (C.1). Here for the $\tilde{\Psi}_C$ field with charge $-g_A$, the action is

$$\mathcal{L}_{\Psi,C} = i\bar{\tilde{\Psi}}_C\left[\mathbf{I}_2\partial_\tau\otimes\gamma^0+\left(\mathbf{I}_2\partial_i+\frac{i}{2}\xi_A\mathcal{H}\boldsymbol{\tau}^i\right)\otimes\gamma_i+i\mu_{\rm m}\mathcal{H}\mathrm{I}_8+2i\xi_\varphi\mathcal{H}\mathbf{I}_2\otimes(\gamma^0\gamma^5)\right]\tilde{\Psi}_C,$$

which can be written in terms of $\tilde{\Psi}$ as

$$\begin{aligned}
\mathcal{L}_{\Psi,C} &= -i\tilde{\Psi}^T\tilde{C}^{-1}\left[\mathbf{I}_2\partial_\tau\otimes\gamma^0+\left(\mathbf{I}_2\partial_i+\frac{i}{2}\xi_A\mathcal{H}\boldsymbol{\tau}^i\right)\otimes\gamma_i+i\mu_{\rm m}\mathcal{H}\mathrm{I}_8+2i\xi_\varphi\mathcal{H}\mathbf{I}_2\otimes(\gamma^0\gamma^5)\right]\tilde{C}\bar{\tilde{\Psi}}^T\\
&= i\tilde{\Psi}^T\left[\mathbf{I}_2\partial_\tau\otimes\gamma^{0T}+\left(\mathbf{I}_2\partial_i+\frac{i}{2}\xi_A\mathcal{H}\boldsymbol{\tau}^i\right)\otimes\gamma_i^T-i\mu_{\rm m}\mathcal{H}\mathrm{I}_8-2i\xi_\varphi\mathcal{H}\mathbf{I}_2\otimes(\gamma^0\gamma^5)^T\right]\bar{\tilde{\Psi}}^T\\
&= -i\bar{\tilde{\Psi}}\left[\mathbf{I}_2\overleftarrow{\partial}_\tau\otimes\gamma^0+\left(\mathbf{I}_2\overleftarrow{\partial}_i+\frac{i}{2}\xi_A\mathcal{H}\boldsymbol{\tau}^i\right)\otimes\gamma_i-i\mu_{\rm m}\mathcal{H}\mathrm{I}_8-2i\xi_\varphi\mathcal{H}\mathbf{I}_2\otimes(\gamma^0\gamma^5)\right]\tilde{\Psi}\\
&= i\bar{\tilde{\Psi}}\left[\mathbf{I}_2\partial_\tau\otimes\gamma^0+\left(\mathbf{I}_2\partial_i-\frac{i}{2}\xi_A\mathcal{H}\boldsymbol{\tau}^i\right)\otimes\gamma_i+i\mu_{\rm m}\mathcal{H}\mathrm{I}_8+2i\xi_\varphi\mathcal{H}\mathbf{I}_2\otimes(\gamma^0\gamma^5)\right]\tilde{\Psi},
\end{aligned}\tag{C.8}$$

where the second to third line has passed by transposition and using the fact that Ψ and $\bar{\Psi}$ anti-commute and in the fourth line we dropped the total derivative terms. By an abuse of notation, it implies

$$\mathcal{L}_{\Psi,C} = \mathcal{L}_\Psi.\tag{C.9}$$

That completed our proof that our action is invariant under the charge conjugation and therefore C-symmetric.

Equation (C.2) implies that the Fourier modes of the spinor and its charge conjugated field are related as

$$\tilde{\Psi}_{C\mathbf{k}} = i\mathbf{I}_2\otimes\gamma^2\ \tilde{\Psi}^*_{-\mathbf{k}}.\tag{C.10}$$

Going to the c-helicity frame, the above reduces to the following form

$$\Psi^\pm_{C\mathbf{k}} = i\gamma^2\ \Psi^{\pm *}_{-\mathbf{k}}.\tag{C.11}$$

C.2 Parity

Now lets explore the action of parity on the setup, which takes $x^\mu = (\tau,\mathbf{x})$ to $x^\mu_P = (\tau,-\mathbf{x})$, and hence

$$\partial_i \to \partial_{i,P} \equiv -\partial_i.\tag{C.12}$$

Besides, the gamma matrices under P transform as

$$P\gamma^0P^{-1} = \gamma^0 \quad\text{and}\quad P\gamma^iP^{-1} = -\gamma^i.\tag{C.13}$$

The VEV of the axion and SU(2) fields transform as

$$P\varphi(t)P^{-1} = -\varphi(t),\tag{C.14}$$

$$PA^a_i(t)P^{-1} = -A^a_i(t),\tag{C.15}$$

which implies that $\xi_{A,P} = -\xi_A$, and $\xi_{\varphi,P} = -\xi_\varphi$. Under the action of parity, the spinor transforms as

$$\tilde{\Psi}_P(\tau,\mathbf{x}) \equiv \tilde{P}\tilde{\Psi}(\tau,\mathbf{x}) = \tilde{\Psi}(\tau,-\mathbf{x}),\tag{C.16}$$

JHEP07(2020)154

where $\tilde{P}$ is the 8×8 parity matrix given as

$$\tilde{P} = \mathbf{I}_2 \otimes P. \tag{C.17}$$

The theory in eq. (C.1) can be written in terms of the parity transformed field as

$$\begin{aligned}\mathcal{L}_\Psi(\tau,\mathbf{x}) &= i\bar{\tilde{\Psi}}_P \tilde{P}\left[\mathbf{I}_2\partial_\tau\otimes\gamma^0+\left(\mathbf{I}_2\partial_i-\frac{i}{2}\xi_A\mathcal{H}\boldsymbol{\tau}^i\right)\otimes\gamma_i+i\mu_{\rm m}\mathcal{H}\mathrm{I}_8+2i\xi_\varphi\mathcal{H}\mathbf{I}_2\otimes(\gamma^0\gamma^5)\right]\tilde{P}^{-1}\tilde{\Psi}_P\\ &= i\bar{\tilde{\Psi}}_P\left[\mathbf{I}_2\partial_\tau\otimes\gamma^0+\left(\mathbf{I}_2\partial_{i,P}-\frac{i}{2}\xi_A\mathcal{H}\boldsymbol{\tau}^i\right)\otimes\gamma_i+i\mu_{\rm m}\mathcal{H}\mathrm{I}_8+2i\xi_\varphi\mathcal{H}\mathbf{I}_2\otimes(\gamma^0\gamma^5)\right]\tilde{\Psi}_P\\ &= i\bar{\tilde{\Psi}}_P\left[\mathbf{I}_2\partial_\tau\otimes\gamma^0+\left(\mathbf{I}_2\partial_{i,P}+\frac{i}{2}\xi_{A,P}\mathcal{H}\boldsymbol{\tau}^i\right)\otimes\gamma_i+i\mu_{\rm m}\mathcal{H}\mathrm{I}_8-2i\xi_{\varphi,P}\mathcal{H}\mathbf{I}_2\otimes(\gamma^0\gamma^5)\right]\tilde{\Psi}_P,\end{aligned} \tag{C.18}$$

which implies that

$$\mathcal{L}_\Psi(\tau,\mathbf{x}) \neq \mathcal{L}_\Psi(\tau,-\mathbf{x}). \tag{C.19}$$

Therefore, the axion-SU(2) gauge field vacuum spontaneously broke the parity in the fermionic sector

D Current: point-splitting regularization

In this appendix, we present the details of computation of the current integral, $\mathcal{K}^+(\tau)$, in eq. (6.21). Here, we use the point-splitting technique to renormalize $\mathcal{K}^+(\tau;\varepsilon)$ as

$$\mathcal{K}^+(\tau;\varepsilon) = -\mathrm{symm}\lim_{\varepsilon\to 0}\sum_{s=\pm}\frac{a\ s\ (2\pi)^2/H^3}{2(a_f a_b)^2}\int \mathrm{d}^3k\left[u_s^{\uparrow *}(k,\tau_f)u_s^{\downarrow}(k,\tau_b)+u_s^{\downarrow *}(k,\tau_f)u_s^{\uparrow}(k,\tau_b)\right],$$

where from eq. (6.11) we have

$$\tau_f = \left(1-\frac{\varepsilon}{2}\right)\tau \quad \text{and} \quad \tau_b = \left(1+\frac{\varepsilon}{2}\right)\tau,$$

while $a_f \equiv a(\tau_f)$ and $a_b \equiv a(\tau_b)$ are the forward and backward scale factors, and the symmetrization is done under $\varepsilon\to-\varepsilon$. Using eqs. (4.11) and (4.16), we can write $\mathcal{K}^+$ as

$$\mathcal{K}^+(\tau;\varepsilon) = \frac{1}{(2\pi)^2}\sum_{s=\pm} is\left[e^{i\kappa_s\pi}\mathcal{I}_{\kappa_s,\mu^+}+\mu_{\rm m}^2 e^{i\tilde{\kappa}_s\pi}\mathcal{I}_{\tilde{\kappa}_s,\mu^+}\right], \tag{D.1}$$

where for a given κ and μ, we define $\mathcal{I}_{\kappa,\mu}(\tau;\varepsilon)$ as

$$\mathcal{I}_{\kappa,\mu}(\tau;\varepsilon) \equiv (2\pi)^2\left(\left(1+\frac{\varepsilon}{2}\right)\left(1-\frac{\varepsilon}{2}\right)\right)^{\frac{3}{2}}\mathrm{symm}\lim_{\varepsilon\to 0}\int_0^\infty \tau^2 k\mathrm{d}k\left[W^*_{\kappa,\mu}(-2ik\tau_f)W_{\kappa,\mu}(-2ik\tau_b)\right]. \tag{D.2}$$

Here we recall that $\mu^+ = i|\mu^+|$, $\kappa_s^+ = \frac{1}{2}+is\kappa_I^+$ and $\tilde{\kappa}_s^+ = -\frac{1}{2}+is\kappa_I^+$. For simplicity, until otherwise stated, we present both κ_s and $\tilde{\kappa}_s$ with κ and μ^+ by μ. Moreover, we drop the $\mathrm{symm}\lim_{\varepsilon\to 0}$ while we will keep in mind that all the terms should be symmetrized with respect to the sign of ε, and eventually we take the ε goes to zero limit.

JHEP07(2020)154

Doing the momentum integral, we arrive at

$$\mathcal{I}_{\kappa,\mu}(\tau;\varepsilon)=\frac{\left[(1+\frac{\varepsilon}{2})(1-\frac{\varepsilon}{2})\right]^{\frac{3}{2}}\mathcal{G}_{\kappa,\mu}(\tau;\varepsilon)}{\Gamma(\frac{1}{2}+\mu-\kappa)\Gamma(\frac{1}{2}-\mu-\kappa)\Gamma^*(\frac{1}{2}+\mu-\kappa)\Gamma^*(\frac{1}{2}-\mu-\kappa)}, \tag{D.3}$$

where $\mathcal{G}_{\kappa,\mu}(\tau;\varepsilon)$ is

$$\mathcal{G}_{\kappa,\mu}(\tau;\varepsilon)\equiv\frac{1}{4}\int_{\mathcal{C}_\alpha}\mathrm{d}\alpha\left(-\frac{1}{1-\frac{\varepsilon}{2}}\right)^{\alpha}\Gamma\left(\frac{1}{2}+\mu+\alpha\right)\Gamma\left(\frac{1}{2}-\mu+\alpha\right)\Gamma(-\kappa-\alpha)G(\alpha), \tag{D.4}$$

and $G(\alpha)$ is defined as

$$G(\alpha)\equiv\int_{\mathcal{C}_\beta}\mathrm{d}\beta\left(1+\frac{\varepsilon}{2}\right)^{-\beta}\Gamma(-\kappa^*-\beta)\Gamma\left(\frac{1}{2}-\mu+\beta\right)\Gamma\left(\frac{1}{2}+\mu+\beta\right)\left(\frac{\varepsilon}{2}\right)^{\alpha+\beta-2}\Gamma(2-\alpha-\beta).$$

The contours $\mathcal{C}_\alpha$ and $\mathcal{C}_\beta$ can be closed in either the left or right half-plane as far as they separate the poles of $\Gamma(\frac{1}{2}+\beta\pm\mu)$ and $\Gamma(-\kappa-\beta)$. (See figure 21)

In doing the complex integral in $G(\alpha)$ and closing the integral on the right-half plane, we have two types of poles

$$\beta_{1n}\equiv-\kappa^*+n, \tag{D.5}$$

$$\beta_{2n}\equiv 2-\alpha+n \qquad \text{where} \quad 2+n-\mathrm{Re}\alpha>0, \tag{D.6}$$

where $n\in\mathbb{N}$. Therefore, we can write $\mathcal{G}_{\kappa,\mu}$ as

$$\begin{aligned}\mathcal{G}_{\kappa,\mu}(\tau;\varepsilon)=&-\frac{2i\pi}{4}\left(\frac{\varepsilon}{2}\right)^{-2}\sum_{n=0}^{\infty}\frac{1}{n!}\left(\frac{-\varepsilon/2}{1+\frac{\varepsilon}{2}}\right)^n\int_{\mathcal{C}_\alpha}\mathrm{d}\alpha\left(\frac{-\varepsilon/2}{1-\frac{\varepsilon}{2}}\right)^{\alpha}\Gamma\left(\frac{1}{2}+\mu+\alpha\right)\Gamma\left(\frac{1}{2}-\mu+\alpha\right)\\&\Gamma(-\kappa-\alpha)\Bigg[\left(\frac{\varepsilon/2}{1+\frac{\varepsilon}{2}}\right)^{2-\alpha}\Gamma(-\kappa^*-2-n+\alpha)\Gamma\left(\frac{1}{2}-\mu+2+n-\alpha\right)\Gamma\left(\frac{1}{2}+\mu+2+n-\alpha\right)\\&+\left(\frac{\varepsilon/2}{1+\frac{\varepsilon}{2}}\right)^{-\kappa^*}\Gamma(2-\alpha+\kappa^*-n)\Gamma\left(\frac{1}{2}-\mu-\kappa^*+n\right)\Gamma\left(\frac{1}{2}+\mu-\kappa^*+n\right)\Bigg].\end{aligned} \tag{D.7}$$

For technical convenience we decompose $\mathcal{G}_{\kappa,\mu}(\tau;\varepsilon)$ as

$$\mathcal{G}_{\kappa,\mu}(\tau;\varepsilon)\equiv\mathcal{G}_1(\tau;\varepsilon)+\mathcal{G}_2(\tau;\varepsilon),$$

where $\mathcal{G}_i(\tau;\varepsilon)$ are the contributions of the ith term inside the square bracket to the $\mathcal{G}(\tau;\varepsilon)$. In the following we compute $\mathcal{G}_1(\tau;\varepsilon)$, and $\mathcal{G}_2(\tau;\varepsilon)$ respectively.

$\mathcal{G}_1(\tau;\varepsilon)$. Taking $\varepsilon\to 0$ and closing the contour on the left-half plane, the first term inside the square-bracket in eq. (D.7) gives

$$\begin{aligned}\mathcal{G}_1=&-\frac{2i\pi}{4}\int_{\mathcal{C}_\alpha}\mathrm{d}\alpha(-1)^{\alpha}\Gamma\left(\frac{1}{2}+\mu+\alpha\right)\Gamma\left(\frac{1}{2}-\mu-\alpha\right)\Gamma\left(\frac{1}{2}-\mu+\alpha\right)\Gamma\left(\frac{1}{2}+\mu-\alpha\right)\\&\Gamma(-\kappa-\alpha)\Gamma(1+\kappa+\alpha)\frac{\Gamma(-\kappa^*+\alpha-2)}{\Gamma(1+\kappa+\alpha)}\left(\left(\frac{3}{2}-\alpha\right)^2-\mu^2\right)\left(\left(\frac{1}{2}-\alpha\right)^2-\mu^2\right),\end{aligned} \tag{D.8}$$

JHEP07(2020)154

which has an infinite number of type $\alpha_{\pm,q}=-q-\frac{1}{2}\mp\mu$, and $\alpha_{0,q}=-q-\kappa-1$ with $q\in\mathbb{N}$. Therefore, it is more convenient to write the above as

$$\mathcal{G}_1=-\frac{2i\pi}{4}\int_{\mathcal{C}_\alpha}\mathrm{d}\alpha(-1)^\alpha\Gamma\left(\frac{1}{2}+\mu+\alpha\right)\Gamma\left(\frac{1}{2}-\mu-\alpha\right)\Gamma\left(\frac{1}{2}-\mu+\alpha\right)\Gamma\left(\frac{1}{2}+\mu-\alpha\right)$$
$$\Gamma(-\kappa-\alpha)\Gamma(1+\kappa+\alpha)\left[w(\alpha)-w(\alpha-1)+\frac{\mathcal{A}_{\kappa,\mu}}{\alpha+\kappa}\right], \tag{D.9}$$

where $w(\alpha)$ and $\mathcal{A}_{\kappa,\mu}$ for each of $\mathrm{Re}\kappa=\pm\frac{1}{2}$ and in terms of $f(\alpha)$

$$f(\alpha)=\left(\left(\frac{3}{2}-\alpha\right)^2-\mu^2\right)\left(\left(\frac{1}{2}-\alpha\right)^2-\mu^2\right), \tag{D.10}$$

are respectively as follows. In case of $\mathrm{Re}\kappa=\frac{1}{2}$, we have

$$w(\alpha)=-\frac{\frac{1}{6}f(\alpha)+2(1-2\kappa)}{\alpha+\kappa}+\frac{\frac{1}{2}f(\alpha+1)-\frac{1}{6}f(\alpha+2)}{\alpha+\kappa-1}-\frac{\frac{1}{6}f(\alpha+1)}{\alpha+\kappa-2}+4\alpha, \tag{D.11}$$
$$\mathcal{A}_{\kappa,\mu}=2(1-2\kappa). \tag{D.12}$$

For $\mathrm{Re}\kappa=-\frac{1}{2}$, $w(\alpha)$ and $\mathcal{A}_{\kappa,\mu}$ are

$$w(\alpha)=-\frac{f(\alpha+1)}{\alpha+\kappa}+\frac{4}{3}\alpha\left(\alpha^2-\frac{3}{4}(1+2\kappa)\alpha+3(\kappa^2-\mu^2+\kappa+\frac{1}{6})\right), \tag{D.13}$$
$$\mathcal{A}_{\kappa,\mu}=-\frac{1}{2}(1+2\kappa)\left(1+4\kappa+4\kappa^2-4\mu^2\right). \tag{D.14}$$

We can further simply eq. (D.9) as

$$\mathcal{G}_1\equiv\mathcal{G}_1'+\mathcal{G}_1'',$$

where $\mathcal{G}_1'$ is

$$\mathcal{G}_1'=-\frac{2i\pi}{4}\left(\int_{\mathcal{C}_\alpha}\mathrm{d}\alpha-\int_{\mathcal{C}_\alpha-1}\mathrm{d}\alpha\right)(-1)^\alpha w(\alpha)\Gamma\left(\frac{1}{2}+\mu+\alpha\right)\Gamma\left(\frac{1}{2}-\mu-\alpha\right)\Gamma\left(\frac{1}{2}-\mu+\alpha\right)$$
$$\Gamma\left(\frac{1}{2}+\mu-\alpha\right)\Gamma(-\kappa-\alpha)\Gamma(1+\kappa+\alpha), \tag{D.15}$$

and $\mathcal{G}_1''$ is

$$\mathcal{G}_1''=-\frac{2i\pi\mathcal{A}_{\kappa,\mu}}{4}\int_{\mathcal{C}_\alpha}\mathrm{d}\alpha\frac{(-1)^\alpha\Gamma(-\alpha-\kappa)\Gamma(\alpha+\kappa+1)}{(\alpha+\kappa)}\Gamma\left(\frac{1}{2}+\mu+\alpha\right)\Gamma\left(\frac{1}{2}-\mu-\alpha\right)$$
$$\Gamma\left(\frac{1}{2}-\mu+\alpha\right)\Gamma\left(\frac{1}{2}+\mu-\alpha\right). \tag{D.16}$$

Doing the integral in eq. (D.15) and closing the contour on the left-half plane, we have only three poles, $\alpha_\pm=-\frac{1}{2}\pm\mu$ and $\alpha_0=-1-\kappa$, which lead to

$$\frac{e^{i\kappa\pi}\mathcal{G}_1'/(2\pi)^2}{\Gamma(\frac{1}{2}-\kappa+\mu)\Gamma(\frac{1}{2}+\kappa-\mu)\Gamma(\frac{1}{2}-\kappa-\mu)\Gamma(\frac{1}{2}+\kappa+\mu)}=$$
$$\frac{1}{4}\left[w(-1-\kappa)+\frac{i}{2}\left(w\left(-\frac{1}{2}+\mu\right)\frac{e^{2i\pi\kappa}+e^{2i\pi\mu}}{\sin(2\mu\pi)}-w\left(-\frac{1}{2}-\mu\right)\frac{e^{2i\pi\kappa}+e^{-2i\pi\mu}}{\sin(2\mu\pi)}\right)\right]. \tag{D.17}$$

JHEP07(2020)154

However, $\mathcal{G}_1''$ includes an infinite number of simple poles

$$\alpha_n^{\pm} = -\frac{1}{2} \pm \mu - n \quad \text{and} \quad \alpha_n^0 = -1 - n - \kappa,$$

where $n \in \mathbb{N}$. The contribution of α_n^0-poles in $\mathcal{G}_1''$ is

$$\frac{e^{i\kappa\pi}/(2\pi)^2 \ \mathcal{G}_1''|_{\alpha^0}}{\Gamma(\frac{1}{2}+\mu+\kappa)\Gamma(\frac{1}{2}-\mu-\kappa)\Gamma(\frac{1}{2}-\mu+\kappa)\Gamma(\frac{1}{2}+\mu-\kappa)} = \frac{A_{\kappa,\mu}}{4}\psi^{(0)}(1). \tag{D.18}$$

Besides, the contribution of $\alpha_n^{\pm}$-poles gives

$$\begin{aligned}&\frac{e^{i\kappa\pi}/(2\pi)^2 \ \mathcal{G}_1''|_{\alpha^{\pm}}}{\Gamma(\frac{1}{2}+\mu+\kappa)\Gamma(\frac{1}{2}-\mu-\kappa)\Gamma(\frac{1}{2}-\mu+\kappa)\Gamma(\frac{1}{2}+\mu-\kappa)} = \\ &\frac{i\mathcal{A}_{\kappa,\mu}}{8}\sum_{n=0}^{\infty}\left(\frac{(e^{2i\kappa\pi}+e^{2i\mu\pi})}{\sin(2\mu\pi)}\frac{1}{(\mu+\kappa-\frac{1}{2}-n)} - \frac{(e^{2i\kappa\pi}+e^{-2i\mu\pi})}{\sin(2\mu\pi)}\frac{1}{(-\mu+\kappa-\frac{1}{2}-n)}\right).\end{aligned} \tag{D.19}$$

Finally, from the combination of eqs. (D.17)–(D.19), we have

$$\begin{aligned}&\frac{e^{i\kappa\pi}\mathcal{G}_1/(2\pi)^2}{\Gamma(\frac{1}{2}-\kappa+\mu)\Gamma(\frac{1}{2}+\kappa-\mu)\Gamma(\frac{1}{2}-\kappa-\mu)\Gamma(\frac{1}{2}+\kappa+\mu)} = \\ &\frac{1}{4}\Bigg[w(-1-\kappa)+\frac{i}{2}\left(w\left(-\frac{1}{2}+\mu\right)\frac{e^{2i\pi\kappa}+e^{2i\pi\mu}}{\sin(2\mu\pi)} - w\left(-\frac{1}{2}-\mu\right)\frac{e^{2i\pi\kappa}+e^{-2i\pi\mu}}{\sin(2\mu\pi)}\right)+\mathcal{A}_{\kappa,\mu}\Bigg\{\psi^{(0)}(1) \\ &+\frac{i}{2\sin(2\mu\pi)}\left((e^{2i\kappa\pi}+e^{2i\mu\pi})\psi^{(0)}\left(\frac{1}{2}-\kappa-\mu\right)-(e^{2i\kappa\pi}+e^{-2i\mu\pi})\psi^{(0)}\left(\frac{1}{2}-\kappa+\mu\right)\right)\Bigg\}\Bigg].\end{aligned} \tag{D.20}$$

We computed $\mathcal{G}_1$ and now we turn to compute $\mathcal{G}_2$.

$\mathcal{G}_2(\tau;\varepsilon)$. Now we turn to compute the contribution of the second term inside the square-brackets of $\mathcal{G}_{\kappa,\mu}$ in eq. (D.7), i.e. $\mathcal{G}_2$ as

$$\begin{aligned}\mathcal{G}_2 \equiv &-\frac{2i\pi}{4}\left(\frac{\varepsilon}{2}\right)^{-2}\left(\frac{\frac{\varepsilon}{2}}{1+\frac{\varepsilon}{2}}\right)^{-\kappa^*}\sum_{n=0}^{\infty}\frac{1}{n!}\left(-\frac{\frac{\varepsilon}{2}}{1+\frac{\varepsilon}{2}}\right)^n\Gamma\left(\frac{1}{2}-\mu-\kappa^*+n\right)\Gamma\left(\frac{1}{2}+\mu-\kappa^*+n\right) \\ &\int_{\mathcal{C}_\alpha}\mathrm{d}\alpha\left(-\frac{\frac{\varepsilon}{2}}{1-\frac{\varepsilon}{2}}\right)^{\alpha}\Gamma\left(\frac{1}{2}+\mu+\alpha\right)\Gamma\left(\frac{1}{2}-\mu+\alpha\right)\Gamma(-\kappa-\alpha)\Gamma(2-\alpha+\kappa^*-n).\end{aligned} \tag{D.21}$$

Closing the contour in the right-half plane, the above complex integral, lets call $\mathcal{G}_2$, can be decomposed as

$$\mathcal{G}_2 \equiv \mathcal{G}_2' + \mathcal{G}_2'',$$

in which $\mathcal{G}_2'$ includes the contribution of simple poles of $\Gamma(-\kappa-\alpha)$, and $\mathcal{G}_2''$ which includes the second order poles. More precisely, for $m \in \mathbb{N}$, the poles are

Simple poles:	$\alpha_m = -\kappa + m$	where	$0 \le m < 2 + 2\mathrm{Re}\kappa - n$,
Second-order poles:	$\alpha_m = 2 + 2\mathrm{Re}\kappa - \kappa - n + m$	where	$n \le 2 + 2\mathrm{Re}\kappa + m$.

JHEP07(2020)154

The contribution of simple poles to $\mathcal{G}_2$ gives $\mathcal{G}'_2$ as

$$\mathcal{G}'_2 = -\frac{(2\pi)^2(-1)^{-\kappa}}{4}\left(\frac{\varepsilon}{2}\right)^{-2-2\mathrm{Re}\kappa}\left(\frac{1-\frac{\varepsilon}{2}}{1+\frac{\varepsilon}{2}}\right)^{\kappa}\left(1+\frac{\varepsilon}{2}\right)^{2\mathrm{Re}\kappa}\sum_{n=0}^{1+2\mathrm{Re}\kappa}\frac{1}{n!}\left(-\frac{\frac{\varepsilon}{2}}{1+\frac{\varepsilon}{2}}\right)^{n}$$
$$\Gamma\left(\frac{1}{2}-\mu-\kappa^*+n\right)\Gamma\left(\frac{1}{2}+\mu-\kappa^*+n\right)\sum_{m=0}^{1+2\mathrm{Re}\kappa-n}\frac{1}{m!}\left(\frac{\frac{\varepsilon}{2}}{1-\frac{\varepsilon}{2}}\right)^{m}\Gamma(2+2\mathrm{Re}\kappa-n-m)$$
$$\Gamma\left(\frac{1}{2}+\mu-\kappa+m\right)\Gamma\left(\frac{1}{2}-\mu-\kappa+m\right). \tag{D.22}$$

Doing the series in the above, we find $\mathcal{G}'_2$ as

$$\lim_{\varepsilon\to 0}\frac{e^{i\kappa\pi}\left[(1+\frac{\varepsilon}{2})(1-\frac{\varepsilon}{2})\right]^{\frac{3}{2}}\mathcal{G}'_2/(2\pi)^2}{\Gamma(\frac{1}{2}+\mu-\kappa)\Gamma(\frac{1}{2}-\mu-\kappa)\Gamma(\frac{1}{2}-\mu-\kappa^*)\Gamma(\frac{1}{2}+\mu-\kappa^*)} = \frac{\mathcal{K}'}{4}, \tag{D.23}$$

where $\mathcal{K}'$ takes the following forms for $\mathrm{Re}\kappa = \pm\frac{1}{2}$ respectively. In case of $\mathrm{Re}\kappa = \frac{1}{2}$ and after symmetrization, we find

$$\mathcal{K}' = \frac{(2\kappa-1)}{2}(1-4\kappa+4\kappa^2-4\mu^2). \tag{D.24}$$

For $\mathrm{Re}\kappa = -\frac{1}{2}$, $\mathcal{K}'$ vanishes

$$\mathcal{K}' = 0. \tag{D.25}$$

As we see in eqs. (D.24) and (D.25), $\mathcal{G}'_2$ only includes finite terms.

Now we turn to compute the contribution of second order poles in $\mathcal{G}_2$ which specifies $\mathcal{G}''_2$ as

$$\mathcal{G}''_2 \equiv \frac{(2\pi)^2}{4}\left(\frac{\varepsilon}{2}\right)^{-2}\sum_{q=0}^{\infty}\sum_{n=0}^{2+2\mathrm{Re}\kappa+q}\frac{(-1)^n}{n!}\left(\frac{\frac{\varepsilon}{2}}{1+\frac{\varepsilon}{2}}\right)^{n-\kappa^*}\Gamma\left(\frac{1}{2}-\mu-\kappa^*+n\right)\Gamma\left(\frac{1}{2}+\mu-\kappa^*+n\right)$$
$$\frac{d}{d\alpha}\left[(\alpha-\alpha_{0,q})^2\left(-\frac{\frac{\varepsilon}{2}}{1-\frac{\varepsilon}{2}}\right)^{\alpha}\Gamma\left(\frac{1}{2}+\mu+\alpha\right)\Gamma\left(\frac{1}{2}-\mu+\alpha\right)\Gamma(-\kappa-\alpha)\Gamma(2-\alpha+\kappa^*-n)\right]_{\alpha=\alpha_{0,q}},$$

where $\alpha_{0,q} = 2+\kappa^*-n+q$. After taking the ε goes to zero limit, we can write $\mathcal{G}''_2$ as

$$\frac{e^{i\kappa\pi}\lim_{\varepsilon\to 0}\mathcal{G}''_2/(2\pi)^2}{\Gamma(\frac{1}{2}-\mu-\kappa)\Gamma(\frac{1}{2}+\mu-\kappa)\Gamma(\frac{1}{2}+\mu+\kappa)\Gamma(\frac{1}{2}-\mu+\kappa)} =$$
$$\frac{1}{4}\Bigg(\mathcal{A}_{\kappa,\mu}\left[\ln\left(\frac{\varepsilon}{2}\right)+i\pi+\psi^{(0)}\left(\frac{1}{2}+\mu-\kappa\right)+\psi^{(0)}\left(\frac{1}{2}-\mu-\kappa\right)-2\psi^{(0)}(1)\right]$$
$$-w(-1-\kappa)+\mathcal{K}''\Bigg), \tag{D.26}$$

where $\mathcal{A}_{\kappa,\mu}$ and $w(-1-\kappa)$ for $\mathrm{Re}\kappa = \pm\frac{1}{2}$ are given in eqs. (D.11)–(D.14) and $\mathcal{K}''$ is as follows. In case of $\mathrm{Re}\kappa = \frac{1}{2}$, $\mathcal{K}''$ is

$$\mathcal{K}'' = \frac{4}{3}\frac{(1-2\kappa)(7-14\kappa+8\kappa^2-4\mu^2)}{(1-4\kappa+4\kappa^2-4\mu^2)}, \tag{D.27}$$

and in case of $\mathrm{Re}\kappa = -\frac{1}{2}$, it is

$$\mathcal{K}'' = -\frac{1}{4}(1+2\kappa)(9+\frac{56}{3}\kappa+\frac{20}{3}\kappa^2+4\kappa^2-4\mu^2). \tag{D.28}$$

From the combination of eqs. (D.23) and (D.26), we have $\mathcal{G}_2$ as

$$\frac{e^{i\kappa\pi}[(1+\frac{\varepsilon}{2})(1-\frac{\varepsilon}{2})]^{\frac{3}{2}}\mathcal{G}_2/(2\pi)^2}{\Gamma(\frac{1}{2}+\mu-\kappa)\Gamma(\frac{1}{2}-\mu-\kappa)\Gamma(\frac{1}{2}-\mu+\kappa)\Gamma(\frac{1}{2}+\mu+\kappa)} = \frac{1}{4}\Bigg[\frac{\Gamma(\frac{1}{2}-\mu-\kappa^*)\Gamma(\frac{1}{2}+\mu-\kappa^*)}{\Gamma(\frac{1}{2}-\mu+\kappa)\Gamma(\frac{1}{2}+\mu+\kappa)}\mathcal{K}'$$
$$+\mathcal{A}_{\kappa,\mu}\left(\ln\left(\frac{\varepsilon}{2}\right)+i\pi+\psi^{(0)}\left(\frac{1}{2}+\mu-\kappa\right)+\psi^{(0)}\left(\frac{1}{2}-\mu-\kappa\right)-2\psi^{(0)}(1)\right)+\mathcal{K}''-w(-1-\kappa)\Bigg]. \tag{D.29}$$

$\mathcal{G}_{\kappa,\mu}(\tau;\varepsilon)$. Working out both $\mathcal{G}_1$ and $\mathcal{G}_2$, we are now ready to compute $\mathcal{G}_{\kappa,\mu}(\tau;\varepsilon)$. From the combination of eqs. (D.20) and (D.29), we find $\mathcal{G}_{\kappa,\mu}(\tau;\varepsilon)$ as

$$\frac{4e^{i\kappa\pi}\left[(1+\frac{\varepsilon}{2})(1-\frac{\varepsilon}{2})\right]^{\frac{3}{2}}\mathcal{G}_{\kappa,\mu}(\tau;\varepsilon)/(2\pi)^2}{\Gamma(\frac{1}{2}-\kappa+\mu)\Gamma(\frac{1}{2}-\kappa-\mu)\Gamma^*(\frac{1}{2}-\kappa-\mu)\Gamma^*(\frac{1}{2}-\kappa+\mu)} =$$
$$\mathcal{K}'+\frac{\Gamma(\frac{1}{2}-\mu+\kappa)\Gamma(\frac{1}{2}+\mu+\kappa)}{\Gamma(\frac{1}{2}-\mu-\kappa^*)\Gamma(\frac{1}{2}+\mu-\kappa^*)}\Bigg\{\mathcal{A}_{\kappa,\mu}\ln\left(\frac{\varepsilon}{2}\right)+\mathcal{K}''-\Delta_1+\left(\frac{e^{2i\pi\kappa}+\cosh 2\pi|\mu|}{\sinh(2|\mu|\pi)}\right)\Delta_2$$
$$+\mathcal{A}_{\kappa,\mu}\left[i\pi-\psi^{(0)}(1)+\frac{e^{2i\kappa\pi}+e^{-2i\mu\pi}}{2\sinh(2|\mu|\pi)}\psi^{(0)}\left(\frac{1}{2}-\kappa-\mu\right)-\frac{e^{2i\kappa\pi}+e^{2i\mu\pi}}{2\sinh(2|\mu|\pi)}\psi^{(0)}\left(\frac{1}{2}-\kappa+\mu\right)\right]\Bigg\}, \tag{D.30}$$

in which we used $\mu = i|\mu|$ and Δ_1 and Δ_2 are

$$\Delta_1 \equiv \frac{1}{2}\left[w\left(-\frac{1}{2}+\mu\right)+w\left(-\frac{1}{2}-\mu\right)\right], \tag{D.31}$$

$$\Delta_2 \equiv \frac{1}{2}\left[w\left(-\frac{1}{2}+\mu\right)-w\left(-\frac{1}{2}-\mu\right)\right]. \tag{D.32}$$

$\mathcal{K}^+(\tau;\varepsilon)$. Upon computing eq. (D.30) for $\kappa = \kappa_s$, we can compute $\mathcal{I}_{\kappa_s,\mu}(\tau;\varepsilon)$ as

$$4\frac{e^{i\kappa_s\pi}}{(2\pi)^2}\mathcal{I}_{\kappa_s,\mu}(\tau;\varepsilon) = \frac{(1-2\kappa_s)(1-4\kappa_s+4\kappa_s^2-4\mu^2)}{2}\left[\ln\left(\frac{\varepsilon}{2}\right)+i\pi-\psi^{(0)}(1)\right]+4\left(\frac{1}{2}-\kappa_s\right)$$
$$\times\left[\left(\frac{1}{2}-\kappa_s\right)^2-\mu^2\right]\left[\frac{e^{2i\kappa_s\pi}+e^{-2i\mu\pi}}{2\sinh(2|\mu|\pi)}\psi^{(0)}\left(\frac{1}{2}-\kappa_s-\mu\right)-\frac{e^{2i\kappa_s\pi}+e^{2i\mu\pi}}{2\sinh(2|\mu|\pi)}\psi^{(0)}\left(\frac{1}{2}-\kappa_s+\mu\right)\right]$$
$$+1-\frac{11}{3}\kappa_s+4\kappa_s^2-\frac{4}{3}\kappa_s^3+\frac{2}{3}\mu(4-9\kappa_s+6\kappa_s^2-4\mu^2)\left(\frac{e^{2i\pi\kappa_s}+\cosh 2\pi|\mu|}{\sinh(2|\mu|\pi)}\right). \tag{D.33}$$

Recalling that $\kappa_s = \frac{1}{2}+is\kappa_I$ and summing over s, we arrive at

$$4\sum_{s=\pm}is\frac{e^{i\kappa_s\pi}}{(2\pi)^2}\mathcal{I}_{\kappa_s,\mu}(\tau;\varepsilon) = 8\kappa_I(|\mu|^2-\kappa_I^2)\left[\ln\left(\frac{\varepsilon}{2}\right)-\psi^{(0)}(1)+i\pi\right]+\frac{4}{3}\kappa_I(1-2\kappa_I^2)$$
$$+4\kappa_I(|\mu|^2-\kappa_I^2)\sum_{s=\pm}\left[\frac{e^{2|\mu|\pi}-e^{-2s\kappa_I\pi}}{2\sinh(2|\mu|\pi)}\psi^{(0)}(-is\kappa_I-i|\mu|)-\frac{e^{-2|\mu|\pi}-e^{-2s\kappa_I\pi}}{2\sinh(2|\mu|\pi)}\psi^{(0)}(-is\kappa_I+i|\mu|)\right]$$
$$+4i\kappa_I|\mu|\left(\frac{\cosh 2\pi|\mu|-\cosh(2\kappa_I\pi)}{\sinh(2|\mu|\pi)}\right)-\frac{4|\mu|}{3}(1-6\kappa_I^2-4|\mu|^2)\frac{\sinh(2\kappa_I\pi)}{\sinh(2|\mu|\pi)}. \tag{D.34}$$

JHEP07(2020)154

The above quantity is complex and we find its imaginary part as

$$\mathrm{Im}\left[4\sum_{s=\pm} is\frac{e^{i\kappa_s\pi}}{(2\pi)^2}\mathcal{I}_{\kappa_s,\mu}(\tau;\varepsilon)\right] = 4i\kappa_I|\mu|\left(\frac{\cosh 2\pi|\mu| - \cosh(2\kappa_I\pi)}{\sinh(2|\mu|\pi)}\right) - \frac{2\kappa_I(|\mu|^2-\kappa_I^2)}{\sinh(2|\mu|\pi)}\sum_{s=\pm}\left[\frac{(e^{2|\mu|\pi}-e^{-2s\kappa_I\pi})}{2(s\kappa_I+|\mu|)} - \frac{(e^{-2|\mu|\pi}-e^{-2s\kappa_I\pi})}{2(s\kappa_I-|\mu|)}\right]. \tag{D.35}$$

Moreover, by computing eq. (D.30) for $\kappa=\tilde{\kappa}_s$, we can compute $\mathcal{I}_{\tilde{\kappa}_s,\mu}(\tau;\varepsilon)$ as

$$\begin{aligned}
&4\frac{e^{i\tilde{\kappa}_s\pi}}{(2\pi)^2}\mathcal{I}_{\tilde{\kappa}_s,\mu}(\tau;\varepsilon) = -2(1+2\tilde{\kappa}_s)\left[\ln\left(\frac{\varepsilon}{2}\right)+1+\frac{1}{3}\left(\frac{6+10\tilde{\kappa}_s+4\tilde{\kappa}_s^2}{1+4\tilde{\kappa}_s+4\tilde{\kappa}_s^2-4\mu^2}\right)\right]\\
&-2(1+2\tilde{\kappa}_s)\left[i\pi-\psi^{(0)}(1)+\frac{e^{2i\tilde{\kappa}_s\pi}+e^{-2i\mu\pi}}{2\sinh(2|\mu|\pi)}\psi^{(0)}\left(\frac{1}{2}-\tilde{\kappa}_s-\mu\right)-\frac{e^{2i\tilde{\kappa}_s\pi}+e^{2i\mu\pi}}{2\sinh(2|\mu|\pi)}\psi^{(0)}\left(\frac{1}{2}-\tilde{\kappa}_s+\mu\right)\right]\\
&+\frac{8\mu}{3}\left(1+\frac{3+5\tilde{\kappa}_s+2\tilde{\kappa}_s^2}{1+4\tilde{\kappa}_s+4\tilde{\kappa}_s^2-4\mu^2}\right)\left(\frac{e^{2i\pi\tilde{\kappa}_s}+\cosh 2\pi|\mu|}{\sinh(2|\mu|\pi)}\right).
\end{aligned} \tag{D.36}$$

Using the fact that $\tilde{\kappa}_s=-\frac{1}{2}+is\kappa_I$ and summing over s, we find

$$\begin{aligned}
&4\sum_{s=\pm} is\frac{e^{i\tilde{\kappa}_s\pi}}{(2\pi)^2}\mathcal{I}_{\tilde{\kappa}_s,\mu}(\tau;\varepsilon) = 8\kappa_I\left[\ln\left(\frac{\varepsilon}{2}\right)+i\pi-\psi^{(0)}(1)+1+\frac{1}{6}\left(\frac{1-2\kappa_I^2}{|\mu|^2-\kappa_I^2}\right)\right]\\
&+4\kappa_I\sum_{s=\pm}\left[\frac{e^{2|\mu|\pi}-e^{-2s\kappa_I\pi}}{2\sinh(2|\mu|\pi)}\psi^{(0)}(1-is\kappa_I-i|\mu|)-\frac{e^{-2|\mu|\pi}-e^{-2s\kappa_I\pi}}{2\sinh(2|\mu|\pi)}\psi^{(0)}(1-is\kappa_I+i|\mu|)\right]\\
&-\frac{4i\kappa_I|\mu|}{(|\mu|^2-\kappa_I^2)}\left(\frac{\cosh 2\pi|\mu|-\cosh(2\pi\kappa_I)}{\sinh(2|\mu|\pi)}\right)-\frac{4|\mu|}{3}\left(\frac{1-6\kappa_I^2+4|\mu|^2}{(|\mu|^2-\kappa_I^2)}\right)\frac{\sinh(2\kappa_I\pi)}{\sinh(2|\mu|\pi)}.
\end{aligned} \tag{D.37}$$

Now, for the plus subspace with $\mu_{\mathrm{m}}^2=|\mu^+|^2-\kappa_I^2$, it can be further simplified to

$$\begin{aligned}
&4\mu_{\mathrm{m}}^2\sum_{s=\pm} is\frac{e^{i\tilde{\kappa}_s\pi}}{(2\pi)^2}\mathcal{I}_{\tilde{\kappa}_s,\mu}(\tau;\varepsilon) = 8\kappa_I\left[\mu_{\mathrm{m}}^2\left(\ln\left(\frac{\varepsilon}{2}\right)+i\pi-\psi^{(0)}(1)\right)+\mu_{\mathrm{m}}^2+\frac{1-2\kappa_I^2}{6}\right]\\
&+4\kappa_I\mu_{\mathrm{m}}^2\sum_{s=\pm}\left[\frac{e^{2|\mu|\pi}-e^{-2s\kappa_I\pi}}{2\sinh(2|\mu|\pi)}\psi^{(0)}(1-is\kappa_I-i|\mu|)-\frac{e^{-2|\mu|\pi}-e^{-2s\kappa_I\pi}}{2\sinh(2|\mu|\pi)}\psi^{(0)}(1-is\kappa_I+i|\mu|)\right]\\
&-4i\kappa_I|\mu|\left(\frac{\cosh 2\pi|\mu|-\cosh(2\pi\kappa_I)}{\sinh(2|\mu|\pi)}\right)-\frac{4|\mu|}{3}(1-6\kappa_I^2+4|\mu|^2)\frac{\sinh(2\kappa_I\pi)}{\sinh(2|\mu|\pi)}.
\end{aligned} \tag{D.38}$$

As we see, it is a complex quantity with an imaginary part given as

$$\mathrm{Im}\left[4\mu_{\mathrm{m}}^2\sum_{s=\pm} is\frac{e^{i\tilde{\kappa}_s\pi}}{(2\pi)^2}\mathcal{I}_{\tilde{\kappa}_s,\mu}(\tau;\varepsilon)\right] = -4i\kappa_I|\mu|\left(\frac{\cosh 2\pi|\mu| - \cosh(2\kappa_I\pi)}{\sinh(2|\mu|\pi)}\right) + \frac{2\kappa_I(|\mu|^2-\kappa_I^2)}{\sinh(2|\mu|\pi)}\sum_{s=\pm}\left[\frac{(e^{2|\mu|\pi}-e^{-2s\kappa_I\pi})}{2(s\kappa_I+|\mu|)} - \frac{(e^{-2|\mu|\pi}-e^{-2s\kappa_I\pi})}{2(s\kappa_I-|\mu|)}\right]. \tag{D.39}$$

Notice that it is exactly cancels the imaginary part of $4\sum_{s=\pm} is\frac{e^{i\kappa_s\pi}}{(2\pi)^2}\mathcal{I}_{\kappa_s,\mu}(\tau;\varepsilon)$ in eq. (D.35). Therefore, our final form for the current function, $\mathcal{K}^+(\tau,\varepsilon)$, in eq. (D.1) is real. More

JHEP07(2020)154

precisely, combining eqs. (D.34), (D.35), (D.38), and (D.39), we find the desired quantity

$$\mathcal{K}^{+}(\tau;\varepsilon) = \\ 4\kappa_I\mu_{\rm m}^2\left[\ln\left(\frac{\varepsilon}{2}\right)-\psi^{(0)}(1)\right]+\frac{2}{3}\kappa_I(1-2\kappa_I^2)+2\kappa_I\mu_{\rm m}^2-\frac{2|\mu|}{3}\left(1-2\kappa_I^2+4\mu_{\rm m}^2\right)\frac{\sinh(2\kappa_I\pi)}{\sinh(2|\mu|\pi)} \\ +\kappa_I\mu_{\rm m}^2\sum_{s=\pm}\left[\frac{e^{2|\mu|\pi}-e^{-2s\kappa_I\pi}}{\sinh(2|\mu|\pi)}\mathrm{Re}\left[\psi^{(0)}(-is\kappa_I-i|\mu|)\right]-\frac{e^{-2|\mu|\pi}-e^{-2s\kappa_I\pi}}{\sinh(2|\mu|\pi)}\mathrm{Re}\left[\psi^{(0)}(-is\kappa_I+i|\mu|)\right]\right]. \tag{D.40}$$

JHEP07(2020)154

References

[1] A.H. Guth, *The Inflationary Universe: A Possible Solution to the Horizon and Flatness Problems*, *Adv. Ser. Astrophys. Cosmol.* **3** (1987) 139 [INSPIRE].

[2] K. Sato, *First Order Phase Transition of a Vacuum and Expansion of the Universe*, *Mon. Not. Roy. Astron. Soc.* **195** (1981) 467 [INSPIRE].

[3] A.D. Linde, *A New Inflationary Universe Scenario: A Possible Solution of the Horizon, Flatness, Homogeneity, Isotropy and Primordial Monopole Problems*, [INSPIRE].

[4] A. Albrecht and P.J. Steinhardt, *Cosmology for Grand Unified Theories with Radiatively Induced Symmetry Breaking*, *Adv. Ser. Astrophys. Cosmol.* **3** (1987) 158 [INSPIRE].

[5] PLANCK collaboration, *Planck 2015 results. XX. Constraints on inflation*, *Astron. Astrophys.* **594** (2016) A20 [arXiv:1502.02114] [INSPIRE].

[6] T. Matsumura et al., *Mission design of LiteBIRD*, *J. Low Temp. Phys.* **176** (2014) 733 [arXiv:1311.2847] [INSPIRE].

[7] M. Hazumi et al., *LiteBIRD: A Satellite for the Studies of B-Mode Polarization and Inflation from Cosmic Background Radiation Detection*, *J. Low Temp. Phys.* **194** (2019) 443 [INSPIRE].

[8] K. Abazajian et al., *CMB-S4 Science Case, Reference Design, and Project Plan*, arXiv:1907.04473 [INSPIRE].

[9] A. Maleknejad and M.M. Sheikh-Jabbari, *Non-Abelian Gauge Field Inflation*, *Phys. Rev. D* **84** (2011) 043515 [arXiv:1102.1932] [INSPIRE].

[10] A. Maleknejad and M.M. Sheikh-Jabbari, *Gauge-flation: Inflation From Non-Abelian Gauge Fields*, *Phys. Lett. B* **723** (2013) 224 [arXiv:1102.1513] [INSPIRE].

[11] A. Maleknejad, M.M. Sheikh-Jabbari and J. Soda, *Gauge Fields and Inflation*, *Phys. Rept.* **528** (2013) 161 [arXiv:1212.2921] [INSPIRE].

[12] A. Maleknejad and E. Komatsu, *Production and Backreaction of Spin-2 Particles of* SU(2) *Gauge Field during Inflation*, *JHEP* **05** (2019) 174 [arXiv:1808.09076] [INSPIRE].

[13] L. Mirzagholi, A. Maleknejad and K.D. Lozanov, *Production and backreaction of fermions from axion-*SU(2) *gauge fields during inflation*, *Phys. Rev. D* **101** (2020) 083528 [arXiv:1905.09258] [INSPIRE].

[14] A. Maleknejad, *Chiral Gravity Waves and Leptogenesis in Inflationary Models with non-Abelian Gauge Fields*, *Phys. Rev. D* **90** (2014) 023542 [arXiv:1401.7628] [INSPIRE].

[15] Y. Zeldovich, I. Kobzarev and L.B. Okun, *Cosmological Consequences of the Spontaneous Breakdown of Discrete Symmetry*, *Zh. Eksp. Teor. Fiz.* **67** (1974) 3 [INSPIRE].

[16] G. Dvali, C. Gomez and S. Zell, *Discrete Symmetries Excluded by Quantum Breaking*, arXiv:1811.03077 [INSPIRE].

[17] E. Dimastrogiovanni and M. Peloso, *Stability analysis of chromo-natural inflation and possible evasion of Lyth's bound*, *Phys. Rev. D* **87** (2013) 103501 [arXiv:1212.5184] [INSPIRE].

[18] P. Adshead, E. Martinec and M. Wyman, *Gauge fields and inflation: Chiral gravitational waves, fluctuations, and the Lyth bound*, *Phys. Rev. D* **88** (2013) 021302 [arXiv:1301.2598] [INSPIRE].

[19] B. Thorne, T. Fujita, M. Hazumi, N. Katayama, E. Komatsu and M. Shiraishi, *Finding the chiral gravitational wave background of an axion-*SU(2) *inflationary model using CMB observations and laser interferometers*, *Phys. Rev. D* **97** (2018) 043506 [arXiv:1707.03240] [INSPIRE].

[20] A. Agrawal, T. Fujita and E. Komatsu, *Large tensor non-Gaussianity from axion-gauge field dynamics*, *Phys. Rev. D* **97** (2018) 103526 [arXiv:1707.03023] [INSPIRE].

[21] A. Agrawal, T. Fujita and E. Komatsu, *Tensor Non-Gaussianity from Axion-Gauge-Fields Dynamics: Parameter Search*, *JCAP* **06** (2018) 027 [arXiv:1802.09284] [INSPIRE].

[22] K.D. Lozanov, A. Maleknejad and E. Komatsu, *Schwinger Effect by an* SU(2) *Gauge Field during Inflation*, *JHEP* **02** (2019) 041 [arXiv:1805.09318] [INSPIRE].

[23] A. Maleknejad, *Gravitational leptogenesis in axion inflation with* SU(2) *gauge field*, *JCAP* **12** (2016) 027 [arXiv:1604.06520] [INSPIRE].

[24] A. Maleknejad, M. Noorbala and M.M. Sheikh-Jabbari, *Leptogenesis in inflationary models with non-Abelian gauge fields*, *Gen. Rel. Grav.* **50** (2018) 110 [arXiv:1208.2807] [INSPIRE].

[25] A. Maleknejad, M.M. Sheikh-Jabbari and J. Soda, *Gauge-flation and Cosmic No-Hair Conjecture*, *JCAP* **01** (2012) 016 [arXiv:1109.5573] [INSPIRE].

[26] A. Maleknejad and E. Erfani, *Chromo-Natural Model in Anisotropic Background*, *JCAP* **03** (2014) 016 [arXiv:1311.3361] [INSPIRE].

[27] A. Maleknejad and M.M. Sheikh-Jabbari, *Revisiting Cosmic No-Hair Theorem for Inflationary Settings*, *Phys. Rev. D* **85** (2012) 123508 [arXiv:1203.0219] [INSPIRE].

[28] M.-a. Watanabe, S. Kanno and J. Soda, *Inflationary Universe with Anisotropic Hair*, *Phys. Rev. Lett.* **102** (2009) 191302 [arXiv:0902.2833] [INSPIRE].

[29] P. Adshead and A. Liu, *Anisotropic Massive Gauge-flation*, *JCAP* **07** (2018) 052 [arXiv:1803.07168] [INSPIRE].

[30] S.L. Adler, *Axial vector vertex in spinor electrodynamics*, *Phys. Rev.* **177** (1969) 2426 [INSPIRE].

[31] J.S. Bell and R. Jackiw, *A PCAC puzzle:* $\pi^0 \to \gamma\gamma$ *in the* σ *model*, *Nuovo Cim. A* **60** (1969) 47 [INSPIRE].

[32] M.E. Peskin and D.V. Schroeder, *An Introduction to quantum field theory*, Addison-Wesley, Reading, U.S.A. (1995).

JHEP07(2020)154

[33] L. Parker and D. Toms, *Quantum Field Theory in Curved Spacetime: Quantized Fields and Gravity*, Cambridge Monographs on Mathematical Physics, Cambridge University Press (2009).

[34] P. Adshead, L. Pearce, M. Peloso, M.A. Roberts and L. Sorbo, *Phenomenology of fermion production during axion inflation*, *JCAP* **06** (2018) 020 [arXiv:1803.04501] [INSPIRE].

[35] T. Hayashinaka, T. Fujita and J. Yokoyama, *Fermionic Schwinger effect and induced current in de Sitter space*, *JCAP* **07** (2016) 010 [arXiv:1603.04165] [INSPIRE].

[36] T. Hayashinaka and S.-S. Xue, *Physical renormalization condition for de Sitter QED*, *Phys. Rev. D* **97** (2018) 105010 [arXiv:1802.03686] [INSPIRE].

[37] A.D. Sakharov, *Violation of CP Invariance, C asymmetry, and baryon asymmetry of the universe*, *Pisma Zh. Eksp. Teor. Fiz.* **5** (1967) 32.

[38] PLANCK collaboration, *Planck 2015 results. XIII. Cosmological parameters*, *Astron. Astrophys.* **594** (2016) A13 [arXiv:1502.01589] [INSPIRE].

[39] F.W. Olver, D.W. Lozier, R.F. Boisvert and C.W. Clark, *NIST Handbook of Mathematical Functions*, Cambridge University Press, New York, NY, U.S.A., 1st ed. (2010).

JHEP07(2020)154